Journal

of

THE ROYAL AERONAUTICAL SOCIETY

NOVEMBER 1959

CONTENTS

NOTICES

THE STRUCTURAL EFFECTS OF KINETIC HEATING

Some Factors Affecting the Choice of Materials — W. G. Heath

Design of Transparencies — J. S. Przemieniecki

Some Practical Aspects of Kinetic Heating Calculations — C. L. Bore

Advantages and Limitations of Models — A. J. Sobey

Summary of the Discussion — Maureen E. Michael and Joan Bruce

ICING FLIGHT DEVELOPMENT — B. T. Cheverton

TECHNICAL NOTES

Iterative Solutions of the Equations for Plane Oblique Shock Waves—A. R. Collar. The Effect of Initial Lateral Tension or Slackness on the Deflection of Long, Thin Plates under Normal Pressure—H. L. Cox and D. Dawson.

GRADUATES' AND STUDENTS' SECTION

THE LIBRARY — REVIEWS — REPORTS

TWELVE SHILLINGS AND SIXPENCE MONTHLY

LONDON

4 HAMILTON PLACE W1

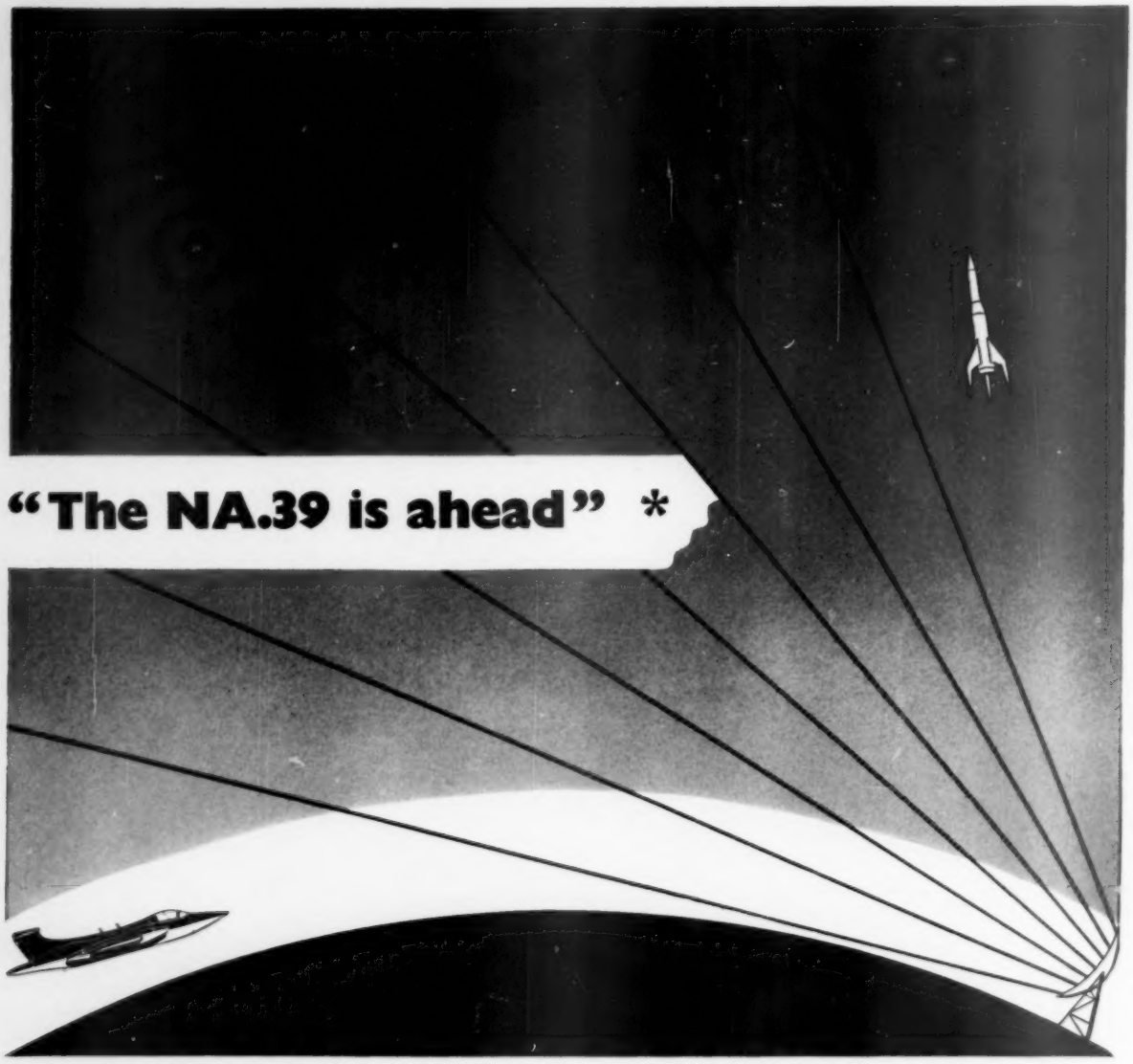

"The NA.39 is ahead" *

Today, in any major war, an enemy would be protected by an almost impenetrable curtain of radar and guided missiles. But there is a gap *beneath* the curtain; a vulnerable level. The NA.39 is designed and constructed to strike at this vulnerable level and that is why the Ministry of Defence has stated—

* *"In the low-level strike role, the NA.39 is ahead of any other aircraft in the world"*

Blackburn

BLACKBURN AIRCRAFT LIMITED, BROUGH, YORKSHIRE

A135/a

Gamma rocket engine delivers 19,000-lb thrust outside the earth's atmosphere - for a weight of under 700lb . . .

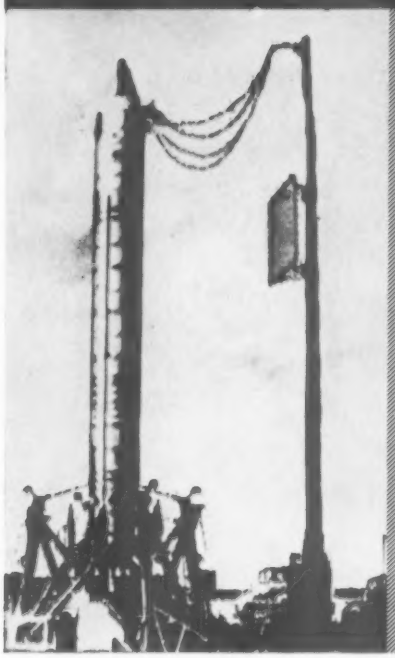

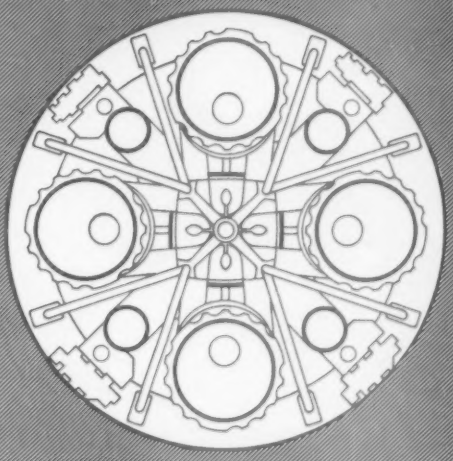

End view showing combustion chambers which can be inclined for vehicle guidance.

...ANOTHER ENGINEERING ADVANCE BY BRISTOL SIDDELEY

One of the largest manufacturers of motive power units in the world, Bristol Siddeley Engines Limited produce the Gamma. A liquid propellent rocket engine, the Gamma delivers 16,400-lb thrust (7,438 kg) at sea level rising to 19,000 lb (8,618 kg) outside the earth's atmosphere for a total engine bay weight of under 700 lb.

The Bristol Siddeley Gamma has four gimbal-mounted combustion chambers which are hydraulically actuated for vehicle guidance. Each combustion chamber is fed with propellents by its own turbopump unit and the four units are joined at the centre by a common manifold. The Gamma burns hydrogen peroxide (HTP) with kerosene and uses silver-plated nickel gauze as a catalyst to decompose the HTP into oxygen and superheated steam.

Gamma powers Black Knight

The Bristol Siddeley Gamma powers the Saunders-Roe Black Knight, Britain's highly successful space research vehicle. The Gamma has proved itself to be exceptionally reliable. In fact, in all firings to date Black Knight has never failed to start, and has reached a height of over 500 miles above the Woomera rocket range in Australia.

Since Bristol Siddeley's rocket division began work in 1946 it has developed a wide range of rocket components. By combining these components in single or multi-chamber layouts, thrust requirements from 500 lb up to very high figures, can be met.

BRISTOL SIDDELEY ENGINES LIMITED

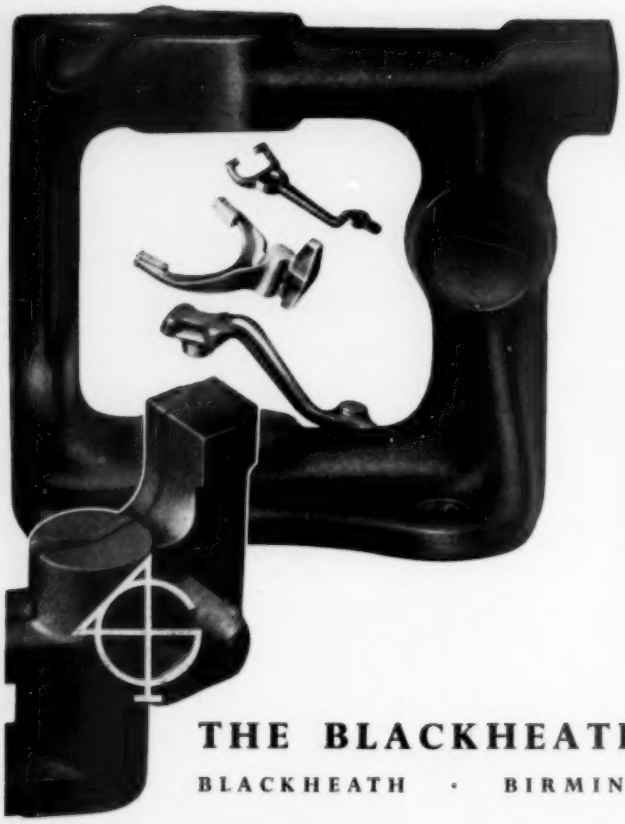

. . . looking ahead,
Blackheath are using
the most up-to-date
equipment for the
continued production of

SUPERIOR DROPFORGINGS

THE BLACKHEATH STAMPING CO. LTD.

BLACKHEATH · BIRMINGHAM · Tel: Blackheath 1448/9

Anti-Icing Controls

Anti-icing and de-icing equipment manufactured by Teddington Aircraft Controls include components used on windscreen de-icing, wing and tail de-icing, engine intake cowl anti-icing, fuel filter ice warning, bomb bay heating and propeller and spinner de-icing systems in many aircraft at present on military service or airline operation. These systems make use of hot air or gas, or electrical heater mat, and the controls are either electrically or pneumatically operated.

CABIN AIR CONDITIONING CONTROL

ANTI-ICING CONTROLS

FUEL TANK PRESSURISATION

HOT AIR AND GAS VALVES

ELECTRO-MAGNETIC VALVES

TIME SWITCHES

PRESSURE SWITCHES

PRESSURE REGULATORS

POTENTIOMETERS, ACCELEROMETERS AND PRESSURE TRANSDUCERS

Teddington CONTROLS
REGD. TRADE MARK

TEDDINGTON AIRCRAFT CONTROLS LTD

MERTHYR TYDFIL, SOUTH WALES Telephone: Merthyr Tydfil 3261

LONDON OFFICE: COLNBROOK BY-PASS, WEST DRAYTON, MIDDLESEX Telephone: Colnbrook 2202-3-4

TAC 163

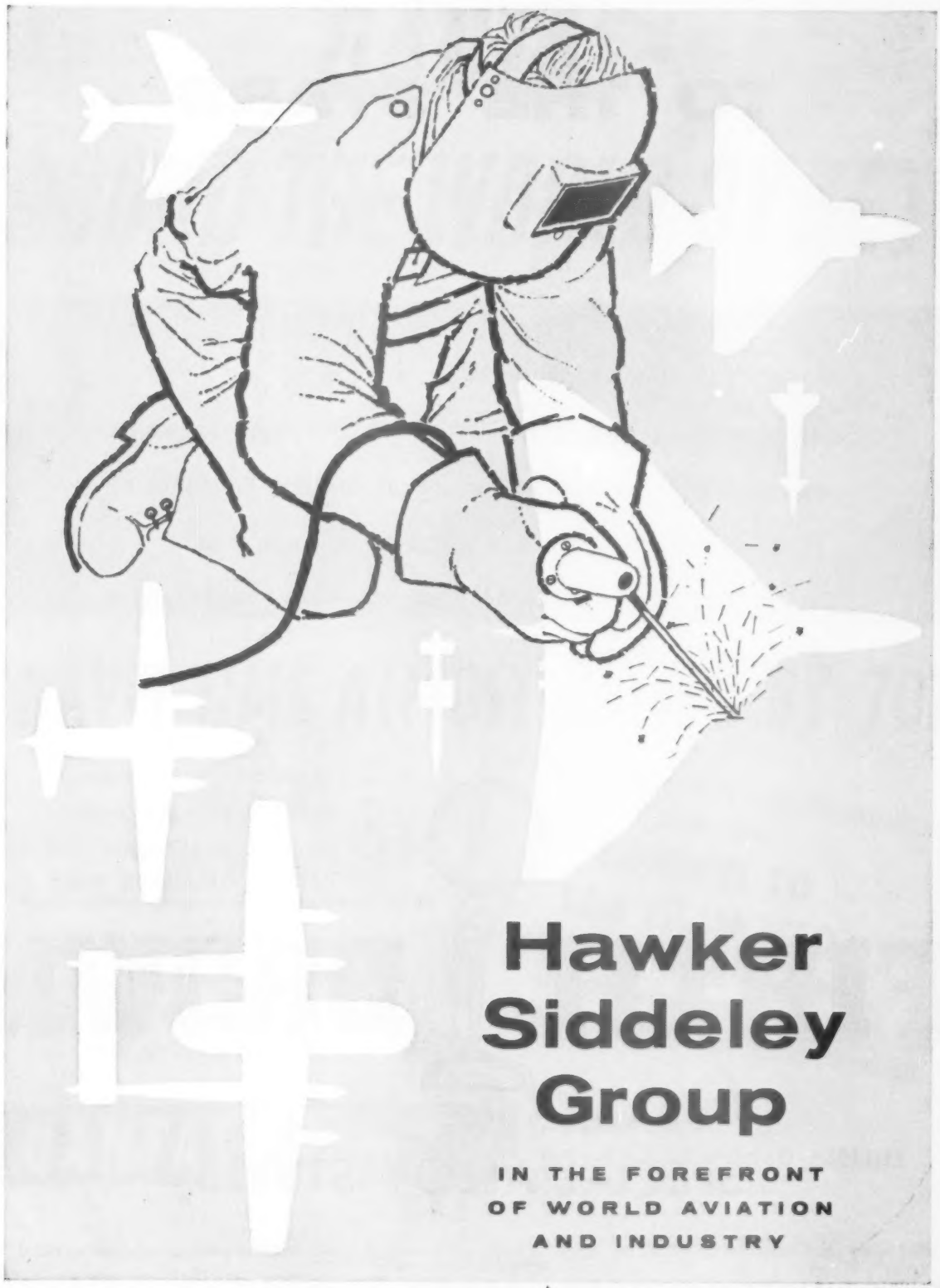
Hawker
Siddeley
Group
IN THE FOREFRONT
OF WORLD AVIATION
AND INDUSTRY

LEADING THE WAY

TO THE STARS

Steels developed by Firth Brown for the Aircraft Industry were assisting world famous Engine and Airframe designers long before the first Schneider race. Unceasing research and advanced metallurgical control has enabled Firth Brown to produce a range of steels to meet the most rigorous requirements of Aeronautics and Astronautics alike.

FIRTH BROWN

SPECIAL ALLOY STEELS

THOS FIRTH & JOHN BROWN LIMITED · SHEFFIELD

QANTAS-
ROUND THE WORLD BY JET

TRAVEL TIME ALMOST HALVED BY 707

Now Flying Westwards
LONDON • NEW YORK
SAN FRANCISCO • HONOLULU • FIJI
NEW ZEALAND* • SYDNEY
**Quick and easy connections to Auckland from Fiji*

Also Flying Eastwards
LONDON • MIDDLE EAST
PAKISTAN • INDIA • THAILAND
MALAYA • SYDNEY

STOP PRESS
LONDON TO SAN FRANCISCO
without changing plane
DE LUXE · TOURIST · ECONOMY CLASSES

QANTAS

AUSTRALIA'S ROUND-THE-WORLD AIRLINE
WITH B.O.A.C, T.E.A.L AND S.A.A

Tickets and helpful advice from all appointed Travel Agents or Qantas, corner of Piccadilly and Old Bond Street, London, W.I. (Mayfair 9200) or any office of B.O.A.C.

prizewinner in 1909

In 1909 Elektron Magnesium Alloys were introduced to the world at an international exhibition in Germany and were awarded the First Prize in a competition for light metals.

ELEKTRON

still the world's lightest structural metal in 1959

The past 50 years have more than justified this initial success of Elektron. Today the latest Elektron alloys, developed by MEL to meet the exacting requirements of industries as diverse as aircraft and textiles, motor transport and nuclear engineering, are still the finest magnesium alloys available anywhere in the world.

In this Golden Jubilee year of Elektron, MEL are proud of the part they have played in pioneering the use of magnesium in Great Britain. As sole producers of the metal, with unique research, development, prototype and fabrication facilities, MEL enterprise and technological skill will continue to make available to all industries the advantages of magnesium—the world's lightest structural metal.

Magnesium Elektron Ltd.

Clifton Junction, Manchester
London Office: 5 Charles II Street, St. James's, SW1
Magnesium Elektron, Inc., New York 20, USA

Design for Mobility

To make a ground-to-air guided weapon system mobile is not simply a matter of jacking it up and running some wheels under it. It needs an entirely different — and more challenging—approach. We know—for we were chosen by the British Government to concentrate on this very problem. And five years of design and development work have gone into the solution. **THE ANSWER IS**

THE 'ENGLISH ELECTRIC' THUNDERBIRD

—a complete mobile and *air transportable weapon system — fully developed—now in service with the British Army.*

Its mobility and ease of redeployment give the flexibility that is so essential to meet the nation's ever-changing defence requirements . . . **AND THE ECONOMY AS WELL**

ENGLISH ELECTRIC AVIATION LIMITED · GUIDED WEAPONS DIVISION: LUTON · STEVENAGE · WOOMERA

A MEMBER OF THE ENGLISH ELECTRIC AVIATION GROUP

Maintaining direct radio-link with their refuelling vehicles out on the airfield, the Shell and BP Aviation Services movement control room directs the vehicle to the apron where the aircraft, needing refuelling, has landed.

4 OUT OF 5 AIRCRAFT* USING LONDON AIRPORT USE SHELL OR BP AVIATION FUELS

"Careful planning and teamwork is the order of the day," says Leslie Hughes, operations room Movement Controller for Shell and BP Aviation Services. "Close co-ordination between ourselves and London Airport's central control tower means that we know well in advance just where and when an aircraft is landing. By consulting our Aircraft Parking Area Plan we can direct the fueller carrying the appropriate grade of aviation fuel to meet the aircraft as it taxies on to the apron. It is this organization that enables us to cut down to a minimum the turn-round time of the aircraft we fuel."

** 25 Leading Airlines use the Shell and BP Aviation Services at London Airport.*

SHELL BP

AVIATION SERVICES

Shell-Mex and B.P. Ltd. Shell-Mex House, Strand, W.C.2.

Registered Users of Trade Marks. Distributors in the United Kingdom for the Shell, BP and Eagle Groups

V810 AIRCRAFT-MILE COSTS

11 cents below forecast!

—That's proof of VISCOUNT Economy for you!

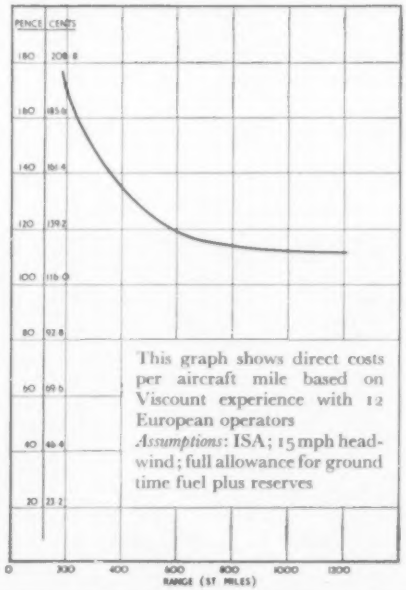

This graph shows direct costs per aircraft mile based on Viscount experience with 12 European operators
Assumptions: ISA; 15 mph head-wind; full allowance for ground time fuel plus reserves

Promised V810 economy more than proved in practice!

The economical performance promised by this graph has been more than fulfilled in the first six months' operation of Continental Airlines' V810 fleet.

After 6 months' V810 operation

CONTINENTAL AIRLINES REPORT

- *Aircraft mile cost 71.33 cents* for an average sector of 500 miles — 11 CENTS BELOW FORECAST!
- *Outstanding V810 economy and passenger appeal brought the airline* $1.3 MILLIONS *in Viscount profit* between May and December 1958 (Average fleet of nine aircraft for the period).

The Viscount V810 is still without a challenger in its class as a modern, medium-sized short/medium haul airliner. Its economy, flexibility, 365 m.p.h. cruise speed, and background of Vickers engineering and Rolls-Royce turbo-prop experience in over 370 Viscounts in service all over the world, make it unique as a profit-earner in this field.

Low fare/High profit note

The V810 in a 70-seat layout has a seat-mile cost of only 1.34 cents at 300 miles, and a proved 1.01 cents at 500 miles! *With only 49 passengers, this aircraft would clear 10% profit at fares 15% down on current U.S.A. coach fares!*

VICKERS VISCOUNT 810

FOUR ROLLS-ROYCE DART TURBO-PROP ENGINES

- ***Fastest and most economical medium-sized airliner in the world***

VICKERS-ARMSTRONGS (AIRCRAFT) LIMITED WEYBRIDGE SURREY

TGA AY638

For Superlative Accuracy . . . .

CROSS

Cross British made products are manufactured by an outstanding process used for the hardening and tempering of steel coils and rings. Covered by many patents, this manufacturing method has enabled components to be made from wire and with superlative accuracy. When top standards are essential you can rely on Cross precision products.

CROSS MANUFACTURING COMPANY (1938) LIMITED

BATH · **SOMERSET** · **ENGLAND** · Phone: Combe Down 2355/8 Telegrams: 'CIRCLE' BATH

This photograph shows a few examples of high-quality precision springs, made by Riley. Some were produced to customers own specifications, others were the result of recommendations by the Riley design and research department. If you have any kind of spring problem, Riley will find the answer to it.

(The diagram shows information required when ordering this type of spring.)

FAMOUS FOR SPRINGS SINCE 1821

There are no finer springs than Springs by **Riley**

ROBERT RILEY LTD., MILKSTONE SPRING WORKS, ROCHDALE, Tel: ROCHDALE 2237 (5 lines) Grams: 'RILOSPRING' ROCHDALE TELEX 63-151

WHICHEVER END THEY PUT IT

Whether it's at one end, as in the quietly efficient Westland Wessex . . . whether it's at both ends, as in the outstanding Bristol 192 . . . whether it's upright, horizontal or in any position in between, the Napier Gazelle free turbine engine will always satisfy the exacting demands of helicopter operation. Designed specifically for helicopter application, the Napier Gazelle, with its "any angle" installation, relieves the designer of many accepted limitations and gives him more opportunity to make proper use of fuselage space.

NAPIER GAZELLE FREE TURBINE ENGINE

D. NAPIER & SON LIMITED, LONDON, W.3. A MEMBER OF THE ENGLISH ELECTRIC AVIATION GROUP

INTERNATIONAL SERIES ON AERONAUTICAL SCIENCES AND SPACE FLIGHT

Joint Chairmen

DR. THEODORE VON KÁRMÁN **DR. HUGH L. DRYDEN**

This series forms a complete source of study and reference covering the whole field of aeronautical sciences and space flight. Each book covers a specific aspect of the subject, and serves as an authoritative review for the well-prepared beginner and a reliable source book for the experienced worker.

Together with the works published by Pergamon Press on behalf of the Advisory Group for Aeronautical Research and Development (AGARD), North Atlantic Treaty Organization, the volumes in Aeronautical Sciences and Space Flight meet much of the increasing demand for up-to-date and authoritative literature prepared by those who fully understand the needs of the student and the experienced worker.

Board of Specialist Editors

R. L. Bisplinghoff, W. S. Hemp
R. T. Jones, W. P. Jones
A. D. Baxter, E. R. Sharp
R. J. Lees, E. Rechtin
G. Melvill Jones, W. R. Lovelace II
M. C. Wilson
M. Alperin, S. F. Singer, M. Stern
W. J. Harris, Jr., C. Zwikker
Individual Editors appointed for each Symposium

Title of Division in the Series

SOLID AND STRUCTURAL MECHANICS
AERODYNAMICS
PROPULSION SYSTEMS INCLUDING FUELS
AVIONICS
AVIATION AND SPACE MEDICINE
FLIGHT-TESTING
ASTRONAUTICS
MATERIALS, SCIENCE AND ENGINEERING

SYMPOSIA

Some of the titles in preparation:

RAREFIED GAS DYNAMICS
Proceedings of the First International Symposium held at Nice
Edited by **F. M. Devienne**
Contains authoritative papers on design and theory, as well as experimental aspects of the subject, of interest to all concerned with aviation and aerodynamics. **£6 net ($17.50)**

ELASTIC STABILITY OF PLATES AND SHELLS
by **H. L. Cox**

FLAME PROPAGATION
by **D. M. Simon**

AGARD FLIGHT TEST MANUAL
Edited by **C. D. Perkins, E. J. Durbin** and **E. Seckel**
(Four Volumes)

An authoritative, comprehensive up-to-date handbook on the analysis and testing of aircraft performance, stability, control and instrumentation. Published for the Advisory Group for Aeronautical Research and Development, North Atlantic Treaty Organization, the AGARD FLIGHT TEST MANUAL will comprise four loose-leaf volumes, and to keep it completely up-to-date annual supplements will be available from 1960 onwards.

£30 net ($100.00) for 4 vols.
Subscription to Supplements: £5 5s. per annum

PERGAMON PRESS London New York Paris Los Angeles

4 & 5 Fitzroy Square, London W.1. 122 East 55th Street, New York 22, N.Y.
24 Rue des Écoles, Paris V^e^.

Journal of

THE ROYAL AERONAUTICAL SOCIETY

WITH WHICH IS INCORPORATED THE INSTITUTION OF AERONAUTICAL ENGINEERS

PUBLISHED MONTHLY AT

4 HAMILTON PLACE, LONDON, W.1

Telephone: Grosvenor 3515-9 *Telegrams:* Didaskalos, Audley, London

SUBSCRIPTIONS: £7 10s. 0d. PER ANNUM, PLUS 9s. POSTAGE AND PACKING
SINGLE COPIES: 12s. 6d. PLUS 9d. POSTAGE AND PACKING

VOLUME 63 NOVEMBER 1959 NUMBER 587

CONTENTS

PAGE

Notices LIII

Christmas Holiday—Lecture Theatre—The Library—Symposium on Flight Safety—Prizes in Aeronautics—Henlow Cadet Prize—Honours Awarded to Members—Message from a Past President of the Society—Annual Subscriptions—The Shuttleworth Collection—Summaries of Lectures—Diary—JOURNAL Binding—Letter from Chief Inspector of Taxes Branch, Inland Revenue—Elections—News of Members.

The Structural Effects of Kinetic Heating 615

Some Factors Affecting the Choice of Materials — W. G. HEATH
Design of Transparencies — J. S. PRZEMIENIECKI
Some Practical Aspects of Kinetic Heating Calculations — C. L. BORE
Advantages and Limitations of Models — A. J. SOBEY
Summary of the Discussion — MAUREEN E. MICHAEL and JOAN BRUCE

Icing Flight Development — B. T. CHEVERTON 659

Technical Notes 669

Iterative Solutions of the Equations for Plane Oblique Shock Waves—A. R. COLLAR. The Effect of Initial Lateral Tension or Slackness on the Deflection of Long, Thin Plates under Normal Pressure—H. L. COX and D. DAWSON.

Graduates' and Students' Section 675

The Library 676

REVIEWS: Sounding Rockets—Guided Missile Engineering—British Civil Aircraft 1919-59—Nine Lives.

ADDITIONS TO THE LIBRARY. REPORTS.

All communications for publication in the JOURNAL *should be addressed to the Editor,* JOAN BRADBROOKE, *A.R.Ae.S.; all communications on general matters affecting the Society should be addressed to the Secretary,* A. M. BALLANTYNE, *T.D., B.Sc., Ph.D., Hon.F.C.A.I., F.I.A.S., F.R.Ae.S.*

None of the papers or paragraphs must be taken as expressing the opinion of the Council of the Royal Aeronautical Society unless otherwise stated.

ADVERTISEMENT OFFICE: *One Arundel Street, Strand, London, W.C.2. Covent Garden* 1612.

PRINTED BY THE LEWES PRESS, WIGHTMAN & CO. LTD., LEWES, SUSSEX, ENGLAND, AND PUBLISHED BY THE ROYAL AERONAUTICAL SOCIETY, 4 HAMILTON PLACE, LONDON, W.1, ENGLAND.

THE ROYAL AERONAUTICAL SOCIETY

Overseas Divisions

AUSTRALIA
President: M. M. WAGHORN, A.F.R.Ae.S.
Hon. Secretary: W. ISBISTER, Science House, [A.F.R.Ae.S. Gloucester & Essex Streets, Sydney, New South Wales.
Branches at: Sydney, Melbourne, Adelaide.

NEW ZEALAND
President: D. A. PATTERSON, M.B.E., A.R.Ae.S.
Hon. Secretary: T. T. N. COLERIDGE, The Shell Com- [A.F.R.Ae.S. pany of New Zealand Ltd., Box 2091, Wellington.
Branches at: Auckland, Wellington, Palmerston North, Christchurch.

SOUTHERN AFRICA
President: COLONEL J. D. T. LOUW, A.F.R.Ae.S.
Hon. Secretary: Mrs. D. D. HUGHES, 14 Keyes Court, Keyes Avenue, Rosebank, Johannesburg.
Branches at: Durban and Salisbury.

Overseas Branch

SINGAPORE *President*: Air Marshal THE EARL OF BANDON, K.B.E., C.B., C.V.O., D.S.O., R.A.F.
Chairman: E. A. CRABBE, A.F.R.Ae.S.
Hon. Secretary: T. C. CHIOLE, A.R.Ae.S., c/o Malayan Airways, Paya Lebar Airport, Singapore.

Branches in the United Kingdom

BELFAST
President: Rear-Admiral Sir MATTHEW S. SLATTERY, C.B., F.R.Ae.S.
Chairman: H. G. PARKER, A.F.R.Ae.S.
Hon. Secretary: D. F. DYSON, A.R.Ae.S., Short Brothers & Harland Ltd., Belfast.

BIRMINGHAM AND WOLVERHAMPTON
President: L. S. GREENLAND, F.R.Ae.S.
Chairman: H. BOTTOMS.
Hon. Secretary: A. JAMES, A.F.R.Ae.S., Sir W. G. Armstrong Whitworth Aircraft Ltd., Warwick Chambers, 14-20 Corporation Street, Birmingham 2.

BOSCOMBE DOWN
President Air Cdre. A. E. CLOUSTON, C.B., D.S.O., D.F.C., A.F.C.
Chairman: Dr. D. CAMERON, F.R.Ae.S.
Hon. Secretary: G. F. LANGDON, Grad.R.Ae.S., A. & A.E.E., Boscombe Down, Amesbury, Wilts.

BRISTOL
President: PROFESSOR A. R. COLLAR, F.R.Ae.S.
Chairman: H. GIDDINGS, F.R.Ae.S.
Hon. Secretary: G. WANSBROUGH-WHITE, A.R.Ae.S., Bristol Aircraft Ltd., Filton, Bristol.

BROUGH
President: N. E. ROWE, C.B.E., F.R.Ae.S.
Chairman: B. P. LAIGHT, F.R.Ae.S.
Hon. Secretary: A. D. HOWARTH, A.R.Ae.S., Blackburn Aircraft Ltd., Brough.

CAMBRIDGE
President: Professor W. A. MAIR, F.R.Ae.S.
Chairman: C. F. C. SNEESBY, A.F.R.Ae.S.
Hon. Secretary: J. LUDFORD, A.R.Ae.S., Marshalls Flying School, Newmarket Road, Cambridge.

CHESTER
President: C. B. V. NIELSON.
Chairman: G. J. SALISBURY, A.R.Ae.S.
Hon. Secretary: H. STRAWSON, A.F.R.Ae.S., Thornton Research Centre, P.O. Box 1, Chester.

CHRISTCHURCH
President: E. W. J. GRAY, F.R.Ae.S.
Chairman: H. E. VINCENT, A.F.R.Ae.S.
Hon. Secretary: N. J. KENT, A.R.Ae.S., c/o Vickers-Armstrongs (Aircraft) Ltd., Hurn Airport, Christchurch.

COVENTRY
President: H. M. WOODHAMS, C.B.E., F.R.Ae.S.
Chairman: W. J. PETERS.
Hon. Secretary: C. T. SCULTHORPE, A.F.R.Ae.S., Sir W. G. Armstrong Whitworth Aircraft Ltd., Whitley, Coventry.

DERBY
President: J. D. PEARSON, F.R.Ae.S.
Chairman: A. A. RUBBRA, F.R.Ae.S.
Hon. Secretary: J. H. STEPHENS, A.F.R.Ae.S., c/o Rolls-Royce Ltd., Nightingale Road, Derby.

GLASGOW
President: Professor W. J. DUNCAN, C.B.E., F.R.Ae.S.
Chairman: Dr. A. W. BABISTER, A.F.R.Ae.S.
Hon. Secretary: W. N. ALCOCK, Shenstone, Dumbuck Crescent, Dumbarton.

GLOUCESTER AND CHELTENHAM
President: L. G. FAIRHURST, F.R.Ae.S.,
Chairman: J. F. CUSS, A.F.R.Ae.S.
Hon. Secretary: C. E. HUTT, A.R.Ae.S., c/o S. Smith and Sons (England) Ltd., Bishops Cleeve, nr. Cheltenham, Glos.

HALTON
President: Air Marshal H. D. SPRECKLEY, C.B., O.B.E., F.R.Ae.S.
Chairman: Air Commodore T. N. COSLETT, O.B.E.
Hon. Secretary: Sqn. Ldr. J. W. G. PARKER, E. & I. Squadron, R.A.F., Halton.

HATFIELD
President: Sir GEOFFREY DE HAVILLAND, C.B.E., A.F.C., Hon. F.R.Ae.S.
Chairman: C. G. LONG, A.F.R.Ae.S.
Hon. Secretary: J. A. KIRK, A.F.R.Ae.S., de Havilland Propellers Ltd., Hatfield, Herts.

HENLOW
President: R. HILLS, F.R.Ae.S.
Chairman: Wg. Cdr. I. D. H. GIBBINS, M.B.E., A.F.R.Ae.S.
Hon. Secretary: Flt. Lt. A. H. CRAVEN, A.F.R.Ae.S., Officers' Mess, R.A.F. Technical College, Henlow, Beds.

ISLE OF WIGHT
President: Sir ARTHUR GOUGE, Hon. F.R.Ae.S.
Chairman: W. BROWNING, F.R.Ae.S.
Hon. Secretary: R. L. WHEELER, A.F.R.Ae.S., Design Office, Saunders-Roe Ltd., Osborne, Isle of Wight.

LEICESTER
Chairman: K. B. AYERS, A.F.R.Ae.S.
Hon. Secretary: M. G. RUSSELL, A.R.Ae.S., c/o Design Office, Auster Aircraft Ltd., Rearsby, Leics.

LONDON AIRPORT
President: G. W. HALL, F.R.Ae.S.
Chairman: R. L. LICKLEY, F.R.Ae.S.
Hon. Secretary: N. BROWN, A.R.Ae.S., B.O.A.C. H.Q., London Airport, Middlesex.

LUTON
President: F. H. POLLICUTT, F.R.Ae.S.
Chairman: H. J. BROOKS, A.F.R.Ae.S.
Hon. Secretary: L. A. WILLOTT, A.F.R.Ae.S., Hunting Aircraft Ltd., Luton Airport.

MANCHESTER
President: Sir ROY H. DOBSON, C.B.E., J.P., Hon.F.R.Ae.S.
Chairman: C. E. FIELDING, O.B.E., F.R.Ae.S.
Hon. Secretary: J. A. E. WATERFALL, 56 Manor Avenue, Ashton-on-Mersey, Cheshire.

MERTHYR TYDFIL
President: C. S. GARDNER.
Chairman: J. INGRAM.
Hon. Secretary: Dr. G. O. FORESTER, Chief of Research, Teddington Aircraft Controls Ltd., Cefn Coed, nr. Merthyr Tydfil, South Wales.

PRESTON
President: Sir GEORGE H. NELSON.
Chairman: E. LOVELESS, A.F.R.Ae.S.
Hon. Secretary: J. F. FOSS, A.F.R.Ae.S., English Electric Aviation Ltd., Warton Aerodrome, nr. Preston.

READING
President: Sir FREDERICK HANDLEY PAGE, C.B.E., Hon.F.R.Ae.S.
Chairman: R. J. FENNER, A.F.R.Ae.S.
Hon. Secretary: N. KITCHING, A.R.Ae.S., Handley Page (Reading) Ltd., The Aerodrome, Woodley, Reading.

SOUTHAMPTON
Chairman: Professor E. J. RICHARDS, O.B.E., F.R.Ae.S.
Hon. Secretary: F. C. KIRKPATRICK, A.R.Ae.S., Folland Aircraft Ltd., Hamble, Southampton.

SOUTHEND
Chairman: T. R. C. BERRETT, A.R.Ae.S.
Hon. Secretary: K. A. COLE, A.R.Ae.S., c/o Aviation Traders (Eng.) Ltd., Southend Airport, Essex.

SWINDON
Chairman: S. R. HUGHES, A.F.R.Ae.S.
Hon. Secretary: D. RIGG, A.R.Ae.S., Vickers-Armstrongs (Aircraft) Ltd., Supermarine Works, South Marston, Swindon.

WEYBRIDGE
President: Sir GEORGE EDWARDS, C.B.E., F.R.Ae.S.
Chairman: H. H. GARDNER, F.R.Ae.S.
Hon. Secretary: E. G. BARBER, A.F.R.Ae.S., Vickers-Armstrongs (Aircraft) Ltd., Weybridge.

YEOVIL
President: E. C. WHEELDON.
Chairmen: D. L. HOLLIS-WILLIAMS, F.R.Ae.S. and Dr. E. W. STILL, F.R.Ae.S.
Hon. Secretary: L. A. LANSDOWN, A.F.R.Ae.S., Westland Aircraft Ltd., Yeovil.

NOTICES

Christmas Holiday

The Office and Library of the Society will be closed from Thursday afternoon 24th December until 9 a.m. on Tuesday 29th December.

The Library

During rebuilding at the Offices of the Society the Library will be operating under some difficulty. Members and other users are therefore asked to make allowances should the service fall slightly short of its usual standard for some months.

The Library will be closed on 8th, 9th and 10th December for the Associate Fellowship Examinations.

Prizes in Aeronautics

The Society's Prizes in Aeronautics, awarded annually to the best student in the Aeronautical Department at Universities and Colleges organising courses in aeronautics, have been awarded for 1959 as follows—:

Bristol University—Joint Award: J. W. Britton and D. R. Philpott.

Cambridge University—C. G. B. Mitchell of St. John's College.

Glasgow University—Kenneth M. Nicoll.

Imperial College, London—B. N. Tomlinson and M. Lacey.

Queen's University, Belfast—Kenneth J. Holden.

Northampton College of Advanced Technology, London—G. N. Sage.

Queen Mary College, London—G. J. Shorey.

Southampton University—R. D. Ford.

Henlow Cadet Prize

The Henlow Cadet Prize for 1959 has been awarded to Pilot Officer D. R. West. The Prize is three years' subscription as a Graduate of the Society, with entrance fee, and a book.

Annual Subscriptions

Members are reminded that their annual subscriptions become due on 1st January 1960. The rates are:—

	Home			*Abroad*		
	£	s.	d.	£	s.	d.
Fellows	8	0	0	7	0	0
Fellows (over 65)	5	0	0	4	0	0
Associate Fellows	6	0	0	5	0	0
Associate Fellows (over 65)	4	0	0	3	0	0
*Associates	5	0	0	5	0	0
Associates (over 65)	3	0	0	3	0	0
Graduates (aged under 26)	2	10	0	2	10	0
Graduates (aged 26 and over)	3	0	0	3	0	0
Students (aged under 21)	1	10	0	1	10	0
Students (aged 21 and over)	2	0	0	2	0	0
Companions	4	0	0	4	0	0
Companions (over 65)	3	0	0	3	0	0
Companions (No Journal)	2	10	0	2	10	0
Founder Members	—	—	—	—	—	—

*Any Associate elected before 1st October 1947 may, if he wishes, elect not to receive the JOURNAL, and in this case his subscriptions will be reduced by £1 10s. 0d. to £3 10s. 0d.

It will avoid delay and confusion if members, when sending remittances for subscriptions, will state their names clearly and give their addresses and grades of membership. Remittances should be made payable to the Royal Aeronautical Society.

Lecture Theatre

Work on the construction of the Lecture Theatre was started at the beginning of October and good progress is being made.

The complete list of contributions received since the October JOURNAL went to press will be published in the December issue.

Donations are still needed.

Symposium on Flight Safety

Admission to the All Day Discussion on Flight Safety to be held at the Institution of Mechanical Engineers on 11th December 1959, will be by special ticket only for members and non-members. Application for tickets should be made to the Secretary of the Society and until 4th December will be issued to members only; thereafter any seats available will be issued to non-members in strict rotation.

The Introductory papers will be:— The Accident Investigator's Viewpoint by Group Captain P. G. Tweedie (M. of A.); The Pilot's View by Captain E. C. Miles (B.O.A.C.); The Operator's View by Captain J. W. G. James (B.E.A.); and The Constructor's View by R. H. Warde (B.A.C.).

The Discussion will begin at 9.45 a.m.

Honours Awarded to Members

Sir Arnold Hall, Immediate Past President of the Society has been awarded the *Ir A. G. von Baumhauer Medal* for the period 1954-1959.

This is awarded periodically to the person who, in the opinion of the Council and advisers of the Royal Netherlands Aero Club, has made the most valuable contribution in either a scientific or practical sense to flight safety.

Sir George Edwards, Past President of the Society has been awarded the *Daniel Guggenheim Medal* for 1959 for a lifetime devoted to the design of military and commercial aircraft culminating in the successful introduction into worldwide commercial service of the first turbine-powered propeller-driven aircraft.

de Havilland Aircraft Co. Comet. The Elmer A. Sperry Award for 1959 was presented to the de Havilland Aircraft Co. on the 7th October in New York during the 7th Anglo-American Aeronautical Conference. The award is made annually for a distinguished contribution which through application, proved in actual service, has advanced the art of transportation, whether by land, sea or air. de Havilland have successfully developed the world's first jet-powered air liner, the de Havilland Comet.

Specifically named in the citation are Sir Geoffrey de Havilland (*Honorary Fellow*), Mr. Charles C. Walker (*Honorary Fellow*), and the late Major Frank B. Halford.

Message from a Past President of the Society

Sir Arthur Gouge, Past President of the Society has sent a note to say that he is retiring and would like all his old friends to know. He wishes to take this opportunity of thanking them for the help and co-operation given to him in the past.

The Shuttleworth Collection

Members may be interested to know that the Shuttleworth Collection is open from Monday to Friday *by appointment*, from 9 a.m. to noon and 2.30 p.m. to 4.30 p.m. and on some Saturdays from 9 a.m. to 11.30 a.m.

Applications for visits, enclosing a stamped addressed envelope, should be sent to L. A. Jackson, Esq., Old Warden Aerodrome, Biggleswade, Bedfordshire.

Summaries of Lectures

Fifteenth British Commonwealth Lecture
to be given on 19th November 1959

SOME RECENT PROGRESS IN AIR SURVEY WITH SPECIAL REFERENCE TO NEWLY DEVELOPED TERRITORIES

by W. P. SMITH, M.B.E., B.A., F.R.I.C.S.
(*Director, Fairey Air Surveys Ltd.*)

The paper considers briefly the state of air survey immediately after the Second World War and then deals in some detail with important aspects of technical progress.

These include the development in camera and lens design leading to improvement in photographic quality, in navigational methods, and to a lesser extent, in aircraft available. The paper then reviews progress in the application of aerial photography to problems of geology, agriculture and forestry in newly developing territories. This is followed by an appreciation of the value of mapping by air survey methods in connection with projects overseas and deals particularly with hydroelectric programmes in Africa, the survey aspects of land tenure problems, and large scale contouring for mining and other purposes. These lead to a consideration of progress made in the use of aerial triangulation and modern plotting machines and to the desirability of reducing the need for ground control. The paper discusses airborne electronic methods such as Shoran, Hiran and the Airborne Profile Recorder, all of which may introduce savings in time and cost when mapping remote areas. More recent systems such as the Tellurometer and Aerodist are touched upon.

The third section of the paper is concerned with geophysical surveys used in mineral exploration and includes reference to recent developments in surveys for radio activity, magnetic anomalies, and conductivity. The recently developed two-aircraft system for electro-magnetic surveys is described and the paper ends with an attempt to forecast some of the directions in which progress may be made in the near future. This section includes references to new "super-wide-angle" aerial cameras, to analytical methods of stereo-restitution, to automatic map plotting, mapping by radar photography and finally to gravimetric survey from the air.

Third Lanchester Memorial Lecture
to be given on 26th November 1959

SOME DEVELOPMENTS IN BOUNDARY LAYER RESEARCH IN THE LAST THIRTY YEARS

by Professor Dr. H. SCHLICHTING
(*Technical University of Braunschweig*)

Boundary layer theory is the cornerstone of our knowledge of the flow of air and other fluids of small viscosity under circumstances of interest in many engineering applications, especially also in aeronautics. Many complex problems in aerodynamics, as for instance the problem of skin friction, which was theoretically attacked very early by F. W. Lanchester, have been clarified by studying the flow within the boundary layer and its effects on the general flow around the body.

Research work on boundary layers, as started by Prandtl in 1904, was for the first twenty years—up to Prandtl's Wilbur Wright Memorial Lecture to the Royal Aeronautical Society in 1927—almost entirely restricted to Prandtl's Institute at Göttingen. But since about 1930 boundary layer theory has been generally accepted, and in the past thirty years there has been an almost exponential rise of the number of contributors to its further development.

The author tries to trace certain lines, along which this important branch of modern fluid dynamics has developed in the last thirty years. In this connection the following topics are treated to some extent:

(I) Transition from laminar to turbulent flow.
(II) Boundary layer control for high lift and low drag.
(III) Aerodynamic heating at high speeds (high Mach numbers).
(IV) Boundary layer effects on swept wings and on rotating bodies.

(I) The theoretical investigations of the problem of transition start from Reynolds' and Lord Rayleigh's hypothesis of the instability of laminar flow. After many unsuccessful attempts Tollmien in 1930 finally succeeded in calculating the critical Reynolds number for the boundary layer on a flat plate. More than ten years later Tollmien's stability theory was completely confirmed by very careful experiments of Dryden and his co-workers.

(II) After many wind tunnel experiments the investigations of boundary layer control for high lift of aerofoils led to the construction of two aeroplanes with boundary suction at the Aerodynamische Versuchsanstalt Göttingen in 1938. Later on also a considerable reduction of the skin friction of aerofoils was obtained with the advent of the laminar flow aerofoil.

(III) In flow at high Mach numbers the velocity boundary layer is accompanied by a thermal boundary layer which is caused by frictional heating. The large increase in the temperature of a solid surface in a high speed stream which can be calculated from boundary layer theory only, poses a serious problem to aeronautical engineers ("thermal barrier").

(IV) The aerodynamic characteristics of swept wings and delta wings are largely governed by the behaviour of their boundary layer. Some of the draw-backs of such wing plan forms can be remedied by boundary layer control, as for instance by a "boundary layer fence." For turbomachines the influence of the centrifugal forces on the boundary layer plays an important role for their aerodynamic coefficients.

DIARY

LONDON

13th November
AGRICULTURAL AVIATION GROUP MEETING—General Discussion on the International Conference at Cranfield. Library, 4 Hamilton Place. 7 p.m.

17th November
LECTURE—Magnetogasdynamics. Dr. J. A. Shercliff. Library, 4 Hamilton Place. 7 p.m.

19th November
FIFTEENTH BRITISH COMMONWEALTH LECTURE—Some Recent Progress in Air Survey with Special Reference to Newly Developed Territories. W. P. Smith. The Institution of Mechanical Engineers, 1 Birdcage Walk, S.W.1. 6 p.m. (Tea at 5.30 p.m.) *See summary.*

24th November
LECTURE—Heat and Mass Transfer in Aeronautical Engineering. Professor D. B. Spalding. Library, 4 Hamilton Place. 7 p.m.

26th November
THIRD LANCHESTER MEMORIAL LECTURE—Some Developments in Boundary Layer Research in the last Thirty Years. Professor Dr. H. Schlichting. Church House, Westminster, S.W.1. 6 p.m. (Tea at 5.30 p.m.) *See summary.*

27th November
MAN POWERED AIRCRAFT GROUP LECTURE—Man as an Aero Engine. Dr. D. R. Wilkie. Library, 4 Hamilton Place. 7 p.m.

1st December

LECTURE—Transonic Flow over Swept Wings. E. W. E. Rogers and Dr. I. M. Hall. 4 Hamilton Place. 7 p.m.

3rd December

MAIN LECTURE AT GLOUCESTER AND CHELTENHAM BRANCH—Some Servo-Mechanisms for Supersonic Aircraft. S. G. Glaze. St. Mary's College, Cheltenham. 7.30 p.m.

8th December

LECTURE—Some Practical Aspects of Compressor Blade Vibration. Dr. E. K. Armstrong and R. E. Stevenson. Library, 4 Hamilton Place. 7 p.m.

11th December

SYMPOSIUM ON FLIGHT SAFETY—All-day Discussion. Institution of Mechanical Engineers, Birdcage Walk, S.W.1. 9.45 a.m. *See Special Notice.*

AGRICULTURAL AVIATION GROUP LECTURE—Aerial Operations Planning in the United Kingdom: Results and Difficulties. Peter King. Library, 4 Hamilton Place. 7 p.m.

17th December

The Engineering Advantages of Rear Engines in Pure Jet Transport. E. S. Allwright. Institution of Mechanical Engineers, Birdcage Walk, S.W.1. 6 p.m. (Tea at 5.30 p.m.).

GRADUATES' AND STUDENTS' SECTION

20th November

Winter Dance. 4 Hamilton Place.

2nd December

Aerodynamics of Racing Cars. F. A. Costin. Library, 4 Hamilton Place. 7.30 p.m.

BRANCHES

16th November

Henlow—Flight Development of a Modern Prototype Aircraft. C. F. Bethwaite. The Assembly Hall, R.A.F. Technical College, Henlow. 7.45 p.m.

17th November

Christchurch—Lecture by Maurice Brennan. Kings Arms Hotel. 7.30 p.m.

Gloucester—Prospects for Space Flight in the Commonwealth. J. E. Allen. Wheatstone Hall, Brunswick Road. 7.30 p.m.

18th November

Coventry—General Aircraft Electrical Systems. G. G. Wakefield. Herbert Art Gallery. 7.30 p.m.

Preston—Aircraft Production Techniques. L. G. Burnard. R.A.F.A. Hall, Preston. 7.30 p.m.

Southampton—Supersonic Propulsion. Dr. R. R. Jamison. Engineering Lecture Theatre, Univ. of Southampton. 8 p.m.

Weybridge—Flight Testing at Supersonic Speeds. Wing Cdr. R. P. Beamont. Apprentice Training School, Vickers-Armstrongs (Aircraft) Ltd. 6.10 p.m.

20th November

Luton—Annual Dinner. Leicester Arms Hotel.

21st November

Hatfield—Visit to N.P.L.

24th November

Belfast—Film Night. Lecture Hall LG8, David Keir Building, Queens University. 7 p.m.

25th November

Bristol—The Training of a Production Engineer for the Aircraft Industry. Professor J. Loxham. Main Lecture Theatre, Faculty of Engineering, University of Bristol. 7 p.m.

London Airport—Air Traffic Control. L. Woodruffe. B.E.A. Viking Centre Cinema, London Airport. 6 p.m.

28th November

Halton—Annual General Meeting and Dinner. Branch H.Q., R.A.F. Halton. 3 p.m.

30th November

Henlow—Film Night. The Assembly Hall, R.A.F. Technical College, Henlow. 7.45 p.m.

1st December

Glasgow—Astronautical Navigation. P. H. Tanner. Royal College of Science and Technology. 7.15 p.m.

Luton—Junior Paper/Discussion Paper Evening. Napier Senior Staff Canteen, Luton Airport. 6.15 p.m.

2nd December

Bristol—Junior Members Paper Competition. Filton House. 6 p.m.

Preston—The Armstrong Whitworth Argosy. E. D. Keen. St. John's Ambulance Hall, Preston. 7.30 p.m.

Swindon—Man Powered Aircraft. B. S. Shenstone. The College, Victoria Road. 7.30 p.m.

3rd December

Gloucester and Cheltenham—MAIN SOCIETY LECTURE—Some Servo-Mechanisms for Supersonic Aircraft. S. G. Glaze. St. Mary's College, Cheltenham. 7.30 p.m.

Isle of Wight—Nuclear Radiation Applications in Industry. E. B. Bell. Clubhouse, Saunders-Roe Sports and Social Club, Church Path, East Cowes. 6 p.m.

7th December

Boscombe Down—Blind Landing. W. J. Charnley. Lecture Hall, A. & A.E.E. 5.30 p.m.

Derby—Mechanical Design Aspects of the R.A. 29. F. Morley. Rolls-Royce Welfare Hall, Nightingale Road. 6.15 p.m.

8th December

Luton—Young People's Lecture. A. W. Bedford. Luton College of Technology.

9th December

Belfast—The Bloodhound. D. J. Farrar. Lecture Hall LG8, David Keir Building, Queen's University. 7 p.m.

Brough—Deck Landing of Naval Jet Aircraft. Lt. Cdr. D. J. Whitehead. Royal Station Hotel Writing Room. 7.30 p.m.

Chester—Experiences of an Airline Pilot. Capt. O. P. Jones. Lecture Theatre, Grosvenor Museum. 7.30 p.m.

Christchurch—Saunders-Roe Hovercraft. D. Stanton-Jones. King's Arms Hotel. 7.30 p.m.

Hatfield—Wind Tunnels. J. A. Kirk. de Havilland Restaurant. 6.15 p.m.

Southampton—Experiences of the Trans-Antarctic Expedition. Wing Cdr. J. H. Lewis. Engineering Lecture Theatre, University of Southampton. 8 p.m.

Weybridge—R. K. Pierson Memorial Lecture. H. H. Gardner. Apprentice Training School, Vickers-Armstrongs (Aircraft) Ltd. 6.10 p.m.

10th December

Cheltenham—The Development of Automatic Landing for Civil Airline Operations. K. Fernside. St. Mary's College. 7.30 p.m.

11th December

Belfast—Annual Dance. Midland Hotel, Belfast.

14th December

Henlow—Presidential Address. R. Hills. The Assembly Hall, R.A.F. Technical College, Henlow. 7.45 p.m.

15th December

Bristol—Junior Committee Lecture. The Supersonic Airliner. R. G. Thorne. Filton House. 6 p.m.

16th December

Coventry—Film Evening. Herbert Art Gallery. 7.30 p.m.

Preston—The Next Generation of Civil Aircraft. G. H. Lee. Queen's Hotel, Lytham. 7.45 p.m.

17th December

Isle of Wight—Annual General Meeting and Film Show. Clubhouse, Saunders-Roe Sports and Social Club, Church Path, East Cowes. 6 p.m.

JOURNAL BINDING

Permanent Binding

1959 Volume (including packing and postage *in the United Kingdom*) .. .. .. £1 5s. 0d.

Previous Volumes (including packing and postage *in the United Kingdom*) .. .. £1 7s. 0d.

Journals, with a note of the name and address of the sender, should be sent direct to The Lewes Press, Friars Walk, Lewes, Sussex, and the remittance to the Secretary at the Offices of the Society.

Members are asked to be certain that the address to which they want their Journals sent is the same on their letters to the Lewes Press and to the Society.

COPY OF LETTER FROM CHIEF INSPECTOR OF TAXES BRANCH, INLAND REVENUE, DATED 17TH OCTOBER 1958
Reference: C.I./SUB/306

Dear Sir,

I have to inform you that the Commissioners of Inland Revenue have approved The Royal Aeronautical Society for the purposes of Section 16, Finance Act, 1958, and that the whole of the annual subscription paid by a member who qualifies for relief under that Section will be allowable as a deduction from his emoluments assessable to income tax under Schedule E of the whole of his annual change in the circumstances of the society should occur in the future you are requested to notify this office.

I should be glad if you would inform your members as soon as possible of the approval of the society. The circumstances and manner in which they may make claims to income tax relief are described in the following paragraphs, the substance of which you may care to pass on to your members.

Commencing with the year to 5th April 1959, a member who is an office holder or employee is entitled to a deduction from the amount of his emoluments assessable to income tax under Schedule E of the whole of his annual subscription to the society *provided that*—

(*a*) the subscription is defrayed out of the emoluments of the office or employment, *and*,

(*b*) the activities of the society so far as they are directed to all or any of the following objects—

(*i*) the advancement or spreading of knowledge (whether generally or among persons belonging to the same or similar professions or occupying the same or similar positions);

(*ii*) the maintenance or improvement of standards of conduct and competence among the members of any profession;

(*iii*) the indemnification or protection of members of any profession against claims in respect of liabilities incurred by them in the exercise of their profession;

are relevant to the office or employment, that is to say, the performance of the duties of the office or employment is directly affected by the knowledge concerned or involves the exercise of the profession concerned.

A member of the society who is entitled to the relief should apply to his tax office as soon as possible *after* 31*st October* 1958, for form P358 on which to make a claim for adjustment of his pay as you earn coding.

Yours faithfully,
(*signed*) T. DUNSMORE,
Senior Principal Inspector of Taxes.

ELECTIONS

The following is a list of elections and transfers of membership of the Society:—

Associate Fellows

Philip Bruce Atkins (*from Graduate*)
Greville Gordon Beale (*from Graduate*)
Geoffrey Bennett
Angus Lochiel Cameron
Frank Jones
Milton Lalas (*from Graduate*)
John David Roberts (*from Graduate*)
Owen James Stevenson (*from Graduate*)

Associates

Kevin Henry Knowles

Graduates

William Eric Bodley
James Dunstan Campbell
Yat Yung Chan
Robert Wallace Grant
Alan Douglas Sussex
Heinz Siegfried Weller

Students

Saeed Ahmed Khan Choudhry
Guy Nils Goodman
Christopher Martin Leech
George Brian Meadley
Thomas James Triggs
Donald John Woodman

NEWS OF MEMBERS

ROY ATKIN (*Graduate*) formerly in the Aerodynamics Department, Blackburn Aircraft, Brough, is now in the Advanced Projects Group, Hawker Siddeley Aviation, Kingston-on-Thames.

F. J. BRADBURY (*Associate Fellow*) formerly a Research and Development Engineer, Automotive Products Co. Ltd., is now Chief Engineer, Lockheed Precision Products Ltd.

H. BROWN (*Graduate*) formerly with Blackburn Aircraft Ltd., is now doing Postgraduate Research Work at Bristol University.

L. J. COATES (*Associate*) formerly Development Engineer, Hymatic Engineering Co., Redditch, has been appointed Experimental Officer, National Engineering Laboratory, Mechanisms and Metrology Division.

G. E. DAVIES (*Graduate*) formerly an Aerodynamicist on Stability and Control, de Havilland Aircraft Company Ltd., is now an Aerodynamicist, Light Aircraft Division, Short Brothers and Harland Ltd., Belfast.

H. J. DAVIES (*Associate Fellow*) of the Mathematics Department, University of Southampton, is now a Research Associate, James Forrestal Research Center on the Hovercraft Project, Princetown, New Jersey.

JOHN E. C. DICKISON (*Associate*) formerly at the Ministry of Supply, St. Giles Court has been posted to Guided Weapons Dept., Ballistic Missile Division, R.A.E.

J. DUNHAM (*Graduate*) formerly a Technical Assistant Rolls-Royce Ltd., Derby, has been elected a Junior Research Fellow, Pembroke College, Cambridge, and is working in the Engineering Laboratory of the University.

A. L. R. DZIWINSKI (*Graduate*) formerly Petroleum Laboratory Technician, Technical College, Henlow, is now an engineer, London office, de Havilland Propellers Ltd.

K. FEARNSIDE (*Associate Fellow*) formerly Technical Executive (Research), Smiths Aircraft Instruments Ltd., has been appointed Director of Research.

Wing Cmdr. A. E. FOSTER (*Associate Fellow*) formerly Group Engineer Officer, Air Headquarters, Malta, is now at R.A.F. Honington as Officer Commanding Technical Wing. (Correction to October Notices.)

D. J. FOSTER (*Graduate*) formerly an Aerodynamicist, Avro Aircraft Ltd., Malton, is now an Engineer, Performance Office, Atomic Power Division, English Electric Co. Ltd., Whetstone.

Flt. Lt. NORMAN GARDNER (*Associate Fellow*) formerly at the R.A.F. Technical College, Henlow, is now Officer Commanding Armament Squadron at Tengah, Singapore.

I. A. B. GAUNT (*Associate Fellow*) of the General Electric Company Ltd., has been appointed Project Engineer and Deputy Manager in Tokyo in connection with the construction of the Nuclear Power Station for the Japan Atomic Power Company.

A. NEIL GOBBY (*Graduate*) formerly with Hunting Engineering Ltd., at Luton Airport is now a lecturer in the Department of Aeronautical and Mechanical Design at Hatfield Technical College.

L. H. GOULD (*Associate Fellow*) formerly a Section Head, Stress Department, Avro Aircraft Ltd., Malton, is now with the Republic Aviation Corp., Farningdale, New York as a Specialist Stress Engineer, Research and Development Division.

J. C. GREEN (*Graduate*) formerly Technical Assistant, Stability and Control Section, Vickers-Armstrongs (Aircraft) Ltd., Winchester, is now an Engineer III, United Kingdom Atomic Energy Authority (Production Group), Capenhurst Works.

G. R. HAMPSHIRE (*Associate*) has left Aden Airways, Aden, and joined Air Links, Gatwick, as Chief Engineer.

J. C. HARDING (*Associate*) formerly Chief Flight Engineer, Airwork Ltd., in the Air Transport Division, is now Flight Test Engineer, Handley Page Ltd., Radlett.

J. F. HARRIMAN (*Associate Fellow*) formerly with Ericsson Telephones Ltd., is now Development Manager, Raleigh Industries Ltd., Nottingham.

The Journal of the Royal Aeronautical Society

WITH WHICH IS INCORPORATED THE INSTITUTION OF AERONAUTICAL ENGINEERS

VOLUME 63 NOVEMBER 1959 NUMBER 587

THE STRUCTURAL EFFECTS OF KINETIC HEATING

An All-Day Discussion on the Structural Effects of Kinetic Heating was held by the Society on 21st April 1959 at the Institution of Mechanical Engineers, Birdcage Walk, London S.W.1. Mr. M. B. Morgan, C.B., M.A., F.R.Ae.S., Deputy Director of the Royal Aircraft Establishment (now Scientific Adviser, Air Ministry) presided throughout the Discussion. Introductory papers were given by Mr. W. G. Heath, Mr. J. S. Przemieniecki, Ph.D., B.Sc., A.F.I.A.S., A.F.R.Ae.S., Mr. C. L. Bore, B.Sc.(Eng.), Grad.R.Ae.S. and Mr. A. J. Sobey, M.A. Miss M. E. Michael and Mrs. J. Bruce acted as rapporteurs for the Discussion.

Some Factors Affecting the Choice of Materials

by

W. G. HEATH

(Assistant Chief Structural Engineer, A. V. Roe and Co. Ltd.)

1. Introduction

For the purpose of this paper, certain fundamental parameters are assumed to be outside the control of the structures designer. It is, however, realised that the designer is often able to show that small changes in one or more of these parameters may have far-reaching effects.

These basic parameters include the aircraft size, weight, operating speed and altitude, aerodynamic characteristics and load factors. Fig. 1 shows how these combine together in various ways to give the loads acting on the structure, the temperature environment and the stiffness required to prevent aeroelastic disturbances.

At this stage the remaining specified parameter is introduced, that of service life. For a particular material this parameter, coupled with the loads and temperature conditions, establishes the stress levels which can be tolerated if undesirable fatigue and creep phenomena are to be avoided.

The structures designer is now in a position to review the various materials of which the properties are known. It is perhaps not unfitting at this juncture to point out that even in 1959 when the design and construction of a trans-Atlantic supersonic air liner is being seriously considered, tremendous gaps exist in our knowledge of material properties at elevated temperatures.

Two other considerations must not be overlooked. Firstly, any material which is considered must be available at the time and in the form (sheet, extrusions, forgings, and so on) which the design necessitates. Secondly, the workshops must be prepared to handle the material. This latter point will also influence the designer in his choice of the type of structure, which may involve the workshops in fabrication processes requiring heavy capital expenditure on new plant.

This paper considers how structural efficiency, stiffness, creep and fatigue may affect the choice of materials which are suitable for structures operating at temperatures up to 500°C. The main concern is with currently available materials, *i.e.* aluminium alloys, titanium alloys and steels. Brief reference is made to the problems of flight at temperatures up to 1,000°C.

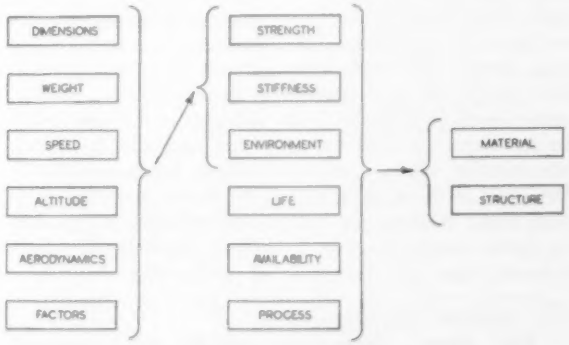

FIGURE 1. Factors affecting the choice of materials.

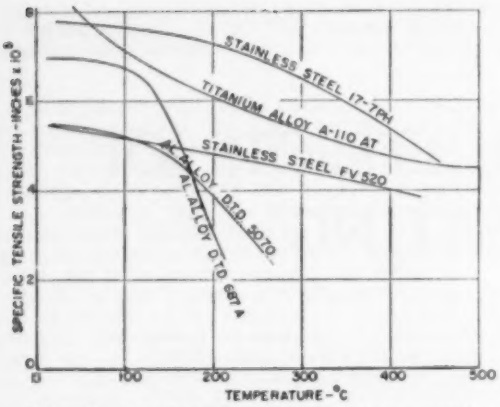
SPECIFIC TENSILE STRENGTH - INCHES x 10⁵
TEMPERATURE - °C
STAINLESS STEEL 17-7PH
TITANIUM ALLOY A-110 AT
STAINLESS STEEL FV 520
AL. ALLOY D.T.D. 5070
AL. ALLOY D.T.D. 687A

FIGURE 2. Specific tensile strength of sheet materials (10 hour soaking time).

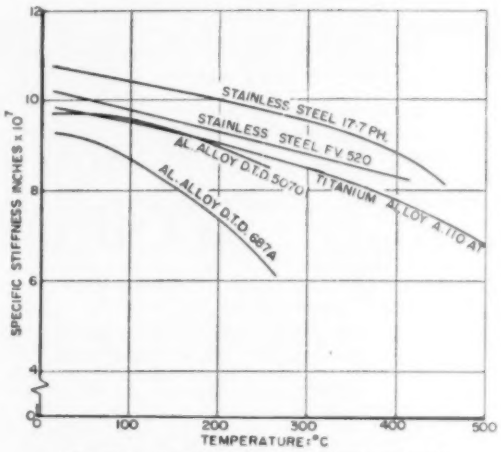

FIGURE 3. Specific stiffness of sheet materials (10 hour soaking time).

2. Structural Efficiency

2.1. GENERAL

Structural efficiency may be defined as a strength/weight or stress/density ratio having the units of length. For materials it is often quoted as the ratio of the ultimate tensile strength to the density and for fabricated components (especially compression panels) it is usually expressed as the load at failure divided by the weight per unit length or width.

The definition is extended slightly in this paper to embrace specific stiffness, *i.e.* the ratio of the elastic modulus to the density.

2.2. SPECIFIC STRENGTH

Most structural designers are familiar with curves of the type shown in Fig. 2, which depict the reduction of specific ultimate tensile strength (U.T.S./density) with increasing temperature. Usually several materials are represented and for a true comparison each material must have been "soaked" for the same period prior to testing.

Curves of this type suffer from several disadvantages, and because these have not always been fully appreciated the curves have often been misused. It is thus worthwhile to consider the various shortcomings of Fig. 2, so that its pitfalls may be avoided.

Very little of an aircraft structure is designed with tensile strength as the sole requirement. More than half of the structure has stability in either compression or shear as its criterion, and the requirements of stiffness, fatigue and creep play such an important part in the design of the remaining structure that tensile strength of itself is of little importance. There may be some use for these curves in the design of the short life missiles, where creep and fatigue are unimportant, but even in these cases the high speeds involved may well make stiffness an over-riding criterion. The use of curves similar to Fig. 2 without reference to other relevant data can therefore be misleading.

2.3. SPECIFIC STIFFNESS

For those components which are designed primarily by aeroelastic considerations, knowledge of the specific stiffness of the various materials can be of use. Fig. 3 shows a typical plot of this parameter, represented by the ratio of Young's modulus to density, plotted against temperature. It is of interest to note that the curves fall in a somewhat different pattern to those of Fig. 2.

2.4. SPECIFIC STABILITY

Since so much of the airframe is designed to be stable under compression and shear loads, it is convenient to consider a parameter which may be used to show the relative merits of various materials in withstanding loads of this type. Stability is essentially a stiffness problem, and at first it may be thought that the specific stiffness values of Fig. 3 are sufficient indication of how the various materials will behave when built up into, say, skin-stringer panels.

It is not difficult to show, however, that the structural efficiency of an element of a compression structure may be written as

$$\frac{P}{W} = C\left(\frac{P}{b}\right)^{\frac{1}{2}} \frac{(\eta E)^{\frac{1}{2}}}{\rho} \frac{I^{\frac{1}{2}}}{t}$$

where P critical load per unit width of element
W weight per unit area of element
C constant, depending on edge conditions, etc.
b leading dimension (length or width) of element
η plasticity reduction factor
E Young's modulus
ρ material density
I second moment of area per unit width of element
t effective thickness of element, *i.e.* thickness of single sheet having same weight.

The structural efficiency thus depends on three variables:—

(*a*) The structural index (P/b), which is a function

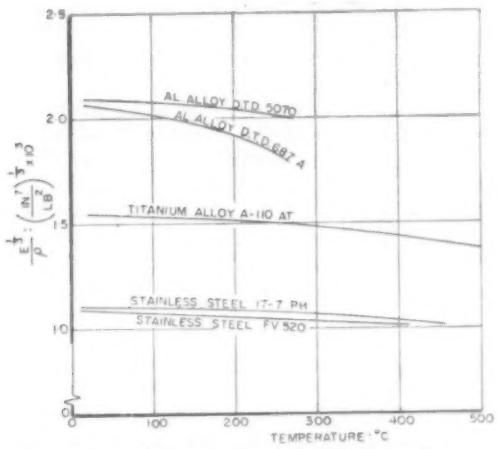

FIGURE 4. Stability parameter of lightly loaded plates (10 hour soaking time).

of the applied loading and the size of the element only.

(*b*) The material property parameter $(\eta E)^{\frac{1}{2}}/\rho$, which depends not only on the shape of the stress/strain curve but also on the stress level, since η varies with stress. The optimum stress is also a function of the structural index.

(*c*) The non-dimensional shape parameter $I^{\frac{1}{2}}/l$, which depends on the type of structural element considered (*e.g.* skin-stringer panel, honeycomb sandwich panel, and so on). The optimum value of this parameter is also a function of the structural index.

There is thus only one independent variable, which is the structural index. For low values of the index, the optimum stress is low and thus $\eta = 1$. For a given type of construction operating at low values of the structural index, the parameter $E^{\frac{1}{2}}/\rho$ is thus a guide to the efficiency of each material. A curve showing typical values of this "specific stability" plotted against temperature is given in Fig. 4. The order of merit of the various materials is quite different to that of the specific stiffness curves of Fig. 3.

For high values of the structural index, the efficiency is limited by the maximum allowable stress, which is taken as the compressive yield or 0·2 per cent proof stress, σ_2.

The maximum obtainable efficiency is thus σ_2/ρ, and a plot of this parameter against temperature is given in Fig. 5.

The two "specific stability" parameters discussed above are valid only at the low and high ends of the structural index scale respectively. The intermediate values are often those on which interest is focused, and these are considered in the next Section.

2.5. TYPE OF STRUCTURE

For compression structures in particular, it is well known that different types of constructions exploit the material properties to different degrees, depending on the value of the structural index. There thus arises the condition where a material exhibiting high values

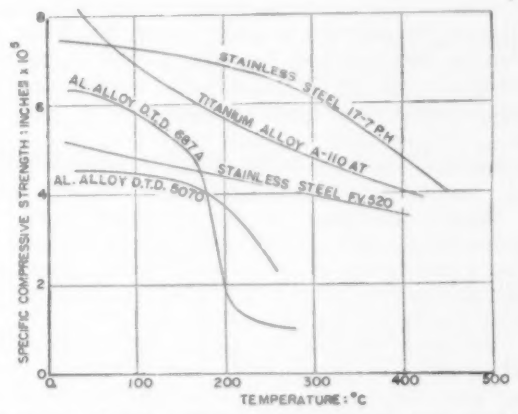

FIGURE 5. Specific compressive strength of sheet materials (10 hour soaking time).

of the "specific stability" parameters may yet give a very low efficiency if it is made into the wrong type of structure. This is particularly true at low to medium values of the structural index (values found, for example, in low aspect ratio wings) where the optimum stress is lower than the yield stress.

Consider, for example, Fig. 6 which shows the relative merits of two similar types of construction, honeycomb sandwich and corrugation sandwich, in three different materials after short-time soaking at 250°C. It is obvious that over a very wide range of values of the structural index, titanium honeycomb sandwich panels are by far the most efficient. But if this type of construction involves difficult workshop processes (as indeed it does) which preclude its use, what is the next most efficient construction? For certain values of the structural index it is certainly not titanium corrugation sandwich; in fact an aluminium corrugation sandwich may be slightly more efficient and a steel honeycomb sandwich considerably more efficient than the "obvious" alternative.

It is therefore concluded that the choice of the material and the type of structure must be made simultaneously, since these two results are mutually

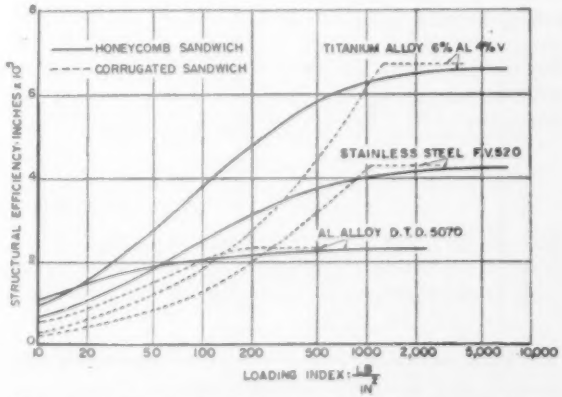

FIGURE 6. Structural efficiency of sandwich construction at 250°C.

dependent. They are also dependent on the configuration of the aircraft; in other words the choice of structure and material for one aircraft does not necessarily apply to another aircraft even though both may be operating at the same temperature.

3. The Effects of Time on Structural Design

3.1. INTRODUCTION OF TIME-DEPENDENT EFFECTS

When considering long-life structures, such as supersonic transport aircraft which will be expected to have a service life of up to 30,000 hours, allowance must be made for at least three time-dependent effects. These are fatigue, corrosion and creep.

The latter effect is new to the airframe designer, and information relevant to the materials, temperature and times of interest to him is scanty. Although fatigue and corrosion are familiar problems, little is known about the effects of high temperature on these phenomena, and even less about their interaction with creep.

3.2. FATIGUE

Fatigue damage depends as much on detail design and working stress level as it does on the basic material. Any assessment of the relative merits of the resistance of test coupons to fatigue must therefore assume that the same standard of detail design can be achieved in practice, no matter what type of construction is contemplated.

Test results from fatigue tests on simple specimens may be used to give a provisional comparison of the *S-N* curves of various materials. If these curves are also plotted as "specific fatigue strength" by dividing the alternating stress by the appropriate density (*see* Fig. 7) some idea can be gained of the relative efficiencies of the materials.

These simple tests will presumably be carried out under rapid fluctuations of stress at the required temperature. Long term tests should be performed in "real time" so that the effect of soaking time can be evaluated. In order to include the usual factor for scatter, periods of up to 100,000 hours (12 years) would be required for transport aircraft.

Within this fantastic time scale more useful results could be obtained by testing portions of actual structures under realistic conditions including transient heating and cooling, take-off, flight and landing loads and periods of rest. A supersonic transport aircraft may well be accumulating flying hours at almost the same rate as its fatigue test specimens—a very good reason for using "fail-safe" structures for such aircraft.

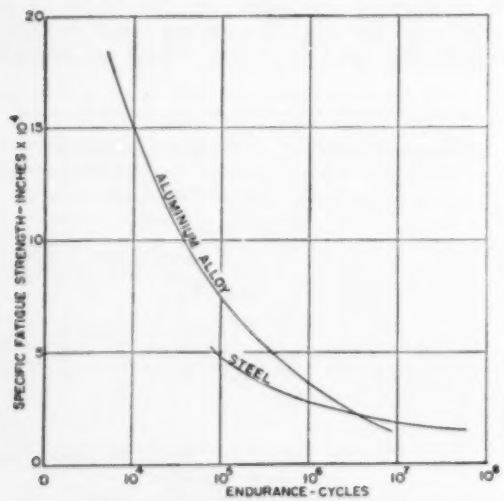

FIGURE 7. Specific fatigue strength. Alternating stress = mean stress.

3.3. CREEP

A criterion for evaluating the creep resistance of a particular material is difficult to define, since creep "damage" can take several forms. These include creep rupture, excessive creep deformation (which may lead to control and aeroelastic problems), and creep buckling of compression members.

Creep is dependent on both time and temperature and it is desirable to link these two together into a single parameter to enable direct comparisons of test results to be made. Larson and Miller[1] have proposed a relationship between tensile rupture time and temperature for a given constant stress in the form

$$T\,(a_1 + a_2 \log t) = \text{constant}$$

where T absolute temperature
a_1, a_2 constants
t time to rupture.

Recent tests by the N.A.S.A. have shown that a similar relationship holds good for the creep buckling of flat plates in compression.

A plot of rupture or buckling stress against the Larson-Miller parameter thus forms one simple guide to the creep resistance of materials. Such a curve is shown in Fig. 8, using specific stress for the vertical scale.

Similar curves may also be drawn for creep in bearing and shear so that the deformation of typical joints may be studied. Fig. 9 shows such a joint,

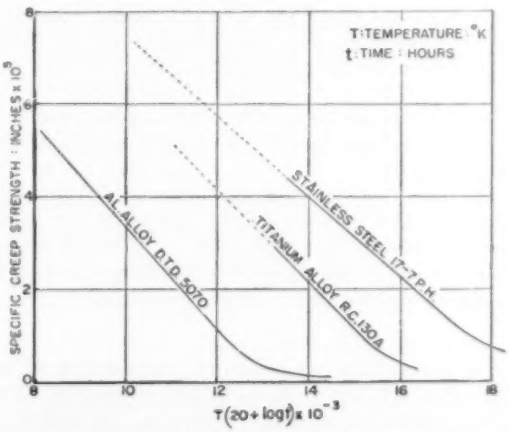

FIGURE 8. Specific creep strength of sheet materials (one per cent creep deformation).

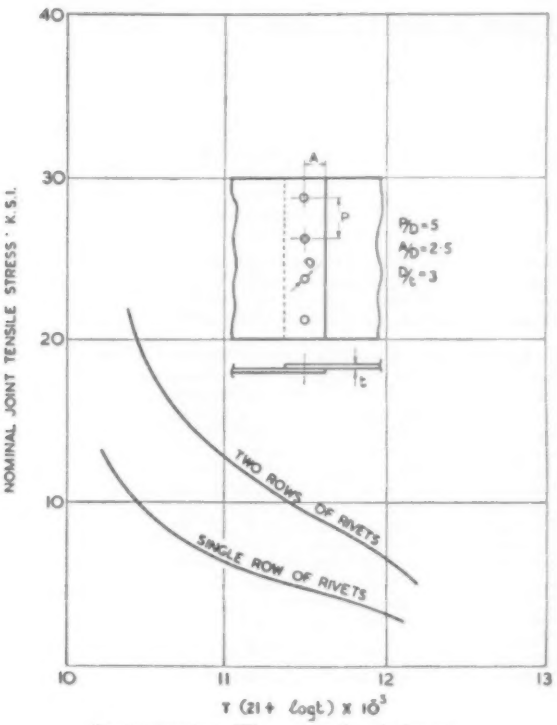

T = temperature °K. t = time in hours.

FIGURE 9. Creep strength of riveted joints. Matl: 2024-T3 (8 per cent rivet deformation).

together with a curve of stress plotted against time required to produce either rupture or 8 per cent (of rivet diameter) deformation. This type of creep deformation can give rise to serious structural troubles, such as looseness of connections and excessive displacements of components.

The various types of stress—tension, bearing and shear—which are present in such a joint must be carefully balanced so that all produce similar rates of creep.

The Larson-Miller relationship holds good only if no metallurgical transformations (*e.g.* precipitation) occur during the soaking period. Both extrapolation and interpolation may be misleading if such changes are likely. There is no reliable substitute for creep tests at the temperature and for the time under consideration.

Like fatigue, the full effects of creep can be assessed only by reference to the load spectrum for the particular aircraft in question. For transport aircraft operating at around a Mach number of 2, studies show that creep may well entail a restriction on the use of aluminium alloys, since short bursts of overspeeding and excess g can produce large creep deformations.

Unlike fatigue, however, creep "damage" is partially recoverable when the applied loads are removed. The extent of this recovery is a matter for controversy, and at this time it is not proposed to discuss this phenomenon.

3.4. INTERACTION OF CREEP AND FATIGUE

Evidence regarding the effects of fatigue loading on creep are conflicting; some results suggest a deterioration in creep properties due to the superimposition of an alternating stress while others suggest an improvement. It is clear that, at present, these two time-dependent phenomena must be considered separately.

4. New Materials

As the design temperature increases the well-known alloys of aluminium, titanium and steel gradually disappear from the field of usefulness, and as temperatures of the order of 1,000°C are approached new materials must be found.

Molybdenum shows considerable promise but it oxidises easily and the oxide is volatile, so that the metal burns away. Chromium plating appears to provide a reasonable surface protection against this catastrophe. At 1,000°C, the 0·5 per cent titanium alloy has a specific stiffness similar to that of the aluminium alloys at room temperature; its "specific stability" values are considerably lower, however, and creep is likely to be the design criterion for quite short soaking times.

Other possible materials include niobium and the cermets and carbides. So little information is available on these materials that comment is valueless; one can only bear them in mind as "possibles" until research reveals their true place in the scheme of things.

5. Conclusion

Simple curves relating the specific strength, stiffness and stability of materials to temperature and soaking time have a limited usefulness. The information they present is often conflicting and the designer may be misled if undue emphasis is placed on one particular aspect.

The final choice of material is strongly linked to the type of structure, and both of these may be considerably influenced by the availability of the material and the workshop processes entailed.

Much more research is needed into the time-dependent effects of creep and fatigue. Over-simplified laboratory tests may give optimistic results when compared with realistic programmed tests on aircraft components, and the choice of any particular material will be ultimately justified only by full operational flying.

ACKNOWLEDGMENTS

The author is indebted to A. V. Roe and Co. Ltd. for permission to publish this paper, and to Mr. G. C. J. Larroucau for his assistance in its preparation.

REFERENCE

1. LARSON, F. R. and MILLER, J. (1952). A Time-Temperature Relationship for Rupture and Creep Stresses. *Trans. A.S.M.E.*, Vol. 74, p. 765, July 1952.

Design of Transparencies

by

J. S. PRZEMIENIECKI, Ph.D., B.Sc., A.F.I.A.S., A.F.R.Ae.S.

(*Bristol Aircraft Limited*)

SUMMARY:— A study of engineering problems encountered in the design of transparencies for supersonic aircraft is presented with a special emphasis on the effects of kinetic heating. The paper is written primarily with optical transparencies in mind but many of the general principles discussed are equally applicable to the design of radomes for elevated temperature applications.

The first parts of the paper consider briefly the methods of calculating temperature distribution in transparent panels subjected to kinetic heating (or cooling) and this leads naturally to discussion of the effects of the non-uniform temperature distribution, differential expansion and the edge restraints preventing thermal deformations. Methods of calculating thermal stresses are suggested through the concept of the "self-equilibrating" temperature distribution; the main attention, however, being concentrated on the derivation of simple engineering formulae rather than on the mathematical rigour of the solution.

The choice of design cases for combined pressure and thermal loading is considered and it is shown that, in general, deceleration manoeuvres combined with outward pressure constitute the design criteria for transparencies. The effects of various parameters on the magnitude of thermal stresses are analysed; these include the effects of altitude, temperature, deceleration and material properties. It is shown that, for given material and panel geometry, the thermal stresses depend mainly on the following parameters: total temperature change, acceleration (or deceleration), and the Biot number based on the panel thickness.

Practical design aspects are also considered, such as choice of materials, strength, panel geometry, mounting of panels and the fail-safe design. Finally, testing of transparencies under pressure and thermal loading is briefly discussed, together with possible methods of strain measurements, and a tentative proving procedure for transparencies is suggested.

1. Introduction

In the design of supersonic aircraft serious consideration must be given to the elevated temperature effects on the transparent materials for window panels and windscreens. The temperature limitation of the present organic plastics imposes severe restrictions on the use of these materials above 80°C. For higher temperatures, glass or fused silica are the alternative materials that may be used; their use, however, creates many engineering problems, largely unexplored, particularly those concerned with thermal effects due to aerodynamic heating and cooling and the safe working stress in the material.

As its principal aim, this paper attempts to present a study of engineering problems encountered in the design of transparencies for supersonic aircraft with a special emphasis on the effects resulting from kinetic heating. Some of the problems discussed are naturally common to all types of structures for high temperatures, others are peculiar only to transparencies treated as structural components.

The design of transparencies for supersonic aircraft poses a difficult and challenging problem to the structural engineer. The material selected must satisfy many requirements, some of which are conflicting; it must be capable of withstanding pressures arising from aerodynamic loading and cabin pressurisation, rapid aerodynamic heating or cooling, heat from de-misting and de-icing systems, and finally impact and erosion, especially from rain and hail. For transparencies designed for space travel additional requirements may be added: resistance to erosion caused by meteoritic dust and adequate protection from radiation hazards.

The paper is written primarily with optical transparencies in mind—with a special emphasis on the design of flat panels—but many of the general principles discussed are equally applicable to the design of curved panels or radomes.

A number of controversial points will most certainly be raised and if the material presented here is sufficient to spark professional argument and lead eventually to a clearer understanding of the design problems of transparencies for elevated temperatures, the main purpose of this paper will be realised.

NOTATION

x, y, z	rectangular co-ordinates (z is measured from the middle surface)
d	panel thickness
a, b	panel dimensions
L	distance from the transition point
t	time
E	Young's modulus
α	coefficient of thermal expansion
ν	Poisson's ratio
k	thermal conductivity
ρ	density
c	specific heat
κ	thermal diffusivity $= k/\rho c$
ε	surface emissivity
c_p	specific heat of air at constant pressure
ρ_a	density of air
V	velocity
σ	Stefan-Boltzmann constant in the radiation law

$D = Ed^3/12(1-\nu^2)$
f_x, f_y stresses in the x- and y-directions respectively
s tensile strength (or modulus of rupture)
w panel deflection in the z-direction
p pressure
T_{w0} adiabatic wall temperature
T_s surface temperature
T_a ambient temperature
T_i initial temperature
T_0 steady state temperature
T temperature distribution through the panel thickness $= T(z, t)$
T_m mean temperature, defined by equation (14)
ΔT temperature gradient, defined by equation (15)
T^* self-equilibrating temperature distribution, defined by equations (12) and (13)
Q heat input
h convective heat transfer coefficient
B Biot number $= hd/k$
M Mach number
Re Reynolds number
St Stanton number
R_b boundary resistance (analogue circuit)
V_{w0} applied voltage proportional to T_{w0} (analogue circuit)
F Airy stress function
w_j the jth root of equation (11)
β_x, β_y parameters defined by equation (19)
ϕ parameter defined by equation (23)
$\gamma_m = m\pi b/2a$

∇^2 Laplace operator $= \dfrac{\partial^2}{\partial x^2} + \dfrac{\partial^2}{\partial y^2}$

∇^4 biharmonic operator $= \dfrac{\partial^4}{\partial x^4} + 2\dfrac{\partial^4}{\partial x^2 \partial y^2} + \dfrac{\partial^4}{\partial y^4}$

2. Design Requirements

The main function of optical transparencies is to provide an adequate field of vision to enable the pilot to control the aircraft and while it is possible to imagine an aircraft flying optically blind, some restricted field of vision must always be provided for take-off and landing or for emergency.

In the early days of aviation no optical transparencies were needed except perhaps for a pair of goggles worn by the pilot who usually had an excellent, unobstructed view, in practically all directions. As aircraft speeds increased and pressurised fuselages were introduced, the need for an enclosed cockpit became essential and this led to the present form of windscreen assemblies and cabin windows. A typical windscreen assembly of a large subsonic aircraft is shown in Fig. 1; here large quadrilateral transparency panels are used and the field of view is generally good. On smaller aircraft the bubble type canopy became a characteristic feature, as illustrated in Fig. 2. For supersonic aircraft, operating at elevated temperatures, transparencies consisting of relatively small flat panels supported in a metal framework must be used. Thus some restriction of the field of vision must inevitably be expected. All panels would be duplicated and have bevelled edge type mounting to give a flush external finish and to avoid unnecessary edge restraints. Naturally it is also possible to use curved panels, and it has already been tried in one British supersonic aircraft, but the inherent difficulties in the manufacture, and the high thermal stresses arising from the edge restraints on the curved boundaries, make this type of construction rather an unattractive proposition.

The requirements for passenger windows are altogether different. Windows are provided mainly for psychological reasons and it is therefore not unreasonable to assume that future airlines and passengers could be educated to accept supersonic air liners without any windows in the passenger compartments. This would undoubtedly remove, at the same time, many difficult problems in the design of pressurised fuselages with numerous cut-outs, and a greater structural safety and economy would be ensured. Of course, a splendid view from a passenger seat of a supersonic air liner flying at a Mach number of 2 or 3 may present an additional attraction for the potential passengers; but surely, this small asset could be easily sacrificed for the sake of safety and economy of the structure. A closed circuit television camera could provide a reasonable view to reassure any passengers suffering from claustrophobia; or they could use slower aircraft with conventional windows.

Public reactions to windowless air liners could be tested now so that any decisions affecting window transparencies for future generations of supersonic air liners

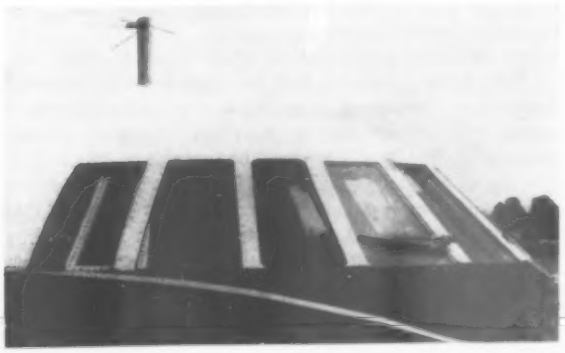

FIGURE 1. Windscreen structure of a large subsonic aircraft.

FIGURE 2. Typical bubble type canopy.

would be formulated accordingly. However this could only be done with the co-operation of a scheduled airline willing to undertake this particular investigation.

3. Aerodynamic Heating or Cooling of Transparencies

The temperature of a transparency can be affected by any of the following:

(*i*) Change in ambient temperature (*i.e.* change in altitude).
(*ii*) Kinetic heating or cooling.
(*iii*) Solar radiation.
(*iv*) De-icing or de-misting methods involving heat.
(*v*) Cabin heating or cooling.

It appears, however, that if a supersonic aircraft is designed to operate at Mach numbers greater than two only the first two causes are of primary importance in the calculation of temperature distribution for design purposes. Attention must be paid also to the proper design of de-icing and de-misting systems to avoid any likelihood of thermal conditions which are worse than those arising from kinetic heating and changes in altitude.

To determine the effects of kinetic heating and rapid changes in altitude on a transparent panel, a knowledge of the temperature distribution as a function of space and time is required for the panel itself and for the surrounding structure. Since the thermal conductivities of materials proposed for elevated temperature transparencies are relatively low, changes in speed and/or altitude produce transient temperature gradients through the thickness of a panel. Therefore all transparent panels may be referred to as "thermally thick" panels for which the heat flow through the thickness must be considered.

3.1. BASIC EQUATIONS FOR HEAT TRANSFER

If an aircraft is accelerated to a high speed, then all external surfaces are heated aerodynamically and the heat input Q per unit surface area is given by

$$Q = h(T_{w_0} - T_s) - \varepsilon\sigma T_s^4 \quad . \quad . \quad (1)$$

where the first term on the right hand side represents forced convection heating (kinetic heating) and the second term is the radiation heat loss from the surface at the temperature T_s.

The so-called adiabatic wall temperature T_{w_0} is a temperature which would be attained at a surface in equilibrium without any radiation losses; it depends mainly on the local ambient temperature T_a, the Mach number M, and the type of boundary layer. It can be calculated simply from:

$$T_{w_0} = T_a(1 + 0{\cdot}167\,M^2) \quad . \quad . \quad . \quad . \quad (2)$$

for laminar boundary layer

and $$T_{w_0} = T_a(1 + 0{\cdot}178\,M^2) \quad . \quad . \quad . \quad . \quad (3)$$

for turbulent boundary layer

The convective heat transfer coefficient h will be discussed in greater detail in Section 3.2.

The relative importance of the radiation term increases with altitude and temperature. However, since the critical design cases for thermal loading on transparencies usually represent deceleration manoeuvres at low altitudes, as will be shown later, the radiation term can be neglected, at least as a first approximation.

The heat input density due to kinetic heating (or cooling) of a panel is approximately uniform and therefore conduction of heat in the panel can be assumed to proceed mainly in the direction normal to the surface, say the z-direction, and thus the problem reduces to finding the solution of the heat conduction equation in one dimension, *i.e.*,

$$\frac{\partial}{\partial z}\left(k\frac{\partial T}{\partial z}\right) = \rho c\frac{\partial T}{\partial t} \quad . \quad . \quad . \quad (4)$$

If, however, thermal conductivity is independent of temperature, the above equation reduces to the well-known diffusion type equation

$$\frac{\partial^2 T}{\partial z^2} = \frac{1}{\kappa}\frac{\partial T}{\partial t} \quad . \quad . \quad . \quad (5)$$

where $\kappa = k/\rho c$ is the thermal diffusivity.

To obtain a complete solution to equation (5) boundary conditions are required at the outer and inner surface. The boundary condition at the outer surface, which can be either heated or cooled depending on whether T_{w_0} is greater or less than T_s, can be expressed as

$$k\frac{\partial T}{\partial z} = h(t)\,[T_{w_0}(t) - T]; \quad z = d/2 \quad . \quad (6)$$

where for convenience the z-direction is measured from the middle surface towards the outer surface. In this boundary condition the rate of heat absorption (or loss) by the material at the outer surface is equated to the rate of heat gain (or loss) by forced convection. For the second boundary condition, one can assume that either the surface is insulated, in which case

$$\frac{\partial T}{\partial z} = 0; \quad z = -d/2 \quad . \quad . \quad (7)$$

or, if the panel is in perfect thermal contact with another panel,

$$k_1\frac{\partial T_1}{\partial z} = k_2\frac{\partial T_2}{\partial z}; \quad z = -d/2 \quad . \quad (8)$$

where suffixes 1 and 2 refer to the two panels in contact.

This latter condition may be used if the transparent panel is of laminated type, such as a laminated glass panel with an interlayer of vinyl or other similar material. Sometimes it may be necessary to provide cooling of the inner surface. The boundary condition would then express the balance between the heat loss from the surface and the heat extracted by the cooling air. In the general discussion that will follow, however, only the boundary condition of zero heat transfer, *i.e.* equation (7), will be used; this forms a suitable design assumption and leads generally to conservative designs (*see* Section 7.1.).

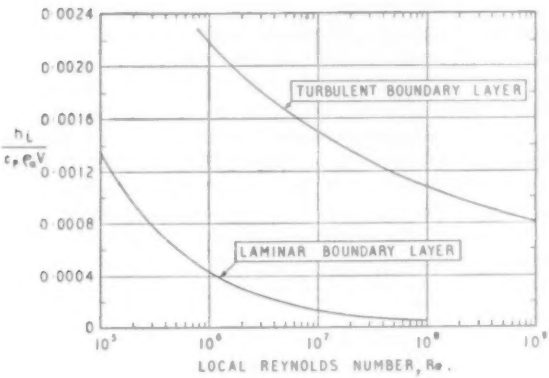

FIGURE 3. Variation of local heat transfer coefficients for laminar and turbulent boundary layers in incompressible flow.

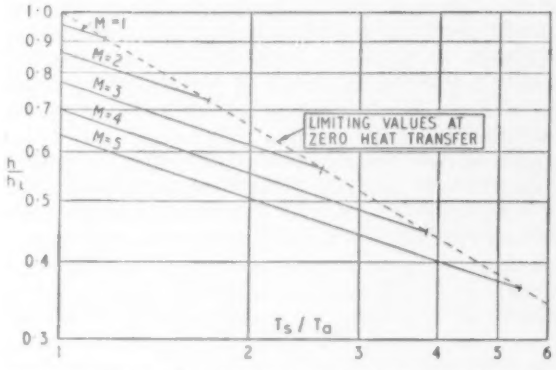

FIGURE 4. Variation of local heat transfer coefficient for turbulent boundary layer in compressible flow (h_i = incompressible value).

3.2. CONVECTIVE HEAT TRANSFER COEFFICIENT

The convective heat transfer coefficient h is determined from the following equation

$$h = St\,(Re, M, T_s/T_a)\,c_p \rho_a V \quad . \quad . \quad (9)$$

where St is the Stanton number, c_p is the specific heat of air at constant pressure, ρ_a is the air density and V is the velocity of air; all these quantities being evaluated for the aerodynamic conditions just outside the boundary layer. The product $c_p \rho_a V$ for any given flight manoeuvre is a known function of time since it depends only on the variation of altitude and speed and c_p can be taken as a constant. The Stanton number St varies not only with the Reynolds and Mach numbers, which are known functions of time, but also with the ratio of external surface temperature to ambient temperature, (T_s/T_a). This latter dependence is more pronounced if the boundary layer is turbulent; it also introduces non-linearity into the boundary condition at the external surface.

A convenient way of determining the heat transfer coefficient is to calculate first its incompressible flow value h_i which depends only on the Reynolds number Re and then to calculate its compressible flow value h from the variation of h/h_i with the Mach number M and the temperature ratio T_s/T_a.[11]

The variation of the incompressible heat transfer coefficients has been plotted in Fig. 3, which shows that h_i is a decreasing function of Re. For laminar boundary layers it would be sufficiently accurate to use h_i instead of the compressible value h; this would give values of h on the high side, but it should not be more than 10 per cent too high for Mach numbers up to 4. For turbulent boundary layers compressible flow formulae must be used since h decreases appreciably with an increase in the Mach number or the temperature ratio T_s/T_a, as shown in Fig. 4. A perusal of Fig. 4 indicates clearly that only for small variations in M and T_s/T_a, the assumption of a constant heat transfer coefficient may be justified. In general, however, variable heat transfer coefficients should be used for calculations on transparencies.

Since it may not always be possible to maintain laminar boundary layers over transparencies, turbulent flow formulae should be used for design purposes. It should be mentioned, however, that the main difficulty in calculating h_i (*see* Fig. 3) is the determination of the effective Reynolds number Re. The equation used for producing Fig. 3 is essentially a flat plate formula for which Re is based on the distance from the transition point which may be particularly difficult to determine on transparencies. To overcome this difficulty the effective transition point for design purposes could be assumed to be one to two feet forward from the edge of the panel; this would probably ensure that the estimate for the heat transfer coefficient is conservative. Experimental data in this field would be extremely valuable.

3.3. METHODS OF SOLUTION OF THE HEAT CONDUCTION EQUATION

The following methods can be used for calculating transient temperature distributions in thermally thick panels:

(*i*) Analytical methods.
(*ii*) Numerical methods.
(*iii*) Semi-numerical methods.
(*iv*) Analogues.

Each of these methods will be discussed briefly and possible methods of solutions will be suggested for calculating transient temperatures in transparencies.

Several objections may be made to the use of the analytical methods. Firstly, solutions may not be sufficiently realistic due to the various simplifications which are necessary to get any solution at all; secondly, the analytical expressions are usually extremely complicated for practical applications; and thirdly, the analytical solutions usually converge poorly near $t=0$ unless special asymptotic solutions are used for small values of time.

The arbitrary variation of h and T_{w_0} with time and also the dependence of h on temperature, rules out any possibility of a successful analytical solution for the temperature distribution through the thickness of a transparency panel. It should, however, be emphasised that in many cases sufficient engineering accuracy may

be achieved with constant average values of the heat transfer coefficient h for which analytical solutions are available. In particular, these methods could be used if only a study of the effects of various parameters is required in the preliminary design rather than an accurate quantitative study.

The temperature distribution through a thermally thick panel for suddenly increased (or decreased) adiabatic wall temperature from T_i to T_0 and for constant heat transfer coefficient is given by:

$$\frac{T-T_i}{T_0-T_i}=1-2\sum_j \frac{\sin w_j \cos w_j\left(\frac{1}{2}+\frac{z}{d}\right)}{(w_j+\sin w_j \cos w_j)} \exp\left(-w_j^2\frac{\kappa t}{d^2}\right) \quad . \quad . \quad . \quad . \quad . \quad . \quad . \quad . \quad (10)$$

where w_j is the jth positive root of the transcendental equation

$$w_j \tan w_j = hd/k \quad . \quad . \quad . \quad (11)$$

The above formula for temperature can also be applied to the case of arbitrary variation of T_{w0} by using the Duhamel's integral.

The numerical methods are based essentially on step by step integration of the equation of heat conduction. These methods have the additional advantage over analytical methods that the variation of thermal properties of the material with temperature and the temperature dependence of the heat transfer coefficient can be included. Similarly any radiation losses and other non-linear effects, *e.g.* free convection, can be included in the solution. Numerical methods applied to heat transfer problems are, in general, time-consuming and require relatively small intervals of time. However, they can be programmed for automatic computation and several such programmes for digital computers are already in existence.

Semi-numerical methods are basically repetitive applications of the exact analytical solution to the response to triangular variation of T_{w0} over a relatively large time interval. This is possible because of the linear character of equations (5), (6) and (7). In these methods, the heat transfer coefficient h is usually approximated as a step function. A semi-numerical method has been described by Hill[2] and the design charts for the application of this method to thermal stress problems in thermally thick plates have been prepared at Bristol[3]. The semi-numerical methods are very rapid and are suitable for computation on desk machines; in general, they are preferable to numerical methods[4].

There are three main types of analogue computers which can be used for calculating temperature distributions in transparencies:

(*i*) Resistance-capacitance network.[5]
(*ii*) General purpose analogue computer (differential analyser).
(*iii*) Pure resistance network.

To discuss the relative merits of various types of computers would be beyond the scope of the present paper; only the basic features of each type will be indicated.

The basic principles of the resistance-capacitance analogue and the differential analyser are similar; the main difference is that in the resistance-capacitance network actual resistances and capacitances are used in each space element while in the differential analyser amplifier units are used for that purpose. On the one hand the accuracy of the differential analyser is generally better than that of the simple resistance-capacitance network. On the other hand the resistance-capacitance analogue is considerably cheaper to construct. Both types use finite differences in space only; time variations are continuous and are therefore suitable for automatic plotting.

The pure resistance network has the advantage of somewhat greater flexibility and versatility since it can handle temperature-dependent coefficients. Its major disadvantage arises from the fact that this type of analogue uses finite differences not only in space but, also, in time, so that unless automatic procedures are used to set up the starting conditions for each time increment the solution of a problem of any size is a lengthy process.

It appears, however, that the resistance-capacitance analogue has certain advantages. In particular, it allows continuous plotting of temperature-time variation and the resulting thermal stress at any point through the thickness of the panel. An analogue computer of the resistance-capacitance type has been built and successfully operated at Bristol Aircraft Limited for routine calculations of temperature distributions in one- or two-dimensional structural components subjected to aerodynamic heating or cooling. The particular application of this analogue to transparent panels will be discussed in Section 3.4.

3.4. THE BRISTOL RESISTANCE-CAPACITANCE ANALOGUE

The resistance-capacitance analogue computer is based on the fundamental similarity of the conductive heat flow within a homogeneous body to that of the charge in a non-inductive electric circuit. The ideal analogue with distributed capacitance must be replaced by a "lumped" system and in that sense the method is similar to the solution of the differential equation of heat flow by finite differences except that, unlike any numerical method based on finite differences, this analogue gives a continuous variation of temperature with time.

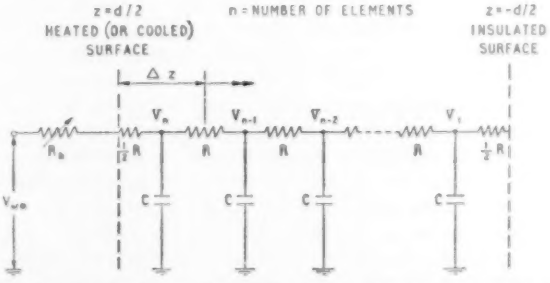

FIGURE 5. Analogue circuit for kinetic heating (or cooling) of thermally thick panels *e.g.* transparencies.

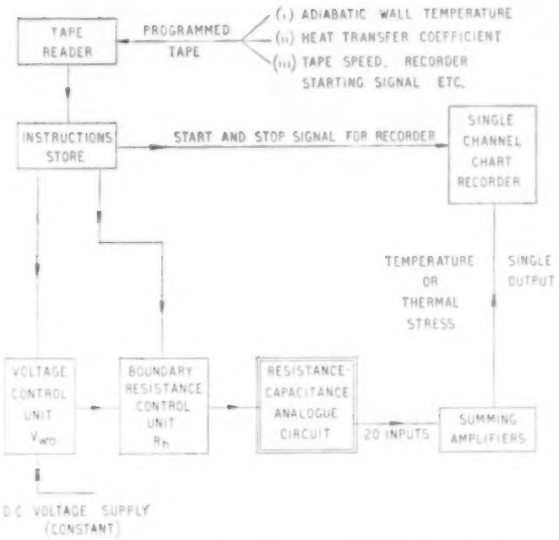

FIGURE 6. Block diagram for kinetic heating analogue.

A typical circuit used at Bristol for solving equation (5) with the boundary conditions (6) and (7) is shown in Fig. 5. Heat storage effects are represented by electrical condensers C, while the electrical resistances R simulate the thermal resistance of the panel. The input voltage V_{w_0} is made proportional to the absolute value of $T_{w_0} - T_i$ while R_b is made inversely proportional to the convective heat transfer coefficient h. By suitable choice of the scale factors this analogue circuit can be operated at any convenient voltages and time intervals.

The variable voltage input V_{w_0} and the boundary resistance R_b are generated in an electro-mechanical control unit operated by a programmed paper tape. A block diagram showing the basic components of the Bristol analogue, connected up for temperature investigation in transparencies, is shown in Fig. 6. The correct variation of $R_b \propto 1/h\,(Re, M, T_s/T_a)$ to be programmed on tape can only be obtained by successive approximations, since the variation of T_s/T_a with time is unknown. This can be achieved by estimating approximately variation R_b with time, operating the analogue while recording the voltage V_s (proportional to the surface temperature T_s) and then re-evaluating h using the variation of T_s obtained on the analogue. In general, one such iteration would be quite sufficient for engineering purposes. However, to avoid the difficulty of the iterative procedure, particularly where a large number of different flight programmes is to be investigated, the following simplified approach has been used.

Consider a typical variation of h with time for either accelerated or decelerated flight at a constant altitude by taking (1) $T_s = T_{w_0}$ and (2) $T_s = T_i$; these two variations are shown in Figs. 7 and 8. The correct variation of h must lie between the curves (1) and (2) (dotted curve). Thus for the successive approximation one could start from either of the two curves. Alternatively two programmed tapes could be prepared: one for $T_s = T_{w_0}$ and the other for $T_s = T_i$. The analogue computer is then operated using the two tapes in turn and all the required voltages are recorded for the two variations in h. Mathematically this means that upper and lower limits for the temperature distribution are obtained by this procedure; these limits in general will differ by not more than 10 per cent which is quite sufficient for the preliminary calculation. If necessary, a second approximation could be used for a few selected cases.

A single channel recorder was used on the Bristol analogue, but more recorders could be connected if required. Up to a maximum of 20 separate outputs can be taken from the analogue network via cathode followers to four summing amplifiers which in turn may be coupled or used separately. The final output voltage from the summing amplifiers can be either the tempera-

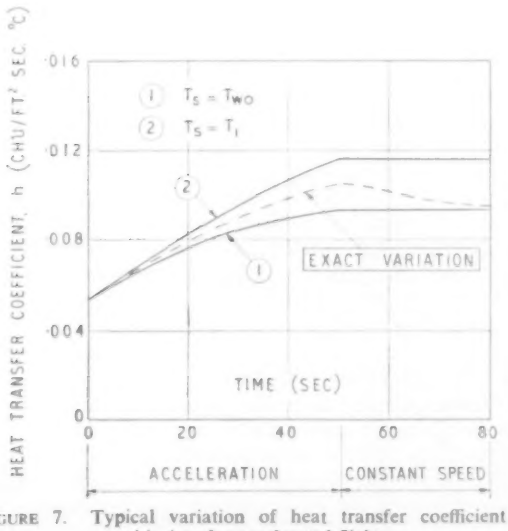

FIGURE 7. Typical variation of heat transfer coefficient h with time for accelerated flight.

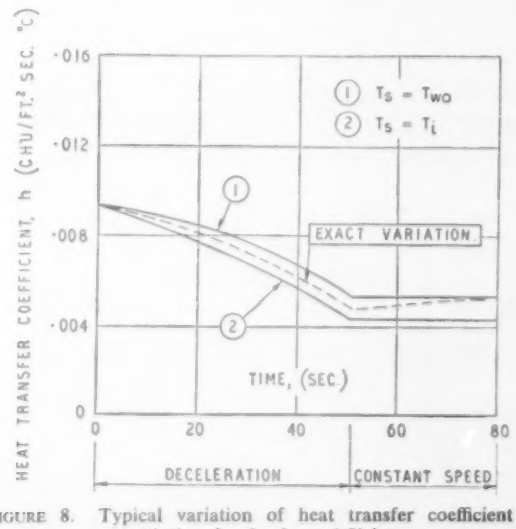

FIGURE 8. Typical variation of heat transfer coefficient h with time for decelerated flight.

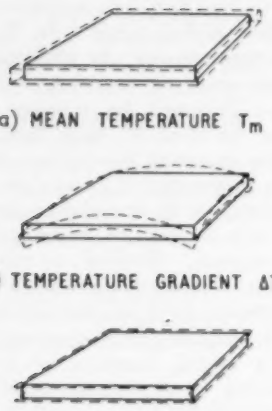

FIGURE 9. Thermal deformations of a flat rectangular panel due to $T = T_m + \Delta T\,(z/d) + T^*$, all edges unrestrained.

ture-time variation at a selected point or the summation $\sum_{n=1}^{20} a_n T_n$ where $-1 \leqslant a_n \leqslant +1$ and T_n is the temperature of the nth point. The latter variation is particularly important since it can be made proportional to the thermal stress in a transparency.

4. Thermal Deformations; "Self-equilibrating" Temperatures

The temperature distribution $T(z, t)$ through the thickness of a panel can be separated into linear and "self-equilibrating" temperature distributions, namely

$$T(z,t) = T_m(t) + \Delta T(t)\frac{z}{d} + T^*(z,t) \quad . \qquad (12)$$

where $T_m(t)$ is the mean temperature, $\Delta T(t)$ is the linear temperature gradient and $T^*(z, t)$ is the self-equilibrating temperature distribution for which

$$\int_{-d/2}^{d/2} T^* dz = \int_{-d/2}^{d/2} T^* z\, dz = 0 \quad . \quad . \qquad (13)$$

Thus only the first two terms on the right hand side of equation (12) contribute to the overall deformation of the panel whereas the T^* distribution, being self-equilibrating, produces zero resultant deformations. T_m and ΔT terms produce thermal stresses only in the presence of edge restraints while stresses due to T^*, away from the edges, are not affected by the edge restraints and they occur even if all edges are completely free.

Using now equations (12) and (13) it follows that the two linear temperature components are given by

$$T_m(t) = \frac{1}{d}\int_{-d/2}^{d/2} T\,dz \quad . \quad . \quad . \qquad (14)$$

and

$$\Delta T(t) = \frac{12}{d^2}\int_{-d/2}^{d/2} T z\, dz \quad . \quad . \qquad (15)$$

Alternatively, ΔT could be obtained by equating the first moment of the temperature $T(z, t)$ to the first moment of the $\Delta T(t)\, z/d$ distribution about the middle plane.

Figure 9 shows the overall thermal deformations on a rectangular panel with free edges; it also illustrates well how the thermal stresses arise in a panel as the result of edge restraint from the surrounding structure. The mean temperature T_m gives overall expansion in the plane of the panel, the temperature gradient ΔT bends the panel into a spherical surface, while the self-equilibrating temperature distribution T^* produces no overall deformation. (However, some small "self-equilibrating" deformations are present near the edges.)

Variation of T_m, ΔT and the self-equilibrating temperature components at both surfaces with the non-dimensional time parameter $N = \kappa t/d^2$ and the Biot number $B = hd/k$ is shown in Figs. 10 to 13 for a sudden change in the adiabatic wall temperature $(T_0 - T_i)$. The variation of the mean temperature T_m is of an exponential type approaching asymptotically the equilibrium value while both ΔT and T^* components increase to some maximum value and then gradually decrease asymptotically to zero. Thus the effects caused by ΔT and T^* are of transient nature. The range of values of B for typical cases is approximately 1 to 10.

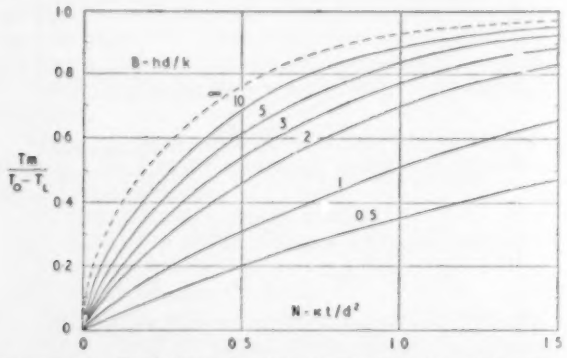

FIGURE 10. Variation of mean temperature T_m with non-dimensional time $N = \kappa t/d^2$ (B = Biot number).

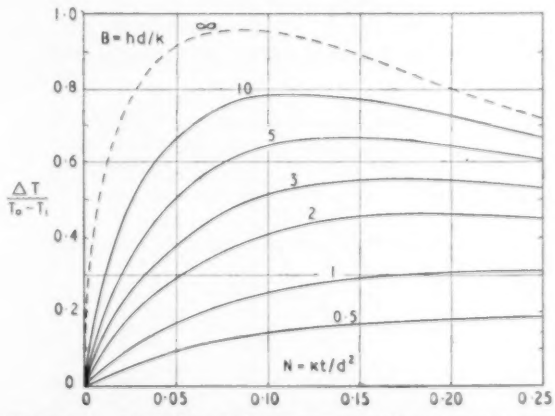

FIGURE 11. Variation of temperature gradient ΔT with non-dimensional time $N = \kappa t/d^2$.

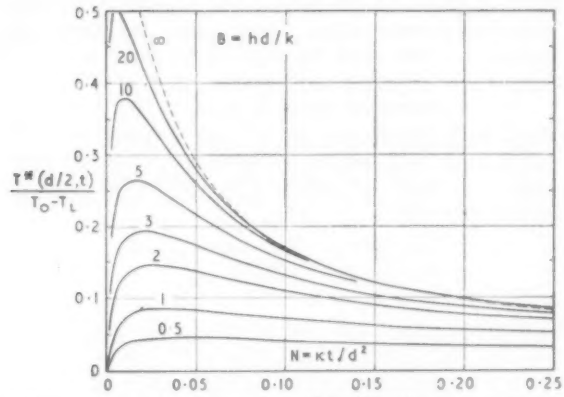

FIGURE 12. Variation of self-equilibrating temperature $T^*(d/2, t)$ with non-dimensional time $N = \kappa t/d^2$.

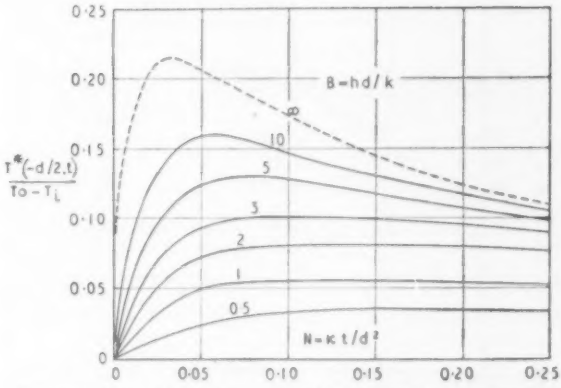

FIGURE 13. Variation of self-equilibrating temperature $T^*(-d/2, t)$ with non-dimensional time $N = \kappa t/d^2$.

5. General Equations for Stresses and Deformations

The large deflection theory of plates subjected to arbitrary pressure and thermal loading indicates that, in general, there is coupling between the membrane stresses in the middle plane of the plate and the bending stresses. The basic differential equations for the general case are as follows[6, 7]:

$$\nabla^4 F = -zE\nabla^2 [T_m(x, y, t)] + E\left\{\left(\frac{\partial^2 w}{\partial x \partial y}\right)^2 - \frac{\partial^2 w}{\partial x^2}\frac{\partial^2 w}{\partial y^2}\right\} \quad . \quad . \quad . \quad . \quad . \quad . \quad . \quad . \quad . \quad (16)$$

$$D\nabla^4 w = -\frac{zEd^2}{12(1-\nu)}\nabla^2 [\Delta T(x, y, t)] + p(x, y, t) + d\left\{\frac{\partial^2 F}{\partial y^2}\frac{\partial^2 w}{\partial x^2} - \frac{2\partial^2 F}{\partial x \partial y}\frac{\partial^2 w}{\partial x \partial y} + \frac{\partial^2 F}{\partial x^2}\frac{\partial^2 w}{\partial y^2}\right\} \quad . \quad (17)$$

$$D = Ed^3/12(1-\nu^2) \quad . \quad . \quad (18)$$

where the x and y co-ordinates refer to any set of mutually perpendicular axes in the plane of the plate, as shown in Fig. 14. The resulting stresses are then determined from the solutions for the Airy stress function F and the transverse deflection, w.

In any design calculations, it is usually sufficiently accurate to assume that both the pressure and thermal loading are constant over the whole panel, so that p, T_m and ΔT then become functions of time only while T^* is a function of z and t.

If one or two pairs of edges are restrained in the plane of the panel then a strong coupling between the membrane stresses and bending stresses may exist. This has been analysed extensively by Williams[8, 9], who solved the problem of the simultaneous loading of pressure and heat (T_m and ΔT) on an infinitely long strip with the lengthwise edges either clamped or pin-ended. Parkes[10] analysed the case of a flat panel, with initial eccentricities and with all edges restrained against expansion subjected to uniform temperature increase (T_m).

If there are no restraints in the plane of the panel, and the deflections are small, the effects due to the pressure p and temperature gradient ΔT can be considered separately. The self-equilibrating temperature distribution produces only self-equilibrating stresses which can also be considered separately and then superimposed on the other stresses.

5.1. PRESSURE STRESSES

The pressure loading on windscreen panels is affected by two components:

(*i*) cabin pressurisation (internal pressure), and

(*ii*) local aerodynamic pressures (external pressure).

The first component is a function of altitude only while the second component is affected by the shape of the windscreen and canopy, incidence, sideslip, speed, Mach number and altitude. In pressurised aircraft, however, the internal pressure component is likely to be the major one, (usually about 5 to 7 lb./in.²) so that although the external pressure loading is far from being uniform, it can be treated as constant when combined with the higher internal pressure.

On forward facing panels, the maximum outward pressure will tend to occur at high incidences, especially in the transonic region, and at maximum cabin pressure, while the maximum inward pressure will occur at low or negative incidences at high speeds and cabin unpressurised. Sideslip can also affect external pressure loading, especially in V windscreens.

On side and upper panels, the maximum outward pressure is similar to that in the forward facing panels

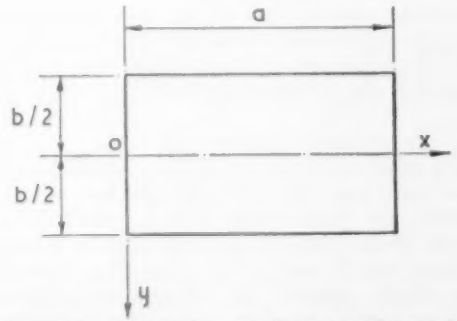

FIGURE 14. Co-ordinate system for rectangular panels.

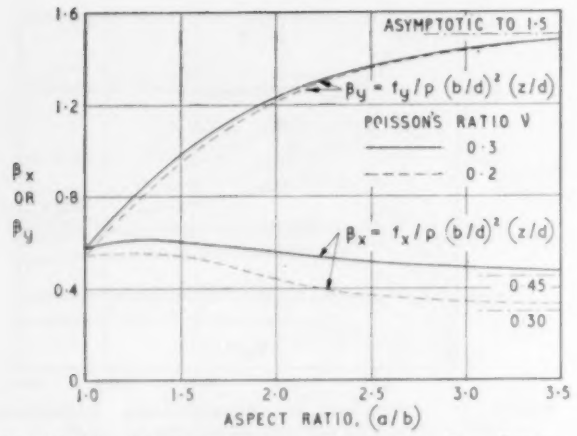

FIGURE 15. Pressure stresses at the centre of a simply-supported rectangular panel.

but sideslip may be more important. Inward pressures will generally be small, even if the cabin is unpressurised.

The solution for calculating stresses in a rectangular panel under uniform pressure with all edges simply-supported is well known. The maximum stress occurs at the centre of the panel and may be expressed as[11]

$$f_x=\beta_x p\left(\frac{b}{d}\right)^2\frac{z}{d} \text{ and } f_y=\beta_y p\left(\frac{b}{d}\right)^2\frac{z}{d} \quad . \quad (19)$$

where β_x and β_y are functions of the aspect ratio a/b; these functions are plotted in Fig. 15.

5.2. THERMAL STRESSES

5.2.1. *Mean Temperature* T_m.

The mean temperature T_m induces stresses only if one or two pairs of edges are restrained against expansion in the plane of the panel. In such cases compressive or tensile stresses are induced if the panel is respectively heated or cooled more rapidly than its surrounding structure (mounting frame). Therefore, it is advisable in designing transparency mounting to avoid any restraint on the expansion of the panel. This also almost certainly excludes any design in which the transparent panel is bolted firmly to the structure, such as is the case with the present laminated glass panels where vinyl layer with light alloy insert round the edges is bolted to the main structure.

Thermal stresses due to T_m are proportional to $\alpha ET_m/(1-\nu)$ and this could have a dangerously high value[12]—in fact over 2½ times higher than the stresses due to ΔT and T^* distributions.

5.2.2. *Temperature Gradient* ΔT.

The effect of ΔT is to produce a uniform curvature in the panel and therefore in the absence of any edge restraints the panel bends into a spherical surface. Because of the restraints along the edges of a rectangular panel, which prevent the edges from leaving the plane of the supports, the temperature gradient ΔT produces certain reactions along the boundary and bending stresses in the panel. For circular panels, with simply-supported edges, these edge reactions and stresses are zero since the edges of the panel remain in the plane of the support under the action of ΔT.

For a rectangular panel clamped at four edges, the bending moments due to ΔT are constant over the entire panel, and twisting moments and transverse shear forces are equal to zero. The thermal stresses are simply given by[13]

$$f_x=f_y=-\alpha E\frac{\Delta T}{(1-\nu)}\left(\frac{z}{d}\right) \quad . \quad . \quad (20)$$

which means that the maximum thermal stress occurring at the surface $(z=\pm d/2)$ is $\pm\alpha E\Delta T/2(1-\nu)$.

For a rectangular panel simply-supported at four edges, thermal stresses have been solved by Maulbetsch[14]; the thermal stresses depend on the aspect ratio of the panel (a/b) but are independent of the Poisson's ratio. These stresses are given by[14, 15]

$$f_x=-\frac{4}{\pi}\alpha E\Delta T\left(\frac{z}{d}\right)\phi \quad . \quad . \quad . \quad . \quad . \quad (21)$$

$$f_y=-\frac{4}{\pi}\alpha E\Delta T\left(\frac{z}{d}\right)(1-\phi) \quad . \quad . \quad . \quad . \quad (22)$$

$$\phi=\sum_{m=1,3,5\ldots}^{\infty}\sin(m\pi x/a)\cosh(m\pi y/a)/m\cosh\gamma_m \quad (23)$$

$$\gamma_m=m\pi b/2a \quad . \quad . \quad . \quad . \quad . \quad . \quad . \quad (24)$$

The function γ can vary between 0 and $\pi/4$ and thus the maximum value of the stress will be

$$f_x \text{ or } f_y=\pm\tfrac{1}{2}\alpha E\Delta T$$

The variation of the thermal stresses f_x and f_y at the centre of a rectangular panel $(x=(a/2), y=0)$ with the aspect ratio a/b is shown in Fig. 16; the maximum stress, $\pm\frac{1}{2}\alpha E\Delta T$ is only realised as a/b tends to ∞, and the minimum thermal stress is only obtained on square panels $(a/b=1)$.

For any aspect ratio $a/b\neq\infty$ the maximum thermal

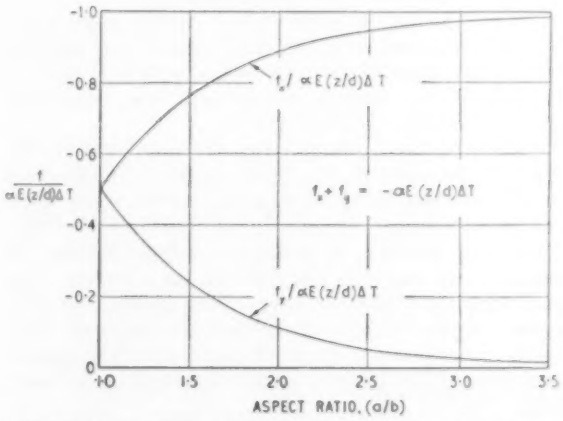

FIGURE 16. Thermal stresses at the centre of a simply-supported rectangular panel due to temperature gradient ΔT.

stresses are always reached at the boundary and are given by

$$(f_x)_{y=\pm b/2} = (f_y)_{\substack{x=0 \\ x=a}} = -\alpha E \Delta T \frac{z}{d} \quad . \quad (26)$$

The analytical solutions obtained by Maulbetsch[14] and Timoshenko[15] indicate that the concentrated reactions and the twisting moments at the four corners tend to infinity. In ductile materials this would probably lead to some local yielding resulting in the redistribution of the stresses near the corners. Maulbetsch[14] suggested a possible solution on these lines and recently this problem has also been discussed by Bijlaard[16] in connection with the analysis of a sandwich panel with bolt attachments subjected to a temperature gradient. With glass panels which exhibit apparently perfect elasticity this mathematical infinity in the solution for the stresses may give cause for concern. A possible practical solution to avoid these stress concentrations is to use generous corner radii.

Other polygonal shapes of panels can also be analysed; for example thermal stresses in triangular panels have been discussed in Ref. 14.

5.2.3. *Self-Equilibrating Temperature Distribution T^*.*

The temperature distribution T^* produces a self-equilibrating stress distribution which is given by[17, 18]

$$f_x = f_y = \frac{\alpha E}{(1-\nu)} \left\{ -T + \frac{1}{d}\int_{-d/2}^{d/2} T\,dz + \frac{12\,z}{d^2}\int_{-d/2}^{d/2} T z\,dz \right\}$$

$$= \frac{-\alpha E T^*}{(1-\nu)} \quad . \quad . \quad . \quad . \quad . \quad (27)$$

For design calculations it is sufficiently accurate to assume that the stress distribution given by equation (27) is uniform over the entire panel. Only at the edges of the panel do the stresses vanish but it may be expected that they reach their full values within a short distance from the edges.

5.2.4. *Order of Magnitude of Thermal Stresses.*

Before discussing the combined pressure and thermal stresses it may be appropriate to indicate the magnitude of the maximum thermal stresses. It has already been mentioned that the probable range of the Biot numbers is between 1 and 10 and therefore attention will be confined to these two extreme values. Assuming Poisson's ratio to be $\nu = 0{\cdot}24$ and using the results of Sections 5.2.1. and 5.2.3. and Figs. 10 to 12, the magnitudes of the thermal stresses due to various temperature components can be estimated. These are shown in Table I for a rectangular panel with all edges simply-supported.

The table applies, strictly speaking, only to the case of a sudden increase in the adiabatic wall temperature $(T_0 - T_1)$ and a constant heat transfer coefficient h. It nevertheless provides a useful guide to the magnitude of the thermal stresses in transparencies; it also shows that it is important to avoid edge restraint in the plane of the panel—particularly on outer panels—as otherwise

TABLE I

THERMAL STRESSES IN TRANSPARENCIES

($\nu = 0{\cdot}24$, glass)

Temperature Component	*Approximate value of thermal stress* $\alpha E (T_0 - T_1)$	
	$B = 1$	$B = 10$
T_m	$-1{\cdot}32$	$-1{\cdot}32$
ΔT	$\pm 0{\cdot}16$	$\pm 0{\cdot}39$
T^* external surface	$-0{\cdot}12$	$-0{\cdot}50$

thermal stresses of the order of $1{\cdot}32\,\alpha E (T_0 - T_1)$ can be induced in the panel.

5.3. COMBINED STRESSES

Assuming that the thermal expansion in the plane of the panel is not prevented, the total stresses will consist of stresses due to T^*, ΔT and the pressure loading p which may be either inward or outward. The peak values of T^* and ΔT do not coincide and therefore separate stress time variations must be added to obtain the maximum thermal stress and the total thermal stress is then combined with the pressure stress.

The design criterion for transparencies is based on the maximum tensile stress. Various design cases are quoted in Table II showing the signs of the stresses.

From this table it can be seen immediately that the maximum tensile stress may occur in any of the following cases:

(*i*) Deceleration; thermal loading combined with outward pressure; stress at $z = d/2$ (external surface).

(*ii*) Deceleration; thermal loading combined with inward pressure; stress at $z = -d/2$ (internal surface).

(*iii*) Acceleration; thermal loading combined with inward pressure; stress at $z = -d/2$ (internal surface).

It has been found, however, that case (*i*), *i.e.* thermal loading due to deceleration of the aircraft and outward pressure, usually gives the highest tensile stress, and may therefore be used as a design criterion.

TABLE II

SIGNS OF MAXIMUM SURFACE STRESSES

+ve *Tension*

−ve *Compression*

Stress Caused by	*Thermal Stresses*			
	Acceleration (Heating)		*Deceleration (Cooling)*	
	Outer Surface $z = d/2$	*Inner Surface* $z = -d/2$	*Outer Surface* $z = d/2$	*Inner Surface* $z = -d/2$
T^*	−	−	+	+
ΔT	−	+	+	−
	Pressure Stresses			
p Outward	+	−	+	−
p Inward	−	+	−	+

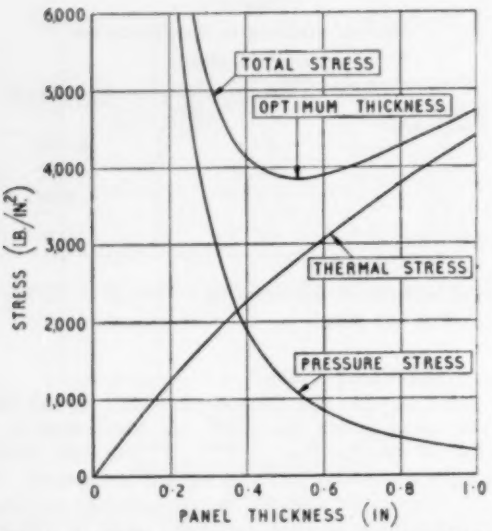

FIGURE 17. Typical variation of total stress with panel thickness; rectangular glass panel.

Since thermal stresses due to T^* and ΔT increase with increasing thickness of the panel (*see* Figs. 11 and 12) and pressure stresses decrease with increasing thickness, there will be some optimum thickness for which the combined stress becomes a minimum. A typical plot showing the variation of the combined stress with thickness for a deceleration case is shown in Fig. 17; here the optimum thickness giving the minimum stress is about 0·5 in. This figure also illustrates the significant feature of thermal stresses, that an increase in the amount of structural material does not necessarily lead to a reduction in the magnitude of thermal stress.

6. Temperature Stresses in Laminated Panels

In laminated glass panels, which are often used in windscreen assemblies, the middle layer is usually made from polyvinyl butyral plastic which has different thermal properties from those of the outer glass layers. When these layers experience changes in temperature, the middle layer expands or contracts at a different rate from the outer layers. Temperature stresses are therefore set up in the layers; in particular large stresses may exist near the edges.

A similar problem has been analysed by Aleck[19] who studied the distribution of thermal stresses in a rectangular beam, clamped along one side, using the principle of least work. The solution obtained could not be applied directly to the analysis of laminated glass panels subjected to temperature changes, because of the assumption of rigid clamping and the essentially two-dimensional character of the problem considered.

Further work by Durelli and Tsao[20, 21], who used a photoelastic technique, on a three-ply laminated panel provided very useful information on the distribution of stresses and their magnitude near the edges. The experimental results were again only applicable to two-dimensional distribution. The correlation of the photoelastic results with the temperature required to produce failure in glass at the interface and with the location of the point of failure near the edge, seems to indicate that two-dimensional thermo-photoelastic technique gives a satisfactory approximation. It may be interesting to mention that the temperature change in these tests was obtained by lowering the temperature to $-40°C$.

Additional experimental and theoretical studies in this field, particularly of the three-dimensional stress field at the corner of three-ply laminated panels, would be extremely valuable.

7. Effects of Design Parameters

7.1. STEADY FLIGHT

In steady flight, when equilibrium conditions are achieved, there will be no thermal stresses unless any differential expansions of the transparency material and the surrounding structure are prevented. The only problem is that of finding a material with sufficient strength at the equilibrium temperature to withstand the pressure loads.

If the duration of the high speed flight is not sufficient to produce a uniform temperature distribution through the thickness of a transparency, then the effective temperature drop due to any subsequent deceleration will be somewhat smaller, resulting in a decrease of the maximum thermal stress; the same is true if the internal surface temperature is kept lower by the supply of cooling air.

7.2. SPEED AND ALTITUDE

Thermal stresses are proportional to the total change in the adiabatic wall temperature which is a function of the Mach number and altitude. Variations in the Mach number and altitude have an additional effect on thermal stresses through the variation in the

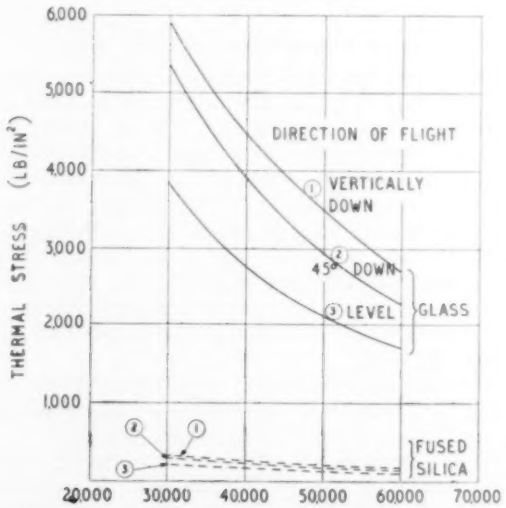

FIGURE 18. Effect of altitude on thermal stress; analogue solution.

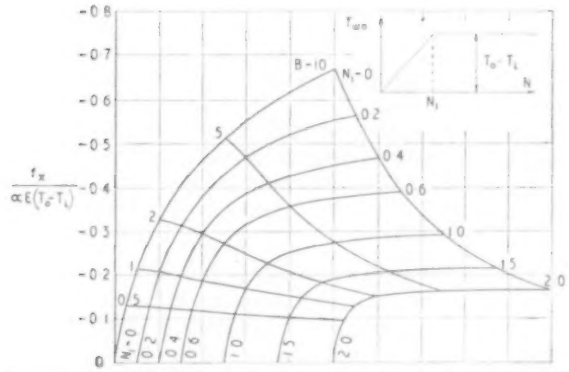

FIGURE 19. Maximum thermal stress f_x in simply-supported rectangular panels; aspect ratio $a/b=2$, Poisson's ratio $\nu=0{\cdot}24$.

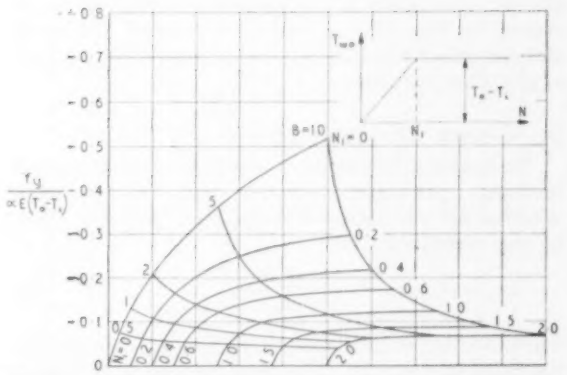

FIGURE 20. Maximum thermal stress f_y in simply-supported rectangular panels; aspect ratio $a/b=2$, Poisson's ratio $\nu=0{\cdot}24$.

convective heat transfer coefficient h or the variation in the Biot number, $B=hd/k$.

To illustrate the effect of altitude on thermal stresses in transparencies, a hypothetical case has been considered in which the aircraft was decelerated with a constant deceleration of $2{\cdot}5g$ starting at various altitudes and flying either level or in a dive. The panel analysed was $\frac{5}{8}$ in. thick, of aspect ratio of about two, and with all edges simply-supported; the materials considered were glass and fused silica. The results of this investigation are shown in Fig. 18; the solutions were obtained on the Bristol resistance-capacitance analogue using variable adiabatic wall temperature and variable heat transfer coefficient.

Figure 18 illustrates well how thermal stresses could be appreciably reduced by decelerating at high altitudes; this procedure should be possible on a supersonic civil transport aircraft, but not necessarily on a fighter aircraft for which no rigid flight programme could be defined.

7.3. ACCELERATION OR DECELERATION

The variation of the total thermal stress due to ΔT and T^* at the external surface with acceleration (or deceleration) will be illustrated for the case of linearly varying adiabatic wall temperature from $T_{w_0}=0$ to (T_0-T_1) in time N_1 (non-dimensional), thereafter remaining constant; the heat transfer coefficient is assumed to be constant. In Figs. 19 and 20 carpet plots of the maximum total thermal stresses f_x and f_y are presented in non-dimensional form for a series of values of N_1 and the Biot number $B=hd/k$; the stresses represented by these plots are for a simply-supported rectangular panel of aspect ratio $a/b=2$ and Poisson's ratio $\nu=0{\cdot}24$ (glass). For fused silica, which has $\nu=0{\cdot}17$, the corresponding curves are only slightly lower. It should be noted that the stresses are negative for positive values of T_0-T_1; thus accelerations induce compressive (negative) stresses and conversely decelerations (negative value of T_0-T_1) induce tensile (positive) stresses. For square panels, f_x and f_y will both be equal to the mean of f_x and f_y for the rectangular panel. This is apparent from the symmetry of equations (21) and (22).

For a given material, panel thickness and flight plan, approximate relations between $N_1=\kappa t_1/d^2$ and average acceleration (or deceleration) and between $B=hd/k$ and the Mach number and altitude can be obtained. This enables the non-dimensional results of Figs. 19 and 20 to be expressed as the variation of stress with altitude, Mach number and acceleration (or deceleration).

It should, however, be emphasised that there may be large variations in the Biot number during the acceleration (or deceleration) period (*see* Figs. 7 and 8) and therefore care should be exercised in interpreting the results of Figs. 19 and 20 which are based on constant values of B. If the variation of the Biot number B is not too great, average values of B can be used and they would give sufficient engineering accuracy. For larger variations more exact methods should be used (*e.g.* Ref. 3), perhaps for a few selected cases.

For convenience, the variation of the Biot number per unit thickness (B/d) with the Mach number and altitude is shown in Fig. 21 for Reynolds number based on a distance $L=3$ ft. and $T_s=T_{w_0}$. (Note that the latter assumption over-estimates the heat transfer co-

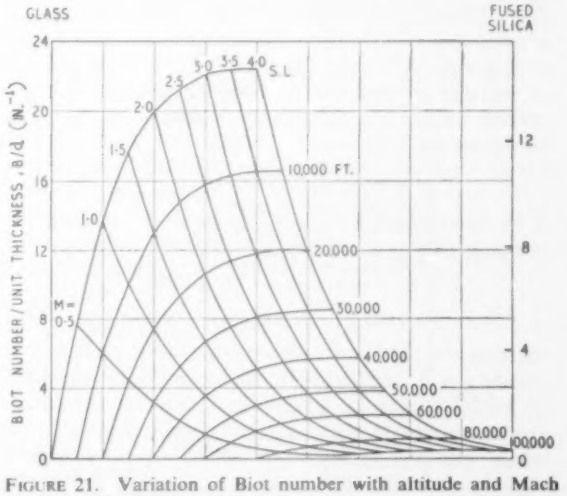

FIGURE 21. Variation of Biot number with altitude and Mach number (Reynolds number is based here on $L=3$ ft., T_s is assumed to be equal to T_{w_0}).

efficient, and hence B, for deceleration manoeuvres, as shown in Fig. 8.) A rather interesting feature is that for $M>2$ the Biot number is practically constant at any given altitude.

8. Choice of Materials

To facilitate the choice of materials, a thermal shock resistance parameter may be used as a possible criterion for comparing different materials; it is given by the expression

$$\frac{\kappa s(1-\nu)}{\alpha E} \quad . \quad . \quad . \quad (28)$$

where s is the tensile strength at elevated temperatures (modulus of rupture). The material with a high value of this parameter will generally have better thermal and strength characteristics.

The low values of the product αE increase the thermal shock resistance parameter. For various types of glasses, however, the Young's modulus E is approximately constant but the coefficient of expansion α can vary appreciably. The use of glass with low thermal expansion to improve thermal shock resistance is not always desirable, if the glass is to be used in the toughened form. Glass is toughened by heating it to a temperature near its softening point and then rapidly chilling both surfaces to produce locked-up strains, compressive in the surfaces and tensile in the centre plane. Thus any resultant tensile stresses in the surface due to the thermal and pressure loading are smaller and consequently the effective strength of glass is increased. The amount of toughening depends on the thermal expansion and it may not be feasible to increase the strength of the low expansion glasses by toughening to the extent possible with glasses of higher thermal expansion. For comparison, coefficients of thermal expansion for various transparent materials and a few typical structural materials are given in Fig. 22; it can be seen that fused silica has the lowest coefficient of expansion ($0{\cdot}54\times10^{-6}$ in./in./°C), followed by borosilicate glass (about $3-5\times10^{-6}$ in./in./°C).

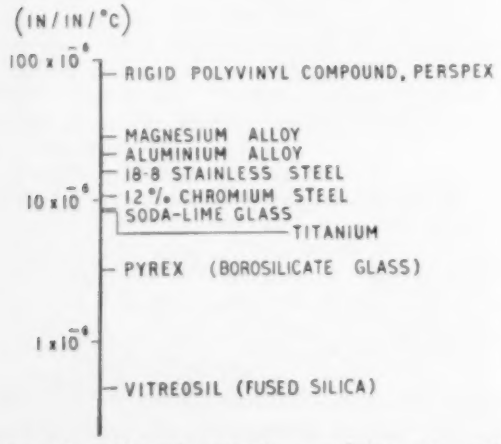

FIGURE 22. Thermal expansion coefficient for various materials.

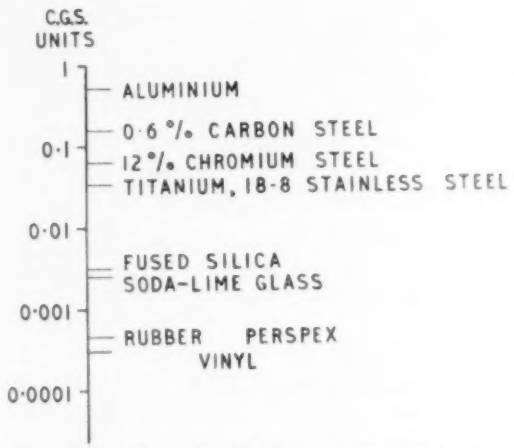

FIGURE 23. Thermal conductivity of various materials.

High values of thermal diffusivity (or conductivity) always decrease thermal stresses. The thermal conductivities of various materials are presented in Fig. 23; here again fused silica appears to be a very attractive material because of its high thermal conductivity. Its thermal conductivity is 0·0032 c.g.s. units, while that of soda-lime glass is about 0·0024. The thermal conductivity of plastic materials is about one order of magnitude smaller.

An additional advantage of fused silica is its low value of the Poisson's ratio; a value of $\nu=0{\cdot}17$ has been quoted but further experimental evidence would be required to confirm this. The Poisson's ratio of ordinary soda-lime glass is about 0·24.

Other properties which must also be considered are: light transmission, ease of manufacture, creep resistance, and resistance to erosion at elevated temperatures.

8.1. ORGANIC TRANSPARENCIES (PLASTICS)

Figure 24 shows the variation of tensile strength with temperature for several typical transparent plastics. Tensile strength is generally high at room temperature but decreases rapidly with temperature imposing severe limitations on the use of these

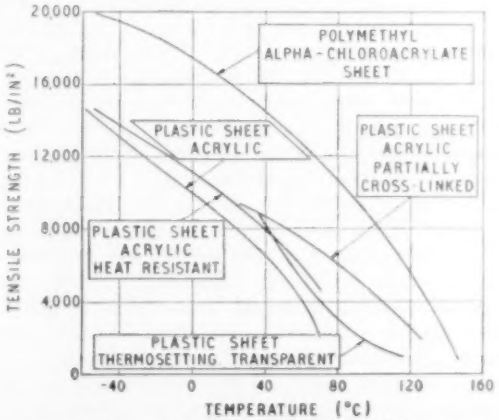

FIGURE 24. Tensile strength of various plastic sheets.

materials at elevated temperatures. The present temperature limit may be taken as around 80 to 100°C but further development may possibly extend this by about sustained loading, fatigue and high rates of creep at elevated temperatures would always make plastic transparencies a somewhat doubtful proposition. Alternative materials for elevated temperatures are inorganic transparencies and since these offer much greater scope, they will be discussed at greater length.

8.2. INORGANIC TRANSPARENCIES (GLASS OR FUSED SILICA)[22]

The strength of glass varies widely with its chemical composition, but even more so with the surface condition, rate of loading, degree of toughening and the presence of moisture at the surface.

The low strength of glass is usually explained by Griffith's concept of surface flaws which act as stress raisers so that the stress at the base of the crack is much greater than the average stress on the surface. The size of the cracks is affected mainly by the moisture and this is primarily responsible for the delayed failure of glass (static fatigue). This theory is generally supported by experiments and a mechanism of dissolution has been proposed[23] in which alkali ion self-diffusion controls the initial steps of water corrosion leading to breakdown of the glass structure; this in turn permits any existing flaws to grow to critical dimensions and bring about spontaneous crack propagation and failure. The rate of this reaction is influenced strongly by temperature.

Figure 25 shows the experimental results of delayed failure tests on soda-lime glass rods[23]. From −50°C to 150°C the maximum tensile stress decreases with the increase in temperature and the time to failure. Above 150°C the failing tensile stress increases slightly with temperature and is practically independent of the time of loading, except perhaps for very short time loading when there is a slight increase in strength. In a similar study Preston[24] found that the minimum strength occurred at about 200°C. This peculiar behaviour is generally true of all glasses including fused silica.

The increase in strength at higher temperatures is attributed to the decreasing effects of moisture which is driven off from the surface. Furthermore, high temperatures produce sufficient movement of atoms to heal the surface flaws and this effect probably outweighs the influence of thermal motion, which in itself lowers the strength of the glass. Treatment of the surface with 5 per cent hydrofluoric acid may also tend to heal the flaws and increases the strength; this effect, however, is only temporary.

All strength calculations should be based on the delayed strength of glass at a temperature corresponding to the minimum failing stress (about 150-200°C). Sometimes in the absence of any other information, short time strength is used with a factor of 2½ in addition to any factor to cover scatter in strength between specimens.

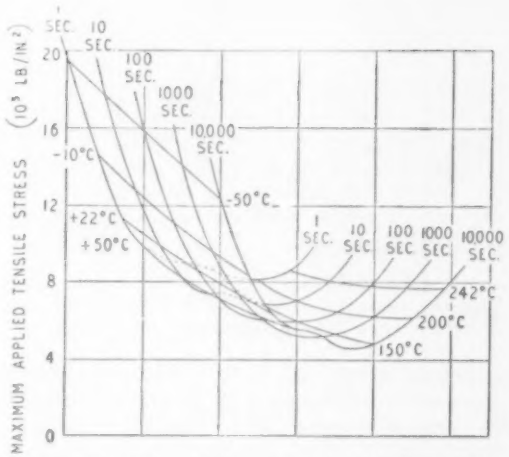

FIGURE 25. Delayed failure curves for soda-lime glass.

8.2.1. *Annealed Glass*

The mechanical and optical properties of annealed plate glass are sufficiently well-known not to be described in detail. Coefficient of thermal expansion is about $8{\cdot}7 \times 10^{-6}$ in./in./°C and this results in high thermal stresses. The accepted maximum allowable working (tensile) stress is about 800 to 1,200 lb./in.². In general, the strength of annealed glass is too low to consider it for transparencies.

8.2.2. *Toughened Glass*

The toughening process (sometimes called tempering), increases the tensile strength of glass. The generally accepted allowable working in stress is about 4,500 lb./in.² for ordinary soda-lime glass in the toughened form.

Borosilicate glasses, of which the most familiar type is Pyrex, have a lower coefficient of thermal expansion compared with the soda-lime glass (*see* Fig. 22). As a result of this they offer good resistance to kinetic heating, but have lower strength in tempered form because the lower coefficient of expansion precludes a high degree of toughening. Whether this will result in a useful material depends on the relative changes in both thermal and allowable stresses and further investigation is obviously needed. The optical properties of borosilicate glasses are usually inferior to those of the soda-lime glasses.

Aluminosilicate glasses have been suggested as a likely material but too little is known yet to evaluate their potentialities.

8.2.3. *Fused Silica*

The most attractive material for high temperature transparencies appears to be fused silica. It has exceptionally low coefficient of thermal expansion (about $\frac{1}{15}$ that of soda-lime glass) and its thermal conductivity is about 1·5 times greater than that of ordinary glass; both these factors tend to reduce thermal stresses appreciably. These important factors are easily demonstrated by the frequent use of silica ware in

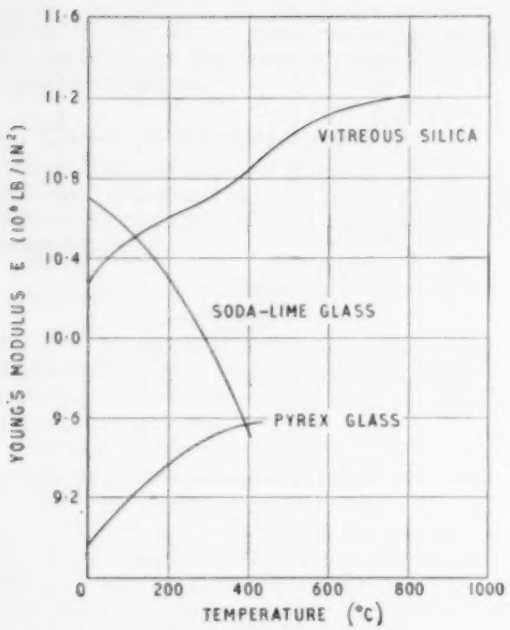

FIGURE 26. *E* for glass at elevated temperatures.

chemical laboratories, in conditions which demand heating to red heat followed by immersion in cold water.

The mechanical strength is less well established for sheet material and further investigation would be required. The working stress would probably be slightly higher than for annealed glass, but bearing in mind that the thermal stresses would generally be about 1/20 of those in a similar soda-lime glass panel (combined effect of low coefficient of expansion and high thermal conductivity), it becomes obvious that fused silica is a material of considerable value. This is also demonstrated in Fig. 18 where a comparison of thermal stresses in soda-lime glass and fused silica is made; the thermal stresses in fused silica are reduced to such an extent that they are small, even compared with the lower allowable stress, and it should therefore be possible to ensure adequate safety with much more certainty.

Unlike other types of materials, the Young's modulus of fused silica increases slightly with temperature (*see* Fig. 26).

9. Practical Design Considerations

9.1. MOUNTING OF PANELS

Present day designs of windscreen panels use laminated glass and the methods of mounting glass panels are dependent on the plastic interlayer being extended beyond the edges and providing a flange which can be bolted to the structure (*see* Fig. 27). This feature will be absent in high temperature applications, and alternative methods will be required without the necessity for drilling the transparent panels. Bevelled edge type mounting may be necessary, as shown also

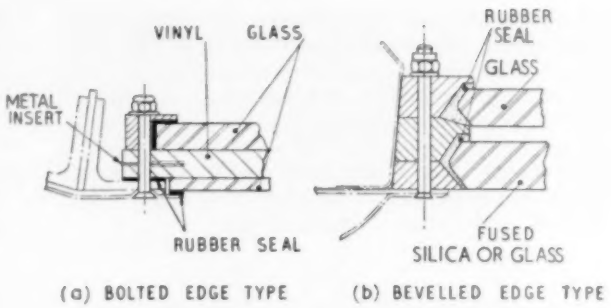

FIGURE 27. Types of edge mounting on transparencies.

in Fig. 27, and this may also have the additional advantage of flush external surfaces. Furthermore, edgewise restraints would not be excessive.

The frames for glass panels should be made as stiff as possible, to avoid straining of the glass due to structural deformations under inertia and aerodynamic loading.

9.2. FAIL-SAFE DESIGN

The fail-safe philosophy can be adopted in the design of transparencies[23]; an obvious solution is the use of a double panel with one panel unloaded but ready to take up the full pressure if the other fails. For example, the interspace between the two panels can be vented to cabin pressure and thus normally only the outer panel is subjected to full pressure and thermal loading. In an alternative design, the interspace could be vented to the air outside and the inner panel would then be subjected to cabin pressurisation, with the outer panel taking the thermal loading.

The fail-safe design has already been demonstrated in tests on double panel transparencies. In Fig. 28 a double panel window is shown after a test in which the

FIGURE 28. Fail-safe test on a window panel.

FIGURE 29. Membrane stresses in vinyl interlayer reacting to pressure loading after initial failure of glass layers.

inner panel was loaded under 8·3 lb./in.^{2} and then fractured instantaneously by punching out a scribed disc and thus subjecting the outer panel to the full pressure suddenly. There was no failure or damage to the outer panel, which continued to hold pressure satisfactorily. The window panels were made of Perspex and were intended for low temperature application. This nevertheless shows the usefulness of the principle.

Naturally designs incorporating duplication as safety measure tend to be heavier than the single panel designs but in view of the uncertainty about the strength, edge restraint, thermal and pressure loading, it may still be better to duplicate the panels.

The use of a vinyl interlayer in laminated glass panels, designed to take the membrane stresses, has the additional advantage in that, should both sheets of glass fail, the vinyl is still capable of carrying the pressure loading. This is manifestly demonstrated in Fig. 29 showing a test on an initially flat rectangular panel in which the vinyl is holding a pressure of eight times the working pressure after both glass sheets had failed.

Laminated glass for inner panels could be used if cooling air could be supplied to the interspace to keep the temperature of the vinyl at a reasonable level. Such a scheme for a double panel window is shown in Fig. 30.

10. Acceptance Tests

10.1. TENTATIVE PROVING PROCEDURE

Realistic tests on transparencies will require artificial cooling of the external surface of a panel. The artificial cooling can be obtained by discharging a fluid coolant and controlling the rate of discharge, or alternatively the flow rate could be maintained constant while the rate of cooling experienced by the surface could be controlled by radiation from a heating source.

The factors required on the transparencies are so high relative to the factors on the rest of the structure that the transparencies in representative mountings could not achieve their factored loads before failures

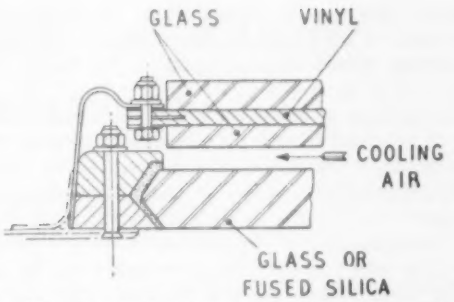

FIGURE 30. Proposed scheme for window mounting on supersonic aircraft.

occurred elsewhere. The use of unrepresentative mountings, to achieve the required factored loading, is a dangerous practice since such mountings would seriously modify the load reactions. As an example of what is involved, a case has been known in which a typical panel mounted in a representative structure had an ultimate strength of less than half of that achieved in a rigid test rig.

Although factored pressure loads could be applied with non-representative mounting, factoring of thermal transient stresses is not easily achieved, and therefore a different proving procedure must be employed. Assuming that a suitable technique for measuring panel stresses can be developed the proving technique might be as follows:

(*i*) Determine the stresses due to unfactored pressure loading.

(*ii*) Determine the maximum thermal stresses under representative temperature drop and representative rate of cooling. (If no suitable experimental technique can be developed, theoretical thermal stresses would be used for this stage).

(*iii*) If possible the maximum stresses should also be determined for the combined loading (*i*) and (*ii*), to check any coupling effects.

(*iv*) Add the stresses from (*i*) and (*ii*), multiply by the appropriate factor and then determine the reserve factor by comparing the resulting stresses with the maximum allowable stress representing a statistically "safe" stress divided by the factor of, say, 5 or 6.

This procedure depends on the development of a successful method of strain measurements in transparencies. It would be outside the scope of this paper to discuss various possible experimental methods. There is, however, a new photoelastic technique[26], developed initially in France, which could be applied to transparencies. This technique is usually known by the trade name "Photo Stress", and the necessary equipment is already being manufactured by an American company.

10.2. "PHOTO STRESS" TECHNIQUE

"Photo Stress" is a photoelastic technique in which the actual full scale structure to be analysed is coated with a special clear plastic that becomes doubly refractive when stressed. Coating can be obtained by means

of liquid plastic or a plastic sheet; the latter can be either clear or metallised on one surface. The material for coating allows measurements to be taken in the range $-55°C$ to $+135°C$.

The method is based on observation and measurement of coloured fringes by a special electronic photostress meter. The minimum measured strain, claimed by the manufacturer, would be more than adequate for the application of this method to transparency testing. The measurements of thermal strain would probably have to be taken on the internal surface since the plastic coating would affect the heat transfer rates unless its effect could be compensated by an increased rate of heating (or cooling).

At the time of writing this paper, there has been no known actual practical experience with the "Photo Stress" method in this country. It is hoped, however, that this experimental technique will be thoroughly explored and, if successful, it will eventually be applied to tests on complete transparency assemblies.

11. Conclusions

In conclusion, I would like to say that I am aware that only the fringes of this topic have been touched. However, I hope that I have been able to present at least a summary of the most important design problems and to suggest a few tentative solutions for the practical design of transparencies for elevated temperatures. The presentation was mainly from the point of view of a structural engineer, and I am very conscious that there are a great number of problems which have not been discussed, particularly those concerning the strength properties and the possible improvements in the existing glass and plastic materials—these are essentially problems for glass and plastics technologists.

I would like also to emphasise that high temperature transparencies still present a great number of challenging problems and in this new field there is undoubtedly a clear need for further research and development.

ACKNOWLEDGMENTS

The author would like to thank Bristol Aircraft Limited for permission to publish this paper. Thanks are also extended to colleagues, particularly to Mr. M. C. Campion, for the considerable help given in the preparation of the paper. The opinions expressed therein are entirely the author's own.

REFERENCES

1. Monaghan, R. J. (1955). Formulae and Approximations for Aerodynamic Heating Rates in High Speed Flight. Unpublished Ministry of Supply Report, Oct. 1955.
2. Hill, P. R. (1957). A Method of Computing the Transient Temperature of Thick Walls from Arbitrary Variation of Adiabatic-Wall Temperature and Heat Transfer Coefficient. N.A.C.A. Tech. Note 4105, Oct. 1957.
3. Przemieniecki, J. S. Design Charts for Transient Temperature and Thermal Stress Distributions in Thermally Thick Plates. (*To be published.*)
4. Buglia, J. J. and Brinkworth, H. (1958). A Comparison of Two Methods for Calculating Transient Temperatures for Thick Walls. N.A.C.A. Tech. Note 4343, August 1958.
5. Paschkis, V. and Baker, H. D. (1942). A Method for Determining Unsteady-State Heat Transfer by Means of an Electrical Analogy. *Trans. ASME*, Vol. 64, No. 2, pp. 105-112, Feb. 1942.
6. Nadai, A. (1925). *Die Elastische Platten.* Julius Springer Verlag, Berlin, p. 264, 1925.
7. Love, A. E. H. (1952). *Mathematical Theory of Elasticity.* Cambridge University Press, 4th Edition, p. 558, 1952.
8. Williams, M. L. (1955). Large Deflection Analysis for a Plate Strip Subjected to Normal Pressure and Heating. *Journal of Applied Mechanics*, pp. 458-464, Dec. 1955.
9. Williams, M. L. (1958). Further Large Deflection Analysis for a Plate Strip Subjected to Normal Pressure and Heating. *Journal of Applied Mechanics*, pp. 251-258, June 1958.
10. Parkes, E. W. (1956). Panels Under Thermal Stress. *Aircraft Engineering*, Vol. 28, pp. 180-186, June 1956.
11. Timoshenko, S. (1940). *Theory of Plates and Shells*, McGraw-Hill, pp. 125-133, 1940.
12. Thompson, A. S. (1952). Thermal Stress in Power Producing Elements. *Journal of the Aeronautical Sciences*, Vol. 19, No. 7, pp. 476-480, July 1952.
13. Timoshenko, S. (1940). *Theory of Plates and Shells*, McGraw-Hill, pp. 53-54, 1940.
14. Maulbetsch, J. L. (1935). Thermal Stresses in Plates. *Journal of Applied Mechanics*, Vol. 2, pp. 141-146, 1935.
15. Timoshenko, S. (1940). *Theory of Plates and Shells*. McGraw-Hill, pp. 176-180, 1940.
16. Bijlaard, P. P. (1959). Thermal Stresses and Deflections in Rectangular Sandwich Plates. *Journal of the Aero/Space Sciences*, Vol. 26, pp. 210-218, 1959.
17. Timoshenko, S. and Goodier, J. N. (1951). *Theory of Elasticity*, Chapter 14. McGraw-Hill, New York, 2nd Edition, 1951.
18. Melan, E. and Parkus, H. (1953). *Wärmespannungen.* Springer Verlag, Wien, pp. 56-70, 1953.
19. Aleck, B. J. (1949). Thermal Stresses in a Rectangular Plate Clamped Along an Edge. *Journal of Applied Mechanics*, pp. 118-122, 1949.
20. Durelli, A. J. and Tsao, C. H. (1955). Determination of Thermal Stresses in Three-Ply Laminates. *Journal of Applied Mechanics*, Vol. 22, pp. 190-193, June 1955.
21. Mylonas, C. (1955). Discussion to reference 20. *Journal of Applied Mechanics*, Vol. 22, p. 611, Dec. 1955.
22. Hahner, C. H. and Kerper, M. J. (1957). Inorganic Transparencies for Aircraft Enclosures. AGARD Report No. 161, Nov. 1957.
23. Charles, R. J. (1958). Static Fatigue of Glass: Parts I and II. *Journal of Applied Physics*, Vol. 29, pp. 1549-1560, Nov. 1958.
24. Preston, F. W. (1942). Mechanical Properties of Glass. *Journal of Applied Physics*, Vol. 13, p. 623, 1942.
25. Russell, A. E. (1957). Safety in Relation to Structural Damage. *Proceedings of the 6th Anglo-American Aeronautical Conference, Folkestone*, Royal Aeronautical Society, 1959.
26. Golubovic, G. (1959). Differentes Applications des Vernis Photoelastiques dans le Domaine des Constructions. *Delft Conference of the Stress Analysis Group*, Institute of Physics (Great Britain), 1959.

Some Practical Aspects of Kinetic Heating Calculations

by

C. L. BORE, B.Sc.(Eng.), Grad.R.Ae.S.

(Project Office, Hawker Aircraft Ltd.)

1. Introduction

This paper is concerned primarily with some of the practical difficulties encountered in connection with the prediction of kinetic heating temperatures. Attention will be concentrated upon methods for estimating temperatures and heat transfer rates for practical aircraft designed to fly at Mach numbers up to about five.

One factor common to all kinetic heating calculations is the variation of temperature through the thickness of the boundary layer, with consequent variation of viscosity. At Mach numbers above about 3, these temperature variations also lead to considerable variations of other properties of air—which are commonly assumed to remain constant—even in classical compressible flow aerodynamics. These factors complicate the aerodynamic equations.

Over certain regions of an aircraft (notably in the air intake ducts) it happens that the *local* Mach number outside the boundary layer may differ considerably from the free stream value. Since the basic heat transfer relationships are derived for flat plate conditions it follows that allowance must be made for differences between local and free stream conditions.

To estimate transient temperatures for the aircraft structure (and, in the limit, equilibrium temperatures) it is necessary to evaluate the overall effect of all the various modes of heat transfer which affect the structure, as well as the heat storage capacity of the structure. For practical estimates it is also necessary to deal with *any* prescribed variation with time of boundary layer temperature and heat transfer coefficient. This calls for numerical methods of estimation, which must be very adaptable, yet not too laborious.

To show the principles of some methods which have been used with success, the aerodynamic heat transfer relationships are first examined, with the object of separating the effects of skin surface temperature from those effects which depend on prescribed sortie conditions. The equation governing transient heating for shell structures is then shown. From this, a step-by-step method of solution is derived. Finally, some typical results are shown.

NOTATION

a speed of sound (ft./sec.)
C_f coefficient of skin friction
C_p specific heat of air at constant pressure (Fig. 1) (C.H.U./slug °K.)
C'_p temperature-mean specific heat (*see* text). (C.H.U./slug °K.)
E emissivity coefficient for Stefan-Boltzmann law
F_M Reynolds number correction factor, equation (14)
h heat capacity of skin material (C.H.U./ft.² °K.)
i enthalpy, or total heat, of air (C.H.U./slug °K.)
k conductivity of air (C.H.U./ft. sec. °K.)
k_H see equation (4) (equivalent to Stanton number)
M Mach number $= u/a$
Pr Prandtl number $= (\mu C_p/k)$
p static pressure, absolute (lb./ft.²)
q heat flux (C.H.U./ft.²sec.)
R gas constant for air (= 3,089 ft. lb./slug °K)
R_e Reynolds number
r temperature or enthalpy recovery factor (equation (2))
T temperature (°Kelvin)
t time (seconds)
u local velocity (ft./sec.)
γ ratio of specific heats
ε pressure recovery factor $= (p_{TOT})$ local: (p_{TOT}) ambient
μ viscosity (slug/ft. sec.)
ρ density (slug/ft.³)
σ Stefan-Boltzmann constant $(= 2{\cdot}78 \times 10^{-12}$ C.H.U./ft.² sec. (°K)⁴)

Suffixes

C central mass
F forcing
f, *e*, H, p *see* above
TOT total, or reservoir condition
W wall
0 ambient
1 local
* evaluated at effective enthalpy condition
$\bar{N}$ quantity N at mid-point of time interval

2. Development

2.1. THERMODYNAMIC PROPERTIES OF AIR

In normal compressible flow aerodynamics it is assumed that the two specific heats of air are both constant, so that the ratio (γ) also is constant. It is also assumed that the Prandtl number (Pr) is constant.

Figure 1 shows the actual variation with temperature of these properties, together with the variation of the viscosity (μ). This shows that for temperatures above,

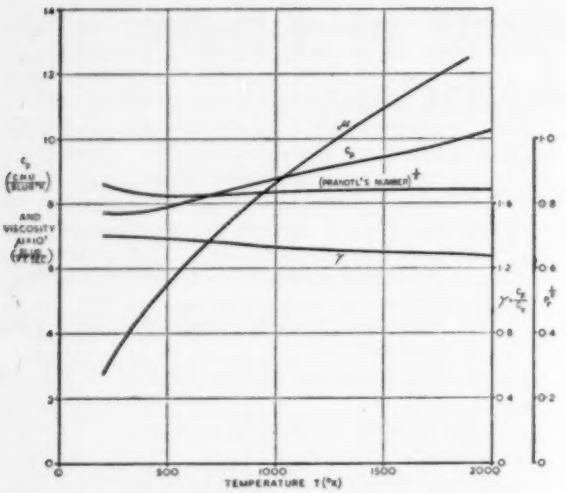

FIGURE 1. Thermal properties of air (from N.B.S. Circular 564).

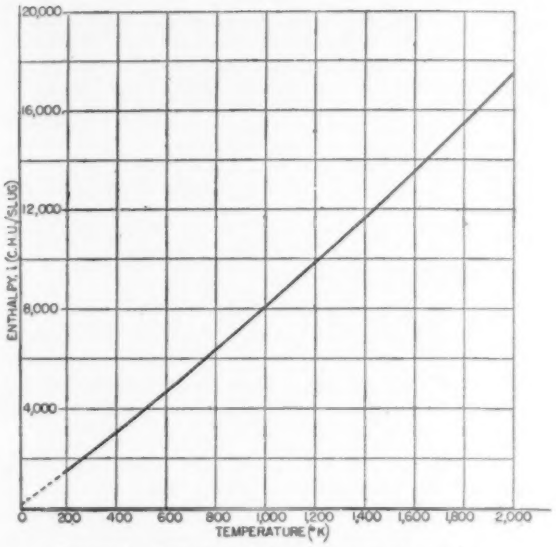

FIGURE 2. Enthalpy of air at atmospheric pressures.

say, 600°K (corresponding with about $M_0=3$) the specific heat at constant pressure (C_p) rises significantly, while γ decreases. The Prandtl number (or its square root, as plotted) varies only a little, except at low temperatures.

It is worth noting at this point that the total heat (or enthalpy, i) of air (Fig. 2) is given by the integral of C_p with respect to temperature T. The mean value of C_p over the temperature range zero to temperature T_1 will be denoted by C'_{p1} while the value of C_p *at* this temperature will be denoted simply by C_{p1}.

Eckert[1] and Monaghan[2,3] have shown that to deal with the variation of specific heat it is preferable to express the heat transfer equations in terms of enthalpy, rather than temperature. The energy equation (for example) becomes:

$$i_{TOT}=i_1+\tfrac{1}{2}u_1^2 \quad . \quad . \quad . \quad (1)$$

instead of

$$C_p T_{TOT}=C_p T_1+\tfrac{1}{2}u_1^2$$

where suffix "1" denotes conditions just outside the boundary layer. Also we assume an enthalpy recovery factor (r), as shown:—

$$r=\frac{i_F-i_1}{i_{TOT}-i_1} \quad . \quad . \quad . \quad (2)$$

instead of the temperature recovery factor r_T:

$$r_T=\frac{T_F-T_1}{T_{TOT}-T_1}\ .$$

Here, suffix "F" denotes the virtual "*forcing*" enthalpy or temperature. This forcing enthalpy is primarily a function of the aerodynamic flow and only to a minor extent is it influenced by *wall* conditions. It is felt that the forcing enthalpy is best regarded as a virtual enthalpy in the boundary layer, and not some property to be assigned to the wall. For this reason the name chosen for this quantity avoids the implication of the word "wall", as involved in such a term as "adiabatic wall" enthalpy, or implied by suffixes such as "AW" or "WO".

Clearly, when kinetic heating is taking place, there are large variations of temperature through the thickness of the boundary layer; consequently the properties of the air vary considerably through the layer—particularly the viscosity. Now Monaghan has argued (after Eckert) that if the properties of the fluid are evaluated at a certain weighted average temperature or enthalpy, then most of the available experimental results can be correlated quite well. Here, this average enthalpy will be called the "effective enthalpy", and conditions evaluated at this enthalpy will be denoted by an asterisk or star. For present purposes the effective enthalpy is given by Monaghan's "mean enthalpy" formula:—

$$i^*=i_1+0{\cdot}54\,(i_W-i_1)+0{\cdot}16\,(i_F-i_1)$$

which can be written:

$$i^*=i^*_B+i^*_W \quad . \quad . \quad . \quad (3)$$

where $i^*_B=0{\cdot}16\,i_F+0{\cdot}30\,i_1$, which depends only on ambient and local conditions, and $i^*_W=0{\cdot}54\,i_W$, which depends on the wall temperature only. It is not suggested that the coefficients given in equation (3) are necessarily the best possible choice, but they are sufficiently plausible for present purposes.

The heat transfer coefficient then becomes:

$$k^*_H=\frac{q}{\rho^*\,u_1\,(i_F-i_W)} \quad . \quad . \quad . \quad (4)$$

compared with

$$k_H=\frac{q}{\rho_1\,u_1\,C_p\,(T_F-T_W)}\ .$$

2.2. HEAT TRANSFER IN TERMS OF KNOWN DATA

In the general case the enthalpies or temperatures outside the boundary layer are not known directly. It is instructive, therefore, to consider how the heat trans-

fer relationships may be expressed in terms of known quantities.

2.3. SORTIES

Let us consider what is known of the boundary layer in advance. Fig. 3 shows a typical sortie for an aircraft operated as a research vehicle or as an interceptor.

This high-speed sortie starts with the aircraft already at a high altitude after a long cruise at subsonic speed, during which the structure has time to soak to a low temperature. The aircraft then accelerates rapidly and climbs to the specified altitude, remaining at the specified altitude and speed until the required distance has been covered. In this type of sortie the rates of heating and therefore the thermal stresses are at a maximum, since the acceleration is rapid and the initial structural temperatures are low. This type of sortie will be considered more closely later.

Note that when the sortie has been specified, both the aircraft Mach number (M_0) and the altitude are known at any time. From the altitude any of the ambient conditions such as pressure (p_0) or temperature (T_0) can be found.

2.4. LOCAL CONDITIONS

As local velocities over certain parts of an aircraft may differ very much from free stream, it is necessary to find relationships between local and ambient conditions. To find local conditions over the various regions of the aircraft in terms of ambient conditions it is convenient to deal with the local Mach numbers (M_1) outside the boundary layer.

Figure 4 shows typical variations. It can be seen that for many regions M_1 is not very far from M_0, although the differences are certainly significant. For the intake ducts, however, the local Mach number is very different from the aircraft Mach number.

Now consider how the basic heat transfer equations may be expressed in terms of the known ambient conditions (suffix "0"), in conjunction with the local Mach number which is presumed known.

The energy equation may be written:

$$i_{TOT} = i_0 + \tfrac{1}{2} u_0^2 = i_1 + \tfrac{1}{2} u_1^2$$

or

$$i_{TOT} - i_0 = \tfrac{1}{2} a_0^2 M_0^2$$

where a_0 = speed of sound in free stream.

Remembering that the temperature-average specific heat, C'_p is defined by $i \equiv C'_p T$ the energy equation may be written:

$$i_{TOT} = i_0 \left\{1 + \left[\frac{\gamma-1}{2} \cdot \frac{C_p}{C'_p}\right]_0 M_0^2\right\}$$
$$= i_1 \left\{1 + \left[\frac{\gamma-1}{2} \cdot \frac{C_p}{C'_p}\right]_1 M_1^2\right\} \quad . \quad (5)$$

2.5. LOCAL ENTHALPY

Therefore
$$i_1 = \frac{i_{TOT}}{\left\{1 + \left[\frac{\gamma-1}{2} \cdot \frac{C_p}{C'_p}\right]_1 M_1^2\right\}} \quad . \quad (6)$$

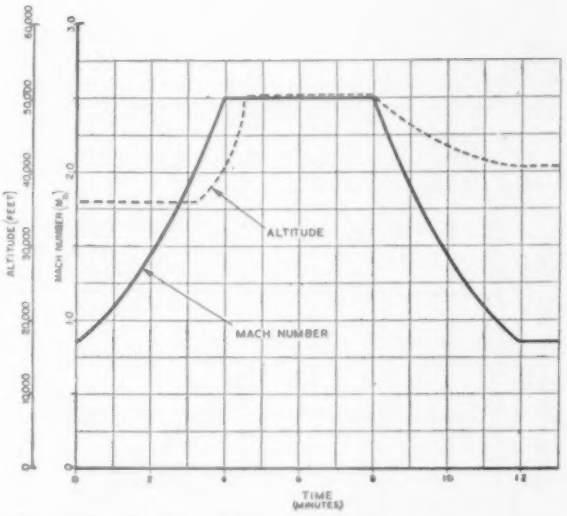

FIGURE 3. Typical sortie (long subsonic cruise, followed by acceleration, climb and high-speed run).

Note that the term in square brackets is a function only of the temperature or enthalpy indicated by the suffix. In ordinary compressible flow aerodynamics, of course, this term is taken to remain constant at $\frac{\gamma-1}{2}$, or for $\gamma = 1{\cdot}4$, at a value of 0·2. Fig. 5 shows the actual variation of the term with local temperature. It can be seen that at 1,300°K (which corresponds roughly with total temperature at a flight Mach number of 5) the term has dropped about 12 per cent below the value usually assumed. For temperatures less than about 600°K, corresponding with M_0 less than 3·0, the error due to taking this term equal to 0·2 is essentially less than 3 per cent. For larger temperatures, of course, it

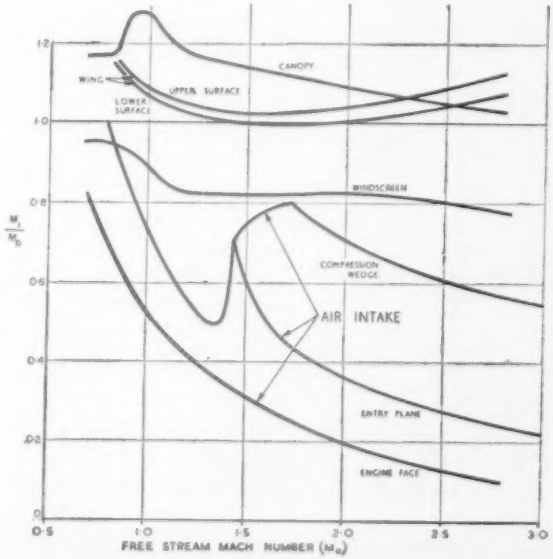

FIGURE 4. Typical local Mach numbers in terms of free stream Mach number.

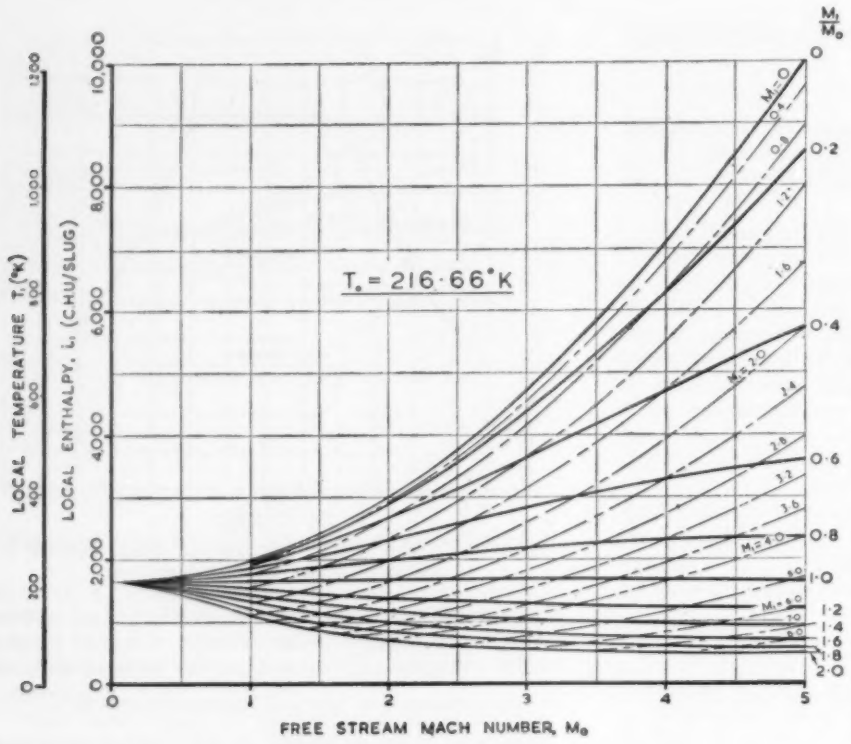

FIGURE 6. Local enthalpy in terms of M_0 and M_1.

is wiser to take note of the variation, as has been done in Figs. 6, 7 and 8.

2.6. FORCING ENTHALPY

Now from equations (2), (5) and (6) it is possible to express the boundary layer "forcing enthalpy" (or "adiabatic wall enthalpy" as it is often called) in terms of the total enthalpy and the local Mach number as shown in equation (7):

$$i_F = \frac{i_{TOT}}{\left\{1+\left[\frac{\gamma-1}{2}\frac{C_p}{C'_p}\right]_1 M_1^2\right\}}\left(1+r^*\left[\frac{\gamma-1}{2}\frac{C_p}{C'_p}\right]_1 M_1^2\right) \quad (7)$$

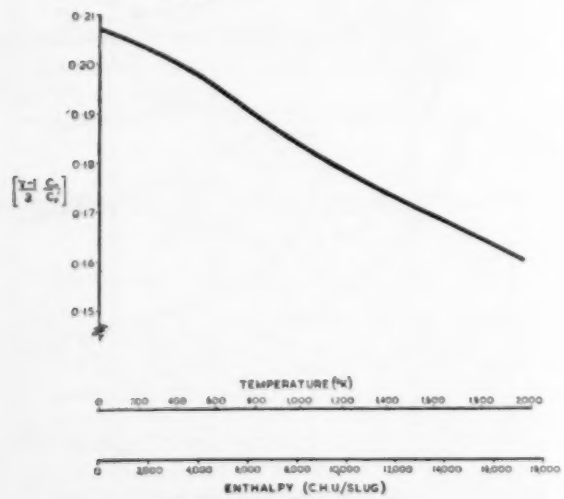

FIGURE 5. Coefficient of M^2.

The enthalpy recovery factor r^* varies only a little, for flight conditions, being roughly 0·84 for laminar flow and about 0·89 for turbulent boundary layers. A rather more detailed consideration is given in the appendix.

2.7. EFFECTIVE ENTHALPY

It was pointed out earlier that part of the effective enthalpy for the boundary layer was independent of the wall temperature. This part (i^*_B) also can be expressed in similar fashion to that shown for the forcing enthalpy, thus:

$$i_B^* = \frac{i_{TOT}}{\left\{1+\left[\frac{\gamma-1}{2}\frac{C_p}{C'_p}\right]_1 M_1^2\right\}} \times \left(0{\cdot}46+0{\cdot}16\,r^*\left[\frac{\gamma-1}{2}\frac{C_p}{C'_p}\right]_1 M_1^2\right). \quad (8)$$

Evidently for the special condition when the wall temperature is equal to the forcing temperature (zero heat transfer) the *whole* of the effective enthalpy can be expressed similarly:

$$i_E^* = \frac{i_{TOT}}{\left\{1+\left[\frac{\gamma-1}{2}\frac{C_p}{C'_p}\right]_1 M_1^2\right\}} \times \left(1+0{\cdot}7\,r^*\left[\frac{\gamma-1}{2}\frac{C_p}{C'_p}\right]_1 M_1^2\right). \quad (9)$$

It is interesting to note the similarity of equations (6) to (9).

Now it is obvious that both the total and the local enthalpies can vary over very wide ranges, but it is convenient that a wide range of possible altitudes can be linked to a few values of ambient temperature. For brevity, the graphs shown are based on the standard stratospheric temperature. It is possible, without serious error, to use the enthalpy graphs for other atmospheric temperatures by applying the appropriate factor to all ordinates.

For given ambient temperature, of course, the total enthalpy depends only on the free stream Mach number. The remaining terms of equations (6) to (9) then depend

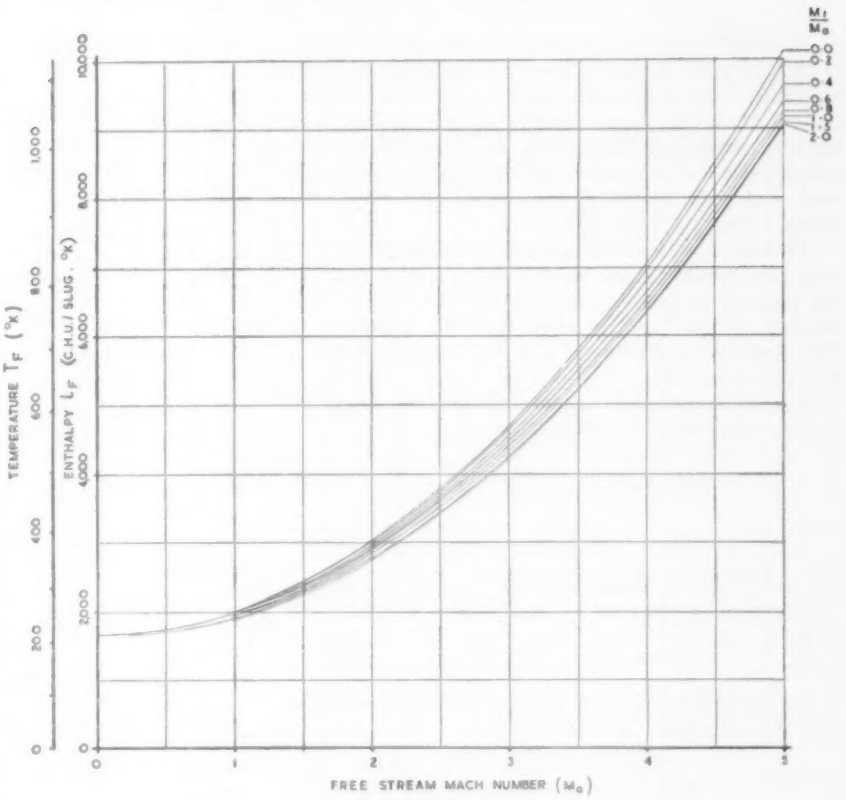

FIGURE 7. Boundary layer "forcing" enthalpy ("adiabatic wall enthalpy").

on both M_0 and the local Mach number, through the local enthalpy. Any of these equations, therefore, can be plotted graphically as a function of M_0 and M_1 only.

Figure 6 shows a graph of local enthalpy in terms of M_0 and M_1/M_0, through equation (6). The curve for $M_1=0$ gives the total enthalpy. It is evident that local enthalpy varies over a wide range. Fig. 7 shows a similar plot of the forcing enthalpy, showing that i_F varies relatively little with local Mach number.

A "carpet" plot could, of course, be used to expand the curves for forcing enthalpy. Such a presentation is shown in Fig. 8 for the boundary layer dependent part of the effective enthalpy.

It has now been shown how many of the required boundary layer enthalpy values can be found from the sortie data, without reference to the wall temperature. The heat transfer rate equations, however, contain terms which depend on the wall temperature, as will be seen next.

3. Heat Transfer Coefficient

The heat transfer relationships will be developed first for the more important case of turbulent boundary layer flow. The laminar flow equations will be shown briefly at a later stage. These developments start on the same lines as used by Monaghan[2].

3.1. TURBULENT BOUNDARY LAYER

$$\left.\begin{aligned} &\text{and} \quad k_H{}^* = 0{\cdot}61\, C_F{}^* \\ &\qquad C_F{}^* = 0{\cdot}288\,(\log_{10} R_e{}^*)^{-2{\cdot}45} \end{aligned}\right\} \quad . \quad (10)$$

$$\text{whence} \quad k_H{}^* = 0{\cdot}176\,(\log_{10} R_e{}^*)^{-2{\cdot}45} \quad . \quad (11)$$

3.2. REYNOLDS NUMBER

How can the effective Reynolds number be found in terms of known data? Let us assume that the Mach number outside the boundary layer is practically constant from the leading edge of the body to the location considered. If this were not the case, the Reynolds number for a local point would have to be based on the boundary layer thickness at the point.

Taking $R_e{}^* = \dfrac{\rho^* u_1 x}{\mu^*}$

and using $\rho^* = \dfrac{p_1}{RT^*}$, $u_1 = a_1 M_1$

we get $R_e{}^* = \dfrac{p_1 a_1 M_1 x}{R T_1 \mu_1}\left(\dfrac{T_1 \mu_1}{T^* \mu^*}\right) = R_{e1}\left(\dfrac{T_1 \mu_1}{T^* \mu^*}\right)$. (12)

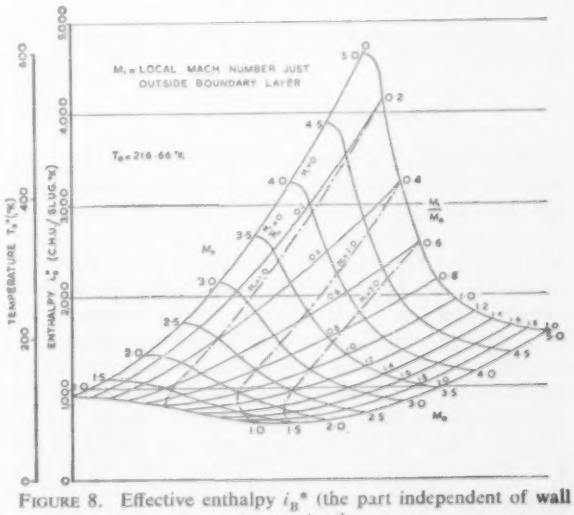

FIGURE 8. Effective enthalpy $i_H{}^*$ (the part independent of wall temperature).

A difficulty enters here since it is not easy to relate p_1 to M_1 by the treatment given for enthalpy changes. Naturally, in some cases the value of p_1 will be obvious, while if M_1 is known the pressure can always be found from an enthalpy-entropy chart. It is interesting, however, to examine the relationship between ambient and local Reynolds numbers on an approximate basis, taking C_p and γ constant.

To make allowance for non-isentropic compression from free stream conditions, the ratio of local reservoir pressure to free stream reservoir pressure may be denoted by the local pressure recovery factor, ε_1. This factor is usually known (*e.g.* for air intake ducts) as a function of M_0.

For constant specific heats, the effective Reynolds number can now be expressed thus:

$$R_e^* = (F_M R_{e0}) \frac{T_0 \mu_0}{T^* \mu^*} \quad . \quad . \quad (13)$$

$$\text{where } F_M = \varepsilon_1 \frac{M_1}{M_0} \left(\frac{1 + \frac{\gamma-1}{2} M_0^2}{1 + \frac{\gamma-1}{2} M_1^2} \right)^{\frac{2\gamma-1}{2(\gamma-1)}} \quad (14)$$

$$\text{or for } \gamma = 1{\cdot}4: \quad = \varepsilon_1 \frac{M_1}{M_0} \left(\frac{1 + \frac{1}{5} M_0^2}{1 + \frac{1}{5} M_1^2} \right)^4$$

Going back to the heat transfer coefficient equation (11), this becomes:

$$k_H^* = 0{\cdot}176 \left[\log_{10} \left(F_M R_{e0} \right) + \log_{10} \left(\frac{T_0 \mu_0}{T^* \mu^*} \right) \right]^{-2{\cdot}45} \quad (15)$$

which can evidently be plotted as a function of the two arguments contained in the parentheses. The first of these arguments can be defined completely from the sortie data, but the term involving $(T^* \mu^*)$ depends on the wall temperature. We now proceed to see how this coefficient fits into the calculation of heat transfer rates.

3.3. HEAT TRANSFER RATE

Equation (4) was:

$$q = \rho^* u_1 k_H (i_F - i_W)$$

but proceeding as above this can be re-written in the form:

$$q = p_0 a_0 M_0 \frac{1}{R} F_M \left(\frac{k_H^*}{T^*} \right) (i_F - i_W) \quad . \quad (16)$$

This equation is instructive, since it shows that the rate of heating is proportional to the atmospheric pressure, to F_M and to (k_H^*/T^*). Now an increase in F_M also leads to a slight decrease in (k_H^*/T^*), as shown in Fig. 9, but the explicit factor is much more powerful.

In Fig. 9, the parameter quoted for the various curves is i^*/i_0. Strictly, the proper parameter is $(T_0 \mu_0)/(T^* \mu^*)$, but for any practical atmospheric temperature the error due to using i^*/i_0 as parameter is negligible. For calculations involving various ambient temperatures it is more accurate to use graphs of k_H^*, instead of (k_H^*/T^*), and make separate allowance for T^*. It is felt that this procedure is simpler and quicker than that outlined in the present Royal Aeronautical Society data sheets.

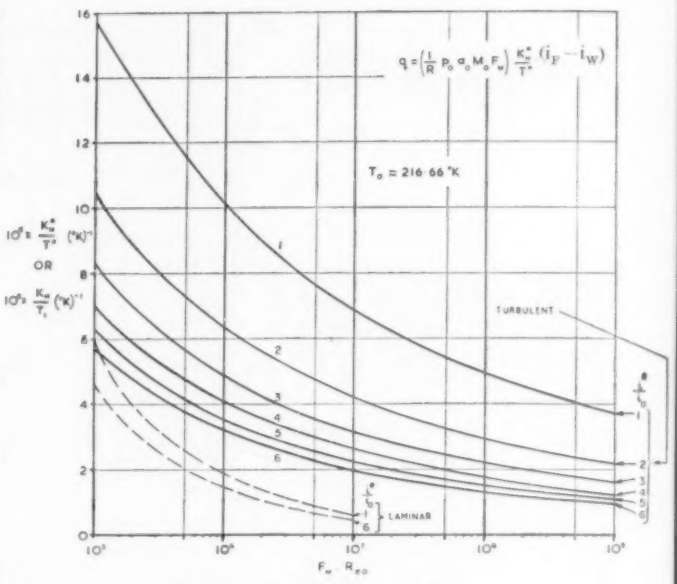

FIGURE 9. Heat transfer coefficient.

Figure 10 shows some typical variations of F_M. The large values of F_M for the air intake are noteworthy; these show why intakes heat rapidly. Note that if $M_1 = M_0$, but $\varepsilon_1 < 1$, as for a blunt-nosed flat plate at high supersonic speed, then F_M is less than unity—so that heat transfer is reduced, and transition is delayed.

3.4. LAMINAR BOUNDARY LAYER

The expressions appropriate to a laminar boundary layer can be developed in a similar way to that given

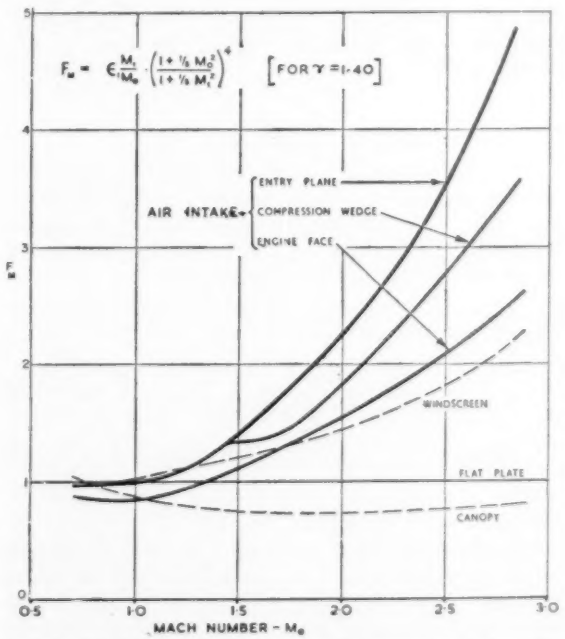

FIGURE 10. Typical Reynolds number correction factor, F_M.

for turbulent flow. The starting point is the familiar equation:

$$k_H^* = \tfrac{1}{2} C_F^* (Pr^*)^{-\frac{2}{3}} \quad . \quad . \quad (17)$$

Taking $$C_F^* = 0{\cdot}664 (R_c^*)^{-\frac{1}{2}} \quad . \quad . \quad (18)$$

we get $$k_H^* = \frac{0{\cdot}332}{(R_c^*)^{\frac{1}{2}} (Pr^*)^{\frac{2}{3}}}$$

Using equation (13) this becomes:

$$k_H^* = \frac{0{\cdot}332}{\left(F_M R_{c_0}\right)^{\frac{1}{2}} \left[\left(\frac{T_0 \mu_0}{T^* \mu^*}\right)^{\frac{1}{2}} (Pr^*)^{\frac{1}{3}}\right]} \quad . \quad (19)$$

Again, this equation can be plotted in terms of the expressions separated in the denominator, as shown in Fig. 9.

It has now been shown how the basic equations of boundary layer heat transfer can be expressed in terms of known data, with the effects of wall temperature isolated, as far as necessary. It is now possible to consider how these equations may be applied to the calculation of transient structure temperatures.

4. Transient Temperatures in a Shell

Figure 11(*a*) shows a simple element of the surface of an aircraft structure. The basic equation involved is simply that of continuity, or conservation of heat. In literal terms this may be written for an arbitrary time interval:

$$\text{Rise in amount of heat stored} = \text{heat input} - \text{heat output} \quad . \quad . \quad (20)$$

The literal form of this equation is emphasised, for in a practical structure there may be a large number of heat input and output terms. This equation, of course, is exact for any time interval. The application of this equation will be illustrated by a simple example.

Consider the state of knowledge about the element during the finite time interval from time (t) to time ($t+\delta t$), as shown in Fig. 11(*b*). To keep the principles clear, for this example it is assumed that the sole heat input to the element is the convective heat transfer from the boundary layer, while the only heat outputs are radiation from the outer surface and convective or conductive heat transfer to an interior mass. The diagram indicates that the boundary layer enthalpy (i_F) is known over the whole of the time interval, but the temperatures of the shell (T_W) and of the interior (T_C) are known only at the beginning of the interval, as a result of the computations for the previous time interval.

If a time interval (δt) is chosen so that the variations of temperature with time of the various interacting masses are not markedly non-linear, and such that the radiating surface temperature at the end of each interval is not much more than, say, 10 per cent greater than that at the beginning of the interval, the parts of the heat transfer equation may be written with good accuracy as follows. (The bar over any quantity denotes a time average over the interval, which is

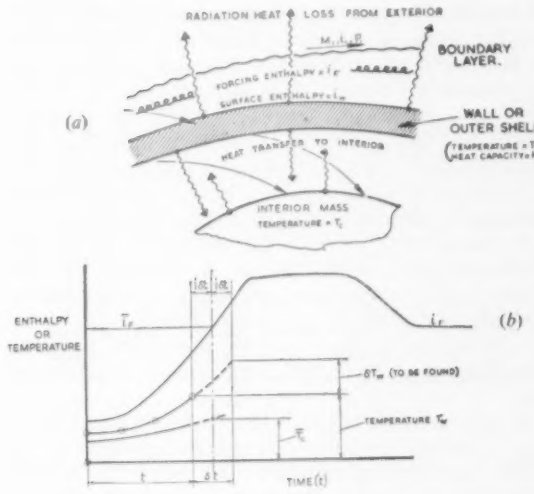

FIGURE 11.

assumed to be practically equal to the value of the quantity at a time halfway through the interval; *i.e.* at $(t+\frac{1}{2}\delta t)$.)

Rise in heat stored $= h_0 \delta T_W$

where h is the heat capacity of the shell (C.H.U./sq. ft. °K).

Heat input from boundary layer

$$= \frac{1}{R} \overline{p_0 a_0 M_0 F_M} (\bar{k}_H^* / \bar{T}^*) (\bar{i}_F - i_W - \tfrac{1}{2} \bar{C}_p \delta T_W) \delta t$$

where $\bar{C}_p$ is evaluated at temperature $\bar{T}_W$.

Heat output due to radiation

$$\simeq E\sigma T_W^4 (1 + \frac{2}{T_W} \delta T_W) \delta t$$

Heat output by internal convection

or conduction $= K (T_W - \bar{T}_C + \tfrac{1}{2} \delta T_W) \delta t$

. . . . . (21)

Collecting all the terms involving the shell temperature increment we get

$$\delta T_W = \frac{\frac{1}{R} \overline{p_0 a_0 M_0 F_M} (\bar{k}_H^* / \bar{T}^*) (i_F - i_W) - K (T_W - \bar{T}_C) - E\sigma T_W^4}{h/\delta t + \tfrac{1}{2} \bar{C}_p (\frac{1}{R} \overline{p_0 a_0 M_0 F_M}) (\bar{k}_H^* / \bar{T}^*) + \tfrac{1}{2} K + 2E\sigma T_W^3}$$

. . . . . (22)

This equation looks rather horrible, but in practice it is easy enough to evaluate, the numerator and denominator being merely sums of simple terms. The only terms involved which are not known quite accurately at the beginning of the time interval are $\bar{T}_C$, $\bar{C}_p$ and $(\bar{k}_H^* / \bar{T}^*)$. To estimate these, graphs can be plotted as the calculations proceed, and extrapolated to the middle of the time interval concerned. This procedure amounts to taking a second approximation

in advance. No case has yet been encountered where a further iteration has been required. Extension of this process to any number of interacting masses and heat sources is obvious. It is also obvious that variations with structure temperature of the surface emissivities, the structural heat capacities and the convective heat transfer coefficients to the interior can all be accommodated readily by using the appropriate coefficients at the mid-points of the time intervals.

A discussion of methods for estimating natural and forced-convection heat transfer coefficients in the interior would require a separate paper. In the absence of a special discussion, it must suffice to state baldly that the estimates shown in this paper are based on generalisations of the usual dimensionless heat transfer data.

It may be asked whether there is any overall gain in time or labour compared with simpler formulae which require shorter time intervals. Comparative calculations have shown that for given accuracy the present method requires only about one-fifth the number of time intervals, so that the computation time overall is reduced appreciably.

5. Typical Results

Let us now look at some typical results of practical kinetic heating calculations. Consider one type of rear fuselage cross section which has to be considered (Fig. 12).

It can be seen that in the cross section shown there are a considerable number of interacting components. Thus surrounding the upper three-quarters of the periphery of the jet pipe is a radiation reflector. Outside this lies the fuselage skin with immediate stringers and frames. At this station very little ventilating air passes down the fuselage between the jet-pipe and the radiation reflector and between the reflector and the fuselage skin, though most sections of this type have

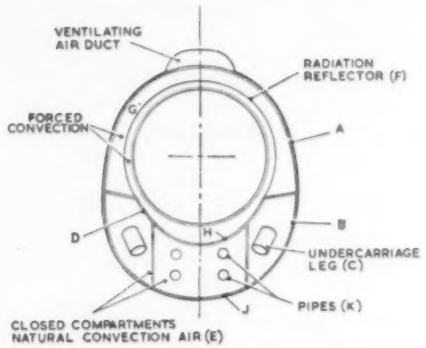

FIGURE 12. Typical cross section of rear fuselage.

large forced convection airflows. Radiative heat transfer occurs between jet-pipe and reflector, and between reflector and fuselage. Convection heating of the ventilating air occurs in both annular passages, and the ventilating air warms up as it passes downstream. The outer skin, of course, undergoes the usual convective and radiative heat transfer processes on the outside.

The lower part of the fuselage is divided into three compartments, inside which natural convection and radiation are the major heat transfer mechanisms, with various pipes in these compartments forming the major masses. The air in these lower compartments acts as an intermediate small mass facilitating convective heat transfer to the pipes.

Results of calculations for this cross section are shown on Fig. 13. The temperatures attained by the various bits of outer skin are practically equal. It is notable that the pipes and the undercarriage legs in the lower bays barely warm up at all, although the air in these compartments gets quite hot. The radiation reflectors also get hot, while keeping the outer skin temperatures down.

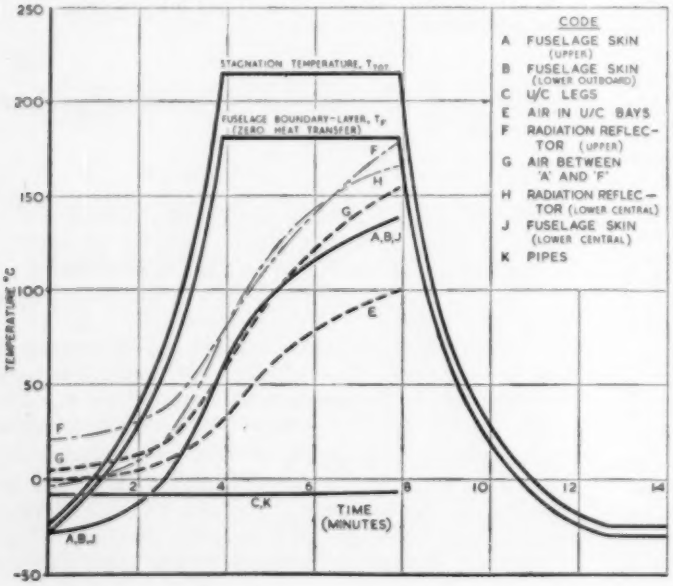

FIGURE 13. Transient temperatures for typical cross section of rear fuselage.

5.1. FURTHER TYPICAL RESULTS

Some more typical results are shown on Fig. 14. The most interesting point about these is the difference of shape of the various transient temperature curves. Other significant results include the high intake skin temperature, due to the large F_M and absence of radiation cooling—and the high final temperature attained by the centre fuselage skin. This was because the radiation reflector was omitted over the jet engine compressor, because this was a relatively cool part of the engine. In practice, a reflector would be installed as a result of this calculation.

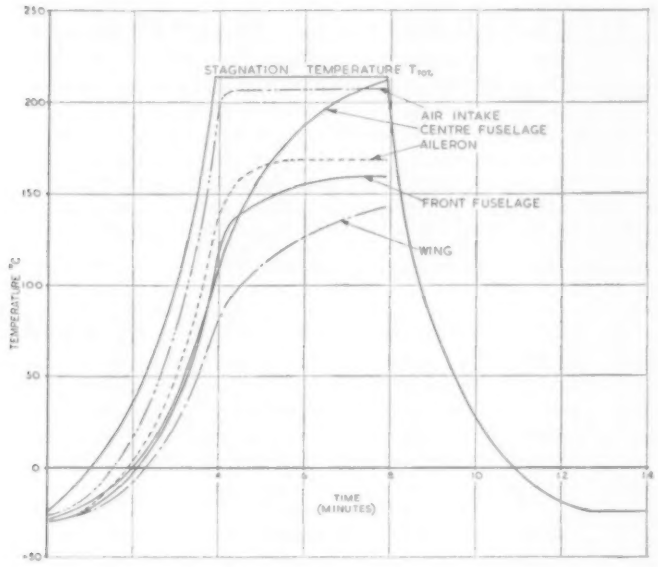

FIGURE 14. Typical transient skin temperatures.

This sort of calculation can be repeated all over an aeroplane. When all the results are complete, it is interesting to see how all the regions fit together. It is then possible to see whether it is necessary in some localities to take account of conduction *along* the length of the skin.

6. Concluding Remarks

An outline has been given of means for predicting the transient and equilibrium temperatures in practical aircraft structures subjected to kinetic heating.

This outline was considered in two parts, the first of which comprised a new presentation of the boundary layer heat transfer relationships, which includes provision for any region of the aircraft where the local Mach number differs from the free stream value. Emphasis was placed on the separation of terms dependent on wall temperature from those which depend only on the prescribed flight path conditions.

The second part outlined a method for the estimation of transient structural temperatures. It was shown that this method could be applied easily to complicated structures with general modes of heat transfer between the various parts. It is simple to deal with variations of heat transfer coefficient, heat capacity and thermal emissivity. Examples have been given of typical results obtained by means of this method.

APPENDIX

ENTHALPY RECOVERY FACTOR

In connection with equation (7) it was remarked that (for flight conditions) the enthalpy recovery factor varied only a little.

In some calculations, however, it may be desirable to work as accurately as possible, so that the known variations should then be taken into account.

For laminar boundary layers, it is well known that the enthalpy recovery factor may be taken as

$$r^* = (Pr^*)^{\frac{1}{2}} \quad . \quad . \quad . \quad (23)$$

For turbulent boundary layers, it is indicated in Ref. 2 that the enthalpy recovery factor tends to decrease with increasing Reynolds number. Taking a plausible mean line through the results quoted, a reasonable law would appear to be:

$$r^* \simeq 0{\cdot}898 - 0{\cdot}015 \log_{10}\left(\frac{R_{e1}}{10^6}\right) \quad . \quad (24)$$

Making allowance for the fact that the quoted results are based on wind tunnel experiments, and making use of equations (12) and (13), it is possible to express (24) as follows:

$$r^* \simeq 0{\cdot}98 - 0{\cdot}015\left[\log_{10}(F_M \cdot R_{e0}) - \log_{10}\left(\frac{T^*\mu^*}{T_0\mu_0}\right)\right] \quad (25)$$

This is plotted in Fig. 15, with i^*/i_0 as parameter.

REFERENCES

1. ECKERT, R. G. (1954). Survey on Heat Transfer at High Speeds. W.A.D.C. Technical Report 54-70. April 1954.
2. MONAGHAN, R. J. (1955). On the Behaviour of Boundary Layers at Supersonic Speeds. *Proceedings of the Fifth Anglo-American Aeronautical Conference, Los Angeles, 1955.* Institute of the Aeronautical Sciences, 1955.
3. MONAGHAN, R. J. (1955). Formulae and Approximations for Aerodynamic Heating Rates in High Speed Flight. Unpublished Ministry of Supply Report, Oct. 1955.

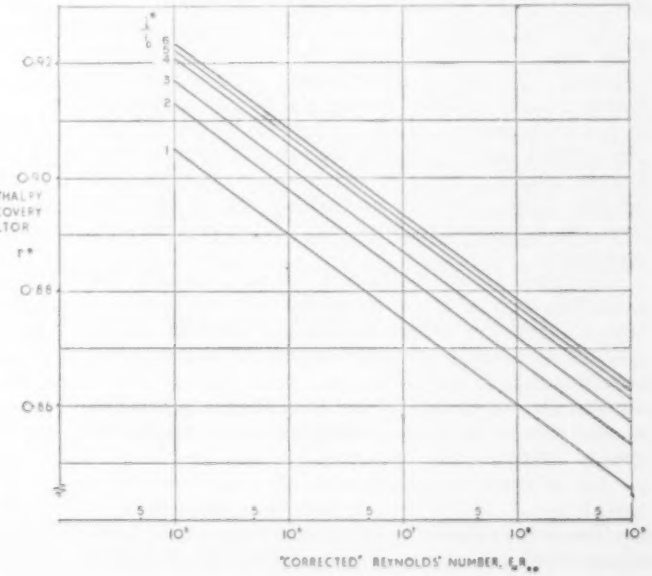

FIGURE 15. Tentative enthalpy recovery factor (turbulent boundary layer).

Advantages and Limitations of Models

A. J. SOBEY, M.A.

(Structures Department, Royal Aircraft Establishment)

SUMMARY: The use of models for structural test investigations in the presence of kinetic heating effects is examined. The principal features of the complex process to be represented are discussed under the classifications external air flow, internal heat transfer, elastic response. Of these the second is found to influence most model design, and an analysis of a typical structure is included to illustrate the various contributions to internal heat transfer.

1. Introduction

To establish the value of an aircraft structure designed to fly at supersonic speeds, certain ground tests will have to be undertaken. Requirements for such an undertaking have been given by Walker[27], who has considered problems of full scale testing.

Models are one possible source of information on the value of a structure and in view of the extensive use of them in aeronautical research in the past, it is pertinent to invite consideration of their assets and liabilities in structural testing.

In aeronautics, models have been used more as small scale work pieces than as working representations of complete systems. As such they have enabled extensive experiments to be made, from among the results of which general observations have been made by interpolation. In this way theory is verified and information relevant to conditions not accurately simulated may be determined.

In the case of a structural test, in the presence of a complex system of mechanical forces under a general thermal field, the replica test, if it is to be of value, must reproduce faithfully the conditions of the prototype. The opportunity for sequence tests and interpolation is not possible. Accordingly, accurate representations of the thermal field are considered as obligatory in any satisfactory testing with models.

The most obvious advantage that a model affords is the reduction in the volume of the complex equipment required for ground examination, should synthetic heating be used. Clearly, loading and heating a structure in a wind tunnel or in an open jet is hardly feasible and synthetic heating of a full scale structure is accepted. For the model a choice of techniques is available, and whether wind tunnels or artificial sources of heat are used, the equipment required will, of necessity, be very specialised.

However, as will be shown, unless a material for modelling with a lower diffusivity may be found, a higher intensity of surface heating in the model will be needed, even though the actual quantity of heat required may be reduced.

In order to rationalise the modelling requirements in the general case, some observations on models in general follow.

NOTATION

Two-letter symbols in parentheses are non-dimensional parametric groups, taking the first two letters of the name with which they are generally associated.

The units used are the most convenient in terms of which to express each parameter. The number of basic dimensions is four, but additional dimensions are introduced for reasons of clarity or when justified in the text.

Small case letters are used, where possible, for scale lengths and suffixes m, p refer to model and prototype respectively*. Thus $l = L_m/L_p$ defining the scale of length. Suffixes a, i, r, s stand for airstream, insulant, refrigerator and structure respectively.

The length L, time T, force F, mass M and heat flux Q quantities are total measurements. Temperature θ is a relative measurement so that ϑ implies

$$\frac{\theta \text{ relative to datum in model}}{\theta \text{ relative to datum in prototype}}.$$

However, the use of the Absolute Scale for temperature in radiative or material property variation requires

$$\vartheta = \frac{\theta \text{ abs., model}}{\theta \text{ abs., prototype}}$$

V	velocity of fluid (external or in cavity)	LT^{-1}
a	velocity of sound in fluid	LT^{-1}
ρ	density	$L^{-3}M$
C_p	specific heat	$MQ\theta^{-1}$
μ	viscosity of fluid	$L^{-1}T^{-1}M$
α	coefficient of linear expansion	θ^{-1}
K	thermal conductivity	$L^{-1}T^{-1}Q\theta^{-1}$
H	heat transfer coefficient	$L^{-2}T^{-1}Q\theta^{-1}$
σ	Stefan-Boltzmann constant	$L^{-2}T^{-1}Q\theta^{-4}$
ξ	surface emissivity	none
R	interface thermal resistance	$L^2TQ^{-1}\theta$
g	gravitational acceleration	LT^{-2}
E	Young's modulus	$L^{-2}F$
ν	Poisson's ratio	none
τ_{ij}	stress components	$L^{-2}F$
U_i	displacements	L
ε_{ij}	strain components	none
V_i	body force components	$L^{-3}F$
t_i	thickness of insulant	L
B_i	parts of surface (*see* Appendix)	

2. Review of Models

Two systems are similar if, in the general case, scale lengths exist (as many as the order of the base of dimensions describing the physical process) in terms of

*Except C_p.

which all physical items in the one system have values determined (*i.e.* derived) in terms of the basic scales. This ideal similarity constitutes a projectivity between kindred systems and is essentially geometric in inspiration. This viewpoint is admirably presented in Duncan's book[7] using the vector concept of base dimension and measure formula. Such a system can rarely be achieved except in simple models with a limited field of enquiry.

In fact a physical model in which work units may have different scales depending on their origin is not unusual. In the thermal structure the energy stored elastically is of an entirely different order of magnitude to the thermal energy and may be considered independent of it, so that thermal effects based on one set of scale lengths may coexist with elastic effects based on a different system, *e.g.* as far as the thermal structure is concerned, the base of dimensions is four for purely thermal effects, plus a fifth appropriate to the elastic case, say the force unit. If, further, dynamical effects are present, of which the mechanical forces are part, the system of scales adopted must be consistent with the elastic similarity established. The mixing of units is permissible if, and only if, there are grounds for dissociating phenomena, and that each class of phenomena is dimensionally self-consistent. A second instance of this occurs in the process of natural convection where the mass unit associated with the fluid motion is, in practice, independent of the unit of heat transported (*see e.g.* Bosworth[5]).

3. Limitations on Experimental Design

Whenever it is necessary to regard as significant a physical parameter, a condition is imposed on the choice of scale lengths which is in the nature of an experimental constraint. Each such constraint reduces the number of such degrees of freedom in the choice of scale lengths, and clearly the number of degrees of arbitrariness in choice of scale length is the excess of base dimension over number of constraints; if this is zero a unique model is possible. In particular we note that if this excess is negative (*e.g.* number N of significant parameters (including base dimensions) is greater than twice the order of the base dimension M) then the existence of a model is fortuitous.

To facilitate model design we require to keep down N. When $N=2M$ and a unique model is possible, it is important that at least one parameter shall change, otherwise the model is identified with the prototype. In particular, if material properties are important, then the number of such parameters which may be scaled cannot be as great as M, unless the material is changed.

The importance of material parameters in model design is obvious. The choice of material implies the acceptance of certain parameters and the appropriate scaling conditions which go with them. If the number of these is large, difficulties are apparent, and in the thermal transfer/elastic response similitude analysis, there are numerous such internal parameters which dominate similitude (*e.g.* K, C_p, α, ν, E).

Although five such material properties are significant in this problem, they do not determine scale lengths entirely since elastic work and thermal work are treated as independent. Further α and E (which, like the non-dimensional ν, are of no interest in the heat transfer problem) only occur in disjunction when strain must be scaled as one to one, which is not obligatory in many of the practical cases.

Accordingly we can expect two constraints from material properties on the heat transfer process (leaving two degrees of freedom in the choice of scales) and a supplementary condition based on elastic similarity which is taken up in an essentially independent fifth scale (say elastic work, or force). Since E, α, ν are all significant parameters peculiar to the elastic problem, there may be additional constraints on the thermal similarity process induced by elastic requirements. For example, if ν varies with temperature in a random manner, and ν is important, then a one-to-one temperature scale would have to be accepted. (For practical materials, such as light alloy or steel, there is no evidence of any significant variation of ν over the working range.)

4. Thermo-Elastic Similitude

The similitude conditions appropriate to the statically/dynamically loaded structure in the presence of thermal effects have been considered by several writers including O'Sullivan[20], Madejski[18] and Heldenfels[11]. The first two writers consider heat transfer within the structure by conduction alone, but Heldenfels notes the significance of external radiation and joints.

Many writers have given similitude criteria for general heat transfer, including Bosworth[5], Fishenden and Saunders[9] and McAdams[17], usually from the viewpoint of understanding the convective transfer process as a substitute for precise quantitative analysis, and other writers have considered dimensional analysis as applied to elastic phenomena. These include Goodier[13], Durelli, Phillips and Tsao[8] and by the three authors cited who consider the compounding of similitude requirements for thermal and elastic effects. In addition thermoelastic similarity has been discussed by Mindlin and Salvadori[12] and by Green, Radok and Rivlin[10].

In the present paper, emphasis on the internal heat transfer process is made, so that similarity conditions for thermoelastic phenomena are dominated by acceptance of the need for accuracy in heat transference. When this is done, the choice of scale lengths is so restricted (except in the simplest case) that the elastic process is seen as supplementary and scaled using as many of the scales derived from thermal arguments as is possible.

5. Similarity Criteria—Supersonic Aerodynamics

The nature of supersonic flow is well understood and the prediction of heat transfer from the supersonic boundary layer has been given extensive mathematical treatment and experimental verification. (*See e.g.* Taylor[25] and the references given there to the work of Monaghan and Eckert.)

The general survey (on a dimensional basis) shows that the non-dimensional heat transfer coefficient (the

Stanton number, St) is a function of the Reynolds number, Re, Prandtl number, Pr, and the Mach number, Ma, for a given profile

where
$$St = H/\rho V C_p$$
$$Re = V\rho L/\mu$$
$$Pr = \mu C_p/K$$
$$Ma = V/a$$

and all the dimensioned parameters refer to the air. In a practical attempt to simulate the supersonic flow, it will, in general, be necessary to have similar Re, Pr, Ma in order to obtain a correct St. If this is attempted in a wind tunnel using air as the working fluid, it is usually impossible to arrange for Re and Ma both to be similar. Moreover, the choice of units appropriate to the air and to the structure must be the same, *e.g.* time and temperature scales must be consistent in fluid and structure [$\vartheta_a = \vartheta_s$].

Because of the well established validity of the supersonic flow theory and its mathematical interpretation, the computed heat transfer may be a more satisfactory basis for experimental heating tests than attempting general aerodynamic similitude. Unless properties of the airstream are significant (as in aeroelastic tests), the synthesis of heat transfer can be considered, using, for example, lamps. (*See* Taylor[26].)

6. Similarity Criteria—Internal Heat Transfer

Thermal conduction, being dependent on material properties (thermal conductivity and thermal capacity) dominates the modelling in as much as conductive heat transfer is always important and the scaling of two parameters limits the choice of modelling scales, two constraints being imposed. Further, surface effects may be important, such as radiation and interface resistance, together with transfer media in contact with the surface (Fig. 1).

Accordingly the modelling criteria are developed from the central idea of conduction always being present. Radiation is added both as an internal distributive phenomenon and as an influence on external heat input. Joints are treated as an adjunct to conduction.

If the transfer to and from, and within the conductive parts of the structure is simulated, the choice of scale lengths is seen to be very limited, if possible, and convection, insulation and refrigerative elements are simulated as additional phenomena to the main transfer process.

When heat transfer within the structure is by conduction alone, we require the identity in the two systems of the

$$\text{Fourier number} = Fo = \frac{KT}{\rho C_p L^2}$$

and the
$$\text{Biot number} = Bi = HL/K.$$

The former requirement governs the correctness of the thermal diffusion within the structure and the latter ensures the appropriateness of the heat intensity on the surface of structure. These conditions follow at once

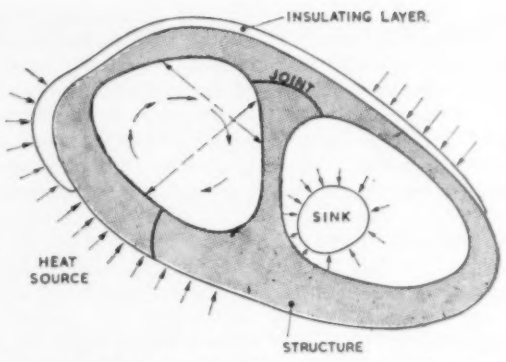

FIGURE 1. Schematic representation of heated aircraft structure.

by noting if K_s and $(\rho C_p)_s$ are to scale consistently

$$K_m/K_p = ql^{-1}t^{-1}\vartheta^{-1}$$
$$(\rho C_p)_m/(\rho C_p)_p = ql^{-2}\vartheta^{-1}$$

so that the scale for time, t, is chosen to be

$$l^2 (K/\rho C_p)_m/(K/\rho C_p)_p$$

and the heat flux, temperature scales are related by

$$q = l^2\vartheta\,(\rho C_p)_m/(\rho C_p)_p.$$

These conditions are consistent with a surface intensity of heating which will scale as $\frac{K_m}{K_p}\, l^{-1}\vartheta$ which in most practical cases will exceed unity. In order to avoid this it is clearly necessary to use a material of lower conductivity in the model. To avoid compression of the time scale, a lower diffusivity is required. Fig. 2 indicates the order of diffusivity of some common materials and it will be seen that avoiding too severe a compression of the time scale requires the use of materials such as steel for light alloy, with some non-metallic medium as a working material for steel, *e.g.* if the prototype is light alloy and the model is in stainless steel, pure conductive requirements are satisfied with scales $q = 1{\cdot}52l^2$, $t = 17{\cdot}5l^2$, and the heat transfer coefficient scales as $0{\cdot}0867l^{-1}$. Surface intensity of heating scales is $0{\cdot}0867l^{-1}\vartheta$.

This system would be feasible for thermal (analogue) investigations were it not that the scaling requirements may not be sustained when allowance is made for the material property changes with temperature.

If radiation and conduction are both significant, as in an integral construction, evacuated box, we require identity of four criteria: namely, two conductive and two radiative.

HL/K, KT/L^2, C_p, $\frac{C}{\vartheta}$ and $\sigma\theta^3 L/K$ must be similar.

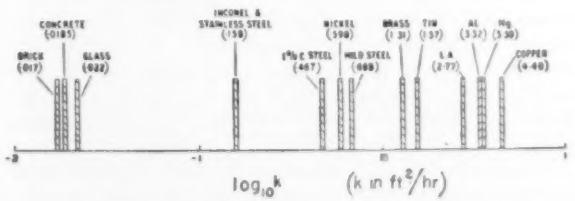

FIGURE 2. Diffusivity of some common materials.

If compatible scale lengths are found, l, q, t, ϑ, we require

$$(K_m/K_p) = ql^{-1}t^{-1}\vartheta^{-1}$$
$$(\rho C_p)_m/(\rho C_p)_p = ql^{-3}\vartheta^{-1}$$
$$ql^{-2}t^{-1}\vartheta^{-4} = 1$$

from which we deduce

$$l = \frac{K_m}{K_p}\vartheta^{-3}$$
$$q = \left(\frac{K_m}{K_p}\right)^3 \frac{(\rho C_p)_m}{(\rho C_p)_p}\vartheta^{-8}$$
$$t = \frac{(K_\rho C_p)_m}{(K_\rho C_p)_p}\vartheta^{-6}$$

e.g. L.A. prototype, stainless steel model yields

$$l = 0{\cdot}09\vartheta^{-3}, \qquad q = 0{\cdot}00113\vartheta^{-8}, \qquad t = 0{\cdot}141\vartheta^{-6}$$

CONCLUSIONS

If the original material is used, and we are forced to use an identical temperature scale, the only model is the identity. For the scales given the surface intensity of heating will scale as ϑ^4. Thus for a reduced intensity we require $\vartheta < 1$ and a reduced total heat input is best achieved by using a low conductivity model, *e.g.* stainless steel for L.A. or even glass for stainless steel.

If the radiation is a direct gain or loss from an external surface* rather than an exchange between interior surfaces, we may relax the condition of independent satisfaction of

$$\mathfrak{C}_m = \mathfrak{C}_p \text{ and } (\sigma\theta^3 L/K)_m = (\sigma\theta^3 L/K)_p$$

to read

$$\left(\frac{\mathfrak{C}}{\mathfrak{C}}\sigma\theta^3 L/K\right)_m = \left(\frac{\mathfrak{C}}{\mathfrak{C}}\sigma\theta^3 L/K\right)_p$$

This may be assumed whenever the "form factor" for the radiation transfer is not critical upon the greyness of the surface to give

$$l = \frac{K_m \mathfrak{C}_p}{K_p \mathfrak{C}_m}\vartheta^{-3}; \quad q = \left(\frac{K_m}{K_p}\right)^3 \left(\frac{\mathfrak{C}_p}{\mathfrak{C}_m}\right)^2 \frac{(\rho C_p)_m}{(\rho C_p)_p}\vartheta^{-8};$$
$$t = \frac{(K_p C_p)_m}{(K_p C_p)_p}\left(\frac{\mathfrak{C}_p}{\mathfrak{C}_m}\right)^2 \vartheta^{-6}$$

The form factor can be estimated (*see e.g.* Fishenden and Saunders[9], Bosworth[5], McAdams[17]) and its dependence on greyness determined.

When the material properties vary with temperature, similarity of two systems is ensured if the two systems are described by a common non-dimensional boundary value problem. The heat conduction uniqueness theorem for this case is given in the Appendix.

In the general conduction case, similarity of two systems (m, p) is assured if

$$l^2 = t \text{ and } \vartheta = 1$$

The boundary conditions impose:

over B_1 no constraint
over B_2 a constraint on the impressed heat intensity
over B_3 a constraint on the heat transfer coefficient.

These are

$$q = lt\vartheta = l^3$$

and

$$H_m/H_p = l^{-1}.$$

We note that the requirement that

$$\vartheta = 1, \quad K_m = K_p, \quad (\rho C_p)_m = (\rho C_p)_p$$

leads to scale lengths with only one degree of freedom, namely,

$$(q, l, t, \vartheta) \text{ are } (l^3, l, l^2, 1).$$

If one further condition is used to determine l then this condition must be between physical properties different in the two systems else $q = l = t = \vartheta = 1$ and no modelling is possible. This eliminates the possibility of further scaling of

(*a*) absolute items (*e.g.* radiation),
(*b*) further material properties (*e.g.* α).

The conclusion reached is that if the variation of material properties is important, the imposition of identity in the temperature scale admits of similitude only in the conductive case. This is of interest only for high solidity structures such as thin solid wings where radiation effects are absent.

Is $\vartheta = 1$ obligatory? To avoid this restriction we must examine the temperature dependence of significant material properties on the absolute temperature.

The characteristic temperature dependence of material properties on temperature is given in Fig. 3* from which we note that over quite large and practical ranges of temperature, the four properties shown are significantly power laws in the absolute temperature. This can be used to scale temperature, namely:

if K is $K_0\theta^\lambda$

(ρC_p) is $(\rho C_p)_0\theta^\mu$

and

$$\theta_m = \vartheta\theta_p \ (\theta_m, \theta_p \text{ on Absolute Scale})$$

then

$$K_m = \vartheta^\lambda K_p, \quad (\rho C_p)_m = \vartheta^\mu (\rho C_p)_p$$

and the heat conduction equation in the model is

$$\operatorname{div}_m (K_m \operatorname{grad}_m \theta_m) = (\rho C_p)_m \frac{\partial \theta_m}{\partial T_m}$$

i.e.

$$\frac{1}{l}\operatorname{div}_p \left\{\vartheta^\lambda K_p \frac{1}{l}\operatorname{grad}_p (\vartheta\theta_p)\right\} = \vartheta^\mu (\rho C_p)_p \frac{\vartheta}{t}\frac{\partial \theta_p}{\partial T_p}$$

which is identical with the equation for the prototype if

$$l^2\vartheta^{\mu-\lambda} = t$$

On the boundary we require that the heat inflow shall be suitably scaled, *i.e.* HL/K the same in both systems, *i.e.*

$$H_m = \vartheta^\lambda l^{-1} H_p$$

*When only the radiation from the external surface is significant, and synthetic methods of heating the structure are used, the radiative constraint on scaling can be avoided, and design proceeds as for the purely conductive model since the appropriate surface heating technique may be presumed to be adjusted to allow for the radiative gain or loss.

*Prepared from Refs. 16 and 19.

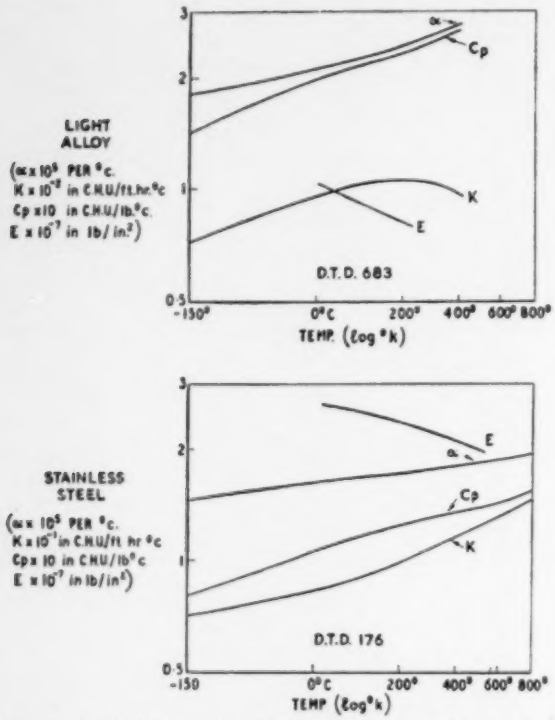

FIGURE 3. Variation of material properties with absolute temperature.

from which there follow for the basic scale lengths: $q=\vartheta^{\mu+1}P$; $t=\vartheta^{\mu-\lambda}P$; l and ϑ arbitrary (two degrees of freedom for pure conductive similarity).

If, in addition, we have radiation effects of importance so that $\mathfrak{F}$ has to be the same and also the radiant/conductive heat units are to scale, then

$$l=\vartheta^{\lambda-3};\quad q=\vartheta^{3\lambda+\mu-3};\quad t=\vartheta^{\lambda+\mu-6}$$

In practice the indices λ, μ are quite small, and the problem of complying with the requirements for this case is not significantly changed from the isotropic case.

Practical values for λ, μ are given in Table I.

For modelling with a reduced linear scale, we require $l<1$, *i.e.* $\vartheta>1$ (*i.e.* surface heat intensity scale >1). If the prototype is operating at $-56°C$ (*i.e.* $\theta_p=217°K$) and the model in the laboratory at 20°C (*i.e.* $\theta_m=293°K$) $\vartheta=1{\cdot}35$ and l is 0·43 for L.A. and 0·46 for steel. These scale lengths are unlikely to be useful in practice for the aircraft case. Further the time scale is severely shortened and likelihood of useful data being obtained diminished.

For a significant modelling scale, l, we need a large change in the emissivity, and the blackening of interior faces of a model may lead to a practicable scaling. However, the prototype surface conditions may be temperature-dependent (McAdams) and the inconstancy of $\mathfrak{F}$ may prove a major limitation. Rough steel surfaces have $\mathfrak{F}$ of the order of 0·5 so that a further 50 per cent reduction in l may be possible. The experimental prospects are, however, slim.

TABLE I

	L.A. (*D.T.D.*683)	*Stainless Steel* (*D.T.D.*176)
Temperature range	0-200°C	0-500°C
λ	0·19	0·40
μ	0·28	0·24

7. Allowance for Resistive Joints

In all the cases considered (conduction with or without radiation, isotropic or non-isotropic materials) the effect of joints has been ignored. They are readily incorporated into the scaled system when the scale lengths are determinate, namely,

$$R_m/R_p=l\frac{K_p}{K_m}$$

This relation must be independent of temperature and will be so, for the cases discussed, if either R is constant, or a power law in the Absolute temperature.

Thus a smaller scale model demands a reduction in joint resistance for the same material, which in practice will prove very difficult to accommodate. If joints are important, they are almost certain to prove obstructive in model design.

8. Influence of Convection

The general (Dimensional Analysis) criteria require the identity in model and prototype of the Nusselt number, Nu, the Grashof number, Gr, and the Prandtl number, Pr, given by

$$\left.\begin{aligned} Nu&=(HL/K)\\ Gr&=(L^3\rho^2g\alpha\theta/\mu^2)\\ Pr&=(\mu C_p/K)\end{aligned}\right\}$$ where the physical properties K, μ, and so on, refer to circulating (convecting) fluid in cavity

If conductive (and/or radiative) effects have been used to fix the scales for q, l, t and ϑ in the structure. these parameters fix properties of the fluid.

The Nu criterion ensures that the units of heat flux in solid and fluid are consistent.

Gr and Pr ensure similarity of the flow process. It is clear that to satisfy all these criteria a fluid with an unusual range of parameters will be required. Attempts to simplify these requirements by insisting only that Nu and $GrPr$ be identical as suggested by Bosworth[5] will alleviate somewhat the experimental difficulty.

The physical properties of fluids are not variable over the range likely to be demanded and if natural convection is known to be important, a mismatching of the convective transfer is likely.

9. Insulants

In practice, an insulating layer is a region of very low conductivity thinly applied so that surface-wise heat transfer is negligible compared with normal heat transfer. Accordingly the full simulation of thermal diffusion in the insulant may be ignored and the thickness of the insulant adjusted so that Ht_i/K_i remains constant in the two systems. This should present no practical difficulty

unless a poor conductor is used as a model material (*e.g.* glass for steel).

10. Heat Sinks

These may be of two kinds: —

(*a*) Heat absorption associated with change of state of the sink material. This requires the temperature of the change of state to scale (Abs.) as ϑ. This should not present practical difficulties. If the heat sink completely changes state, complications arise, but this case is not of interest.

(*b*) Heat is absorbed by a refrigerative element according to

$$Q_r = H_r(\theta_r - \theta)$$

This requires $H_r L_s / K_s$ to scale in order to have a consistency of the thermal units. Implicitly $\theta_{rm} = \theta_{rp}\vartheta$.

11. Similarity Criteria—Elastic Effects

In the general isotropic case we have P, E, ν, L, τ_{ij}, α, θ involved, requiring τ_{ij}/E, P/EL^2, ν, $\alpha\theta$ to be consistent in both model and prototype.

In this context E, ν and α are assumed independent of θ. Thus

$$\tau_{ij}/E = f(\rho/EL^2,\ \nu,\ \alpha\theta).$$

Under special conditions, we may drop the dependence of τ_{ij} on ν and may expect to change the scale for $(\alpha\theta)$ or strain. To do this we require a mathematical examination of the boundary value problems associated with (linear) small-strain elasticity. Similarity criteria based on this kind of assumption have been given by Mindlin and Salvadori[13], and by Green, Radok and Rivlin[10], but the non-isotropy of the material properties has not been investigated. When material properties vary with temperature, these requirements imply that if the original material is used, $\vartheta = 1$, which has been seen in the section on heat transfer to be necessary when radiation and convection are important. To examine $\vartheta \neq 1$ requires the detailed elaboration of the linear problem of elasticity with its less restrictive criteria. To justify the similarity criteria based on a common form we require a uniqueness theorem, which is given in the Appendix.

If two elastic systems have the same non-dimensional boundary value equations they lead to the same stress system.

Elastic Similarity Conditions in a three-dimensional medium with elastic constants dependent on temperature can be most readily developed by the following argument.

Strain
$$\varepsilon_{ij} = \frac{1+\nu}{E}\tau_{ij} - \frac{\nu}{E}\delta_{ij}\tau_{aa} + \delta_{ij}\alpha\theta \quad . \quad . \quad (1)$$

using the tensor notation of Sokolinkoff[24].

The compatibility of strain and equilibrium of stress subject to certain stress boundary conditions ensure the correctness of the stress/strain system.

Compatibility requires

$$\varepsilon_{ij,\,mn} + \varepsilon_{mn,\,ij} = \varepsilon_{im,\,nj} + \varepsilon_{nj,\,im} \quad . \quad . \quad (2)$$

Equilibrium

$$\tau_{ij,\,j} + V_i = 0 \quad . \quad . \quad . \quad (3)$$

where V_i are the body force vector components per unit volume.

If we arrange that

$$(\varepsilon_{ij})_m = e\,(\varepsilon_{ij})_p \quad . \quad . \quad . \quad (4)$$

at all points, e being a constant, then for isotropic length scaling, if (2) is satisfied in the model it is automatically satisfied in the prototype.

For equation (4) to hold universally

$$\left(\frac{1+\nu}{E}\tau_{ij}\right)_m = e\left(\frac{1+\nu}{E}\tau_{ij}\right)_p \quad . \quad . \quad (5)$$

$$\left(\frac{\nu}{E}\tau_{kk}\right)_m = e\left(\frac{\nu}{E}\tau_{kk}\right)_p \quad . \quad . \quad (6)$$

$$(\alpha\theta)_m = e\,(\alpha\theta)_p \quad . \quad . \quad . \quad (7)$$

From (5), (6),

$$\nu_m = \nu_p \quad . \quad . \quad . \quad . \quad (8)$$

$$\frac{(\tau_{ij})_m}{(\tau_{ij})_p} = \text{Scale for stress} = e\frac{E_m}{E_p} = \frac{(E\alpha\theta)_m}{(E\alpha\theta)_p} = \frac{(E\alpha)_m\vartheta}{(E\alpha)_p} \quad (9)$$

If E and α are together proportional to some power of the absolute temperature, (9) gives a constant scaling factor for stress even when temperature is scaled.

From equation (3)

$$V_m/V_p = \frac{(E\alpha)_m}{(E\alpha)_p}\vartheta l^{-1} \quad . \quad . \quad (10)$$

giving the scale for body force intensities.

If we are dealing with two-dimensional stress systems in the isotropic case, it is well known that for the problem with boundary conditions or stress, ν is unimportant for singly connected regions since the Airy stress function (stress potential) is independent of ν. Only when conditions at the boundaries involve displacement is ν important, or when we have multiply connected regions when the displacement analysis is implicit.

Thus the requirement that ν is to be reproduced is important in all cases except the special one of plane strain or generalised plane stress (when ν may be arbitrary) for singly connected zones. This has more pertinence to components than full scale structures. The special conditions on the scales for plane strain and generalised plane stress have been given by Green, Radok and Rivlin[10] who use an advanced treatment based on complex stress potentials. Their conclusions —that ν is important except in the single connected case—are that no subset of the similarity criteria holds. This follows from connectivity arguments of the kind given.

The scale for stress implies a scale for force, and also for work. Units of energy can be mixed in this way (heat and work having, in general, different scales) provided that there is no significant interaction. This has been considered by Hemp[12], and by Broglio and

Santini[16] and found not to be significant for the non-thermal shock case.

If we have dynamical effects, *e.g.* in the analysis of the natural frequencies of systems, we should amend the equations of equilibrium to read:

$$\tau_{ij,j} + V_i = \rho \frac{\partial^2 U_i}{\partial T^2}$$

leading to

$$(\rho U)_m/(\rho U)_p = \frac{(E\alpha)_m}{(E\alpha)_p} l^2 \vartheta l^{-1}.$$

But the scale for strain

$$e = \frac{U_m L_p}{U_p L_m} = \frac{\alpha_m}{\alpha_p} \cdot \vartheta$$

whence

$$\frac{U_m}{U_p} = \frac{\alpha_m l \vartheta}{\alpha_p}$$

gives scale for displacements and therefore

$$\rho_m/\rho_p = E_m t^2/E_p l^2$$

gives scale for density. This is a condition which will be difficult to achieve in practice owing to impositions on the time scale from conduction considerations.

Elastic properties may be examined for the elastostatic case, but dynamical effects will be difficult to accommodate.

12. Plasticity

When the elastic limit is exceeded and time-dependent strains are significant, the cumulative strain is a function of time, stress, temperature, and, possibly, the strain already produced. Madejski[18] has examined an idealised case, but similarity will, in general, require an identity of the strain, stress, temperature scales, and possibly of time as well (if the strain rate is dependent on the cumulative strain as in work hardening). Such conditions are not tenable except in idealised component study and the presence of plastic strains is regarded as a major limitation on the design of experiments.

13. A Design Study

To show the likely significance of some of the internal heat transfer parameters discussed, calculations have been made using the structure of the original Hoff-Torda[14] study modified in the following ways:

(*i*) By the inclusion of web-flange interface resistances.

(*ii*) By allowance for radiation heat transfer between flange and web.

(*iii*) By allowance for free convective heat transfer between flange and web.

The geometry of the system is given in Fig. 4. The material is steel and the significant properties are as follows. The structure is subjected to an instantaneous heating according to

$Q = H(\theta_{ow} - \theta_{flange})$

Q being the heat intensity

H the heat transfer coefficient

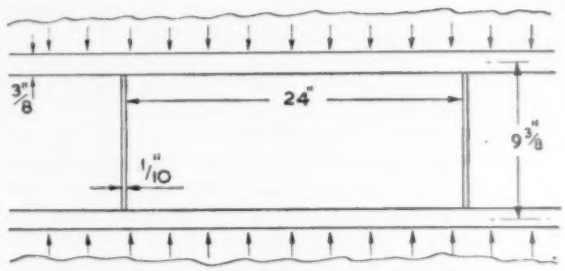

FIGURE 4. The Hoff study wing.

θ_{ow} is the zero heat transfer wall temperature (taken as 300°C).

Following Hoff, H is taken as 90 CHU/ft.² hr. °C, a heat transfer coefficient consistent with $Ma = 5$, $Re = 10^7$ at 40,000 ft. (*see* Taylor [25]).

This example has been discussed extensively in the literature, in addition to the original reference, by Parkes[21] who added the effect of flange-web solidity variation, by Pohle and Oliver[22] who gave the exact conductive solution, and by Biot[4] who used the installation as an application of his variational technique.

In none of the papers cited is the effect of joint resistance, internal convection or radiation examined.

The calculations include the effect of a thermal resistance joint at the web-flange junction, the resistance of which is varied over a wide range (of 200 to 1) and is likely to include all practical constructions. See, *e.g.* Barzelay and Holloway[1] and Barzelay, Tong and Hollo[2], who give measured values of joint resistances for sheet constructions of the stringer-panel type. Bernard[3] gives an indication of the effect of impact pressure on the joint resistance for blocks.

The radiative transfer is calculated using the classical theory (*see, e.g.* Fishenden and Saunders[9] or Bosworth[5], and as Hoff[15]) assuming an internal surface emissivity of one half. The evidence available on the likely value of $\frac{\varepsilon}{0}$ is scant, but McAdams[17] gives an extensive list of known values which bracket the one-half region. As this survey is intended only to be comparative, the value chosen is not critical, and the selected value is thought to be representative of typical interior surfaces. The problem of the dispersal of non-absorbed radiation is ignored, and is unlikely to have a significant influence on the trends of the calculations.

To estimate convection effects, the following hypotheses have been used:

(*i*) The thermal capacity of the convective fluid is zero.

(*ii*) The wall fluid heat transfer coefficient may be estimated from flat plate formulae, *e.g.* a value of heat transfer coefficient of $H = 1{\cdot}2$ CHU/ft.² hr. °C (McAdams[17] and Zemansky[26]) so that the heat transfer between walls is at the rate of $H(-\theta_{mean} + \theta_{wall})$ where θ_{mean} is the effective transfer temperature of the convective fluid and is calculated on the basis of assumption (*i*).

Numerical analyses have been conducted using a matrix technique suitable for use on an electronic com-

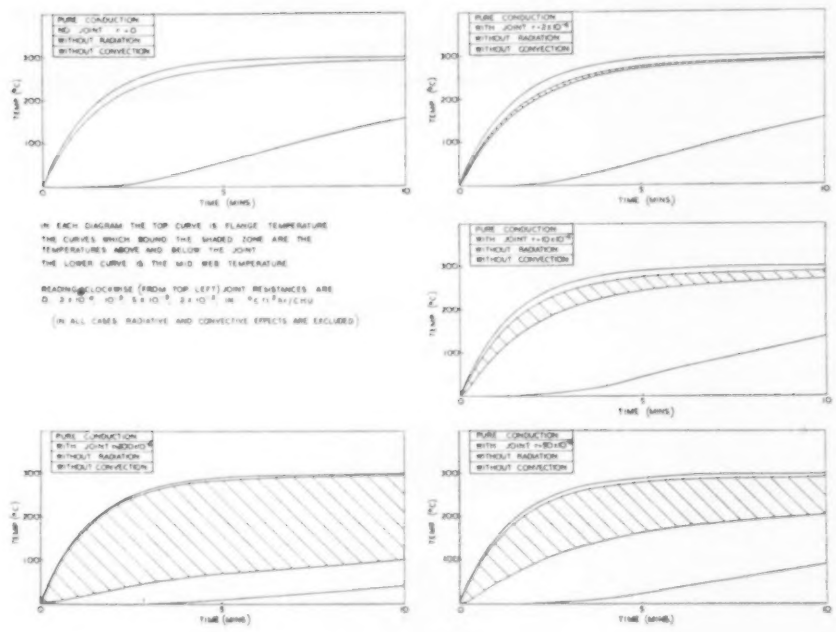
PURE CONDUCTION
WITHOUT RADIATION
WITHOUT CONVECTION
TEMP (°C)
TIME (MINS)
IN EACH DIAGRAM THE TOP CURVE IS FLANGE TEMPERATURE
THE CURVES WHICH BOUND THE SHADED ZONE ARE THE
TEMPERATURES ABOVE AND BELOW THE JOINT
THE LOWER CURVE IS THE MID WEB TEMPERATURE
(IN ALL CASES RADIATIVE AND CONVECTIVE EFFECTS ARE EXCLUDED)

FIGURE 5. Temperature distributions through the study wing as a function of joint resistance.

puter. Results are presented for a range of resistances from 2×10^{-4} to 2×10^{-2} °C ft.² hr. per CHU, which covers the measured range of values (Figs. 5, 6). A likely value of interface resistance for riveted or bolted constructions is 5×10^{-3} °C ft.² hr. per CHU[1], at which value a significant transfer is brought about by convection and radiation.

This particular example has been selected because of its historical significance and the relative solidity of the flange and web imply (for the heating rate given) a thermal stress which is very high (in the Hoff-Torda case of about 80 per cent the maximum possible zE times the excess of adiabatic wall temperature over initial temperature). In this case the effect of the joint is to increase the maximum tensile stress from 80 per cent to 90 per cent of the maximum possible over the extreme range of joint resistance. The resulting alleviation of stress by flange-web transfer (convection and radiation) is shown in Fig. 7.

When the flange soak temperature is raised, the effect of radiation and convection is intensified and a survey of the relative proportions of heat received by the web due to pure conduction across the joint, to radiation, and to convection is given in Fig. 8 as a function of flange temperature and joint resistance.

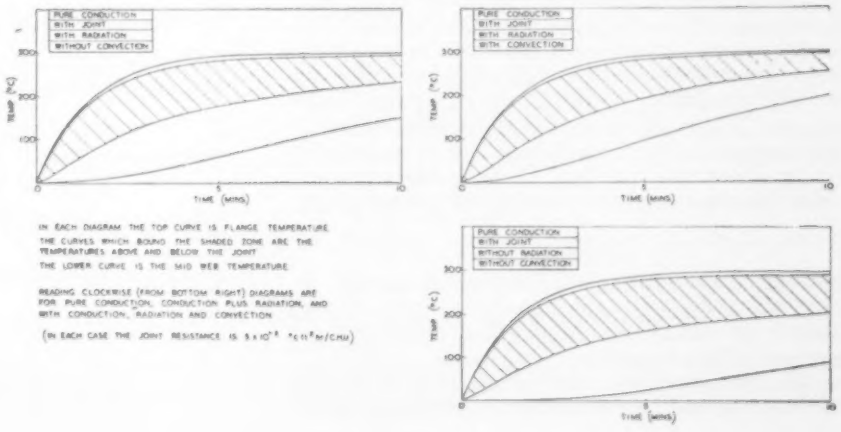
PURE CONDUCTION
WITH JOINT
WITH RADIATION
WITHOUT CONVECTION
WITH CONVECTION
WITHOUT RADIATION
TEMP (°C)
TIME (MINS)
IN EACH DIAGRAM THE TOP CURVE IS FLANGE TEMPERATURE
THE CURVES WHICH BOUND THE SHADED ZONE ARE THE
TEMPERATURES ABOVE AND BELOW THE JOINT
THE LOWER CURVE IS THE MID WEB TEMPERATURE
READING CLOCKWISE (FROM BOTTOM RIGHT) DIAGRAMS ARE
FOR PURE CONDUCTION, CONDUCTION PLUS RADIATION, AND
WITH CONDUCTION, RADIATION AND CONVECTION
(IN EACH CASE THE JOINT RESISTANCE IS 5 x 10⁻³ °C ft² hr/CHU)

FIGURE 6. Effect of radiation and convection on the heat transfer within the study wing.

The evidence of this example is that for the jointed structure, the simplification of heat transfer to a purely conductive process is misleading and a proper allowance for all these effects will have to be made in any practical testing.

14. Conclusions

In the simplest of cases, a solid structure, the internal heat transfer may be represented satisfactorily by a scale model with two degrees of freedom. Allowance for surface radiation (when aerodynamic sources of heat are used) reduces the model to a one degree of freedom one. Size of model may be chosen arbitrarily. In this case the elastic properties may be represented also. Change of material is possible only when the material properties are constant throughout the experiment, *i.e.* when they are independent of temperature.

When properties vary with temperature it is possible to use the same material with an identical temperature scale. In this case the conductive representation leaves only one degree of freedom and external radiation cannot be catered for. For practical materials a shift in temperature scale is possible owing to the special nature of the temperature dependence of the appropriate physical properties. When this is done a model is possible, but when conduction and radiation are allowed for, a unique scaling is determined. This leads to a smaller model only if the absolute temperature is increased in scale. This will be the case for stratosphere to laboratory scaling. Elastic effects are scaled as before.

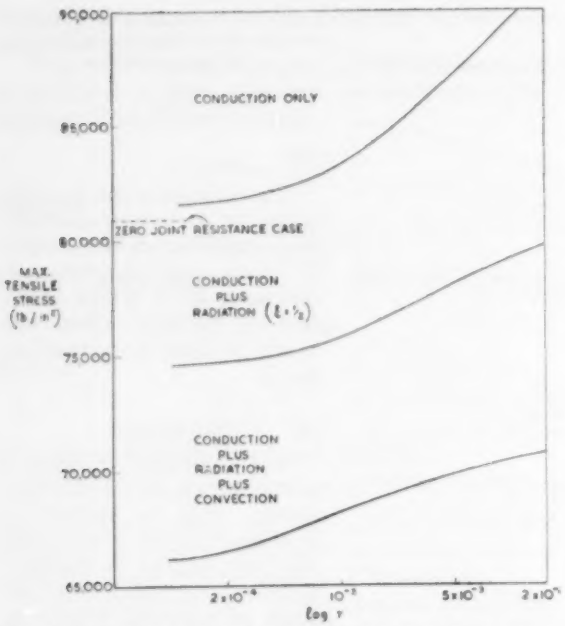

FIGURE 7. Estimates of maximum thermal stress (tensile) as a function of joint resistance.

If a high solidity structure is built up of components whose faces of contact are not on surfaces of zero heat transfer then the interface resistance will have to be scaled, and this will be very difficult in practice. For a reduced linear scale, the joint resistance has to be reduced unless a change of material is possible to one of greater conductivity.

For structures of low solidity the conditions of the examples given are complicated by internal radiation and convection, which are of increasing significance as joint resistance increases. If these phenomena are to be scaled, the experimental constraints are severe. A unique scaling is possible when the internal radiation is correctly simulated. To arrange for the convective process to be simulated correctly requires the fluid properties to change, and the appropriate fluid may not be available.

Elastic effects are correctly reproduced in the small strain case with a change of temperature scale owing to the apparent constancy of Poisson's ratio and the power law dependence of E with temperature over the working temperature range. Effects of interest outside the small strain theory (*e.g.* post buckling behaviour and permanent set) will require a one-to-one temperature scaling and restrict the field of application to purely conductive heat transfer cases, *e.g.* the solid structure.

APPENDIX 1

UNIQUENESS THEOREM FOR THERMAL CONDUCTION

In the non-isotropic case we may no longer use the method of dimensional analysis but boundary value problem analysis is required.

The heat conduction equation in the case of non-isotropic and/or temperature-dependent properties follows

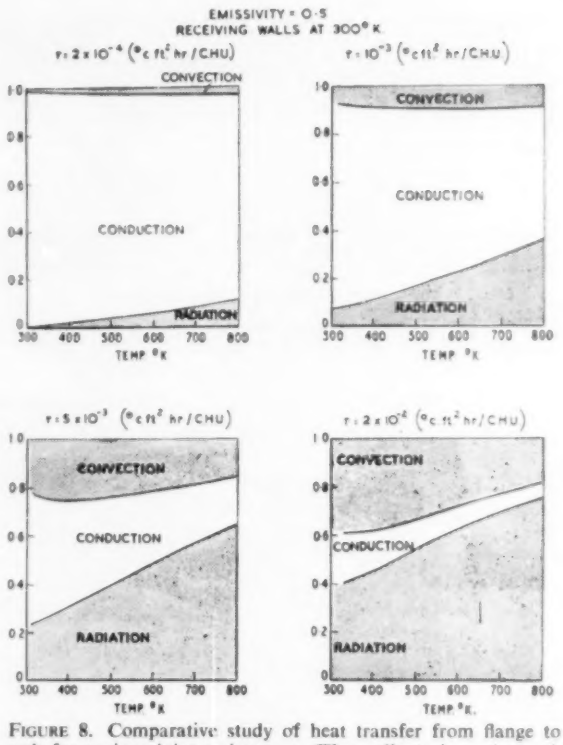
EMISSIVITY = 0·5
RECEIVING WALLS AT 300° K
γ = 2 × 10⁻⁴ (°c ft² hr/CHU)
γ = 10⁻³ (°c ft² hr/CHU)
γ = 5 × 10⁻³ (°c ft² hr/CHU)
γ = 2 × 10⁻² (°c ft² hr/CHU)
CONVECTION
CONDUCTION
RADIATION
TEMP °K

FIGURE 8. Comparative study of heat transfer from flange to web for various joint resistances. (The ordinate in each graph indicates the proportion of the total heat received by the web due to the three agencies indicated.)

at once from the conservation of energy within a volume V, as

$$\text{div}\,(K\ \text{grad}\,\theta)=\rho C_p\frac{\partial\theta}{\partial T}. \quad . \quad . \quad . \quad (1)$$

and the appropriate boundary conditions of practical interest are:

$$\left.\begin{array}{l}\text{over part } B_1 \text{ of the boundary, } \theta=\bar{\theta}\,(x,y,z,T) \text{ specified}\\ \text{over part } B_2 \text{ of the boundary, } \dfrac{\partial\theta}{\partial n}=\bar{\theta}'\,(x,y,z,T) \text{ specified}\\ \text{over part } B_3 \text{ of the boundary, } \dfrac{\partial\theta}{\partial n}=H'(\theta_0-\theta) \quad \text{specified}\end{array}\right\} \quad (2)$$

(n being a unit normal vector).

Subject to (2), (1) has a unique solution. For if there are two possible solutions

$$\theta_1\,(x,y,z,T) \text{ and } \theta_2\,(x,y,z,T)$$

with common

$$\theta_0\,(x,y,z,0) \text{ in } V$$

satisfying (1) and (2), then the difference

$$\theta=\theta_1-\theta_2 \quad \text{satisfies}$$

$$\text{div}\,(K\ \text{grad}\,\theta)=\rho C_p\frac{\partial\theta}{\partial T} \quad . \quad . \quad . \quad (3)$$

$$\theta=0 \text{ on } B_1;\ \frac{\partial\theta}{\partial n}=0 \text{ on } B_2;\ \frac{\partial\theta}{\partial n}=-H'\theta \text{ on } B_3. \quad (4)$$

Consider

$$\iint_B K\theta\frac{\partial\theta}{\partial n}\,dS=\iint_{B_1+B_2+B_3}\theta\,(K\ \text{grad}\ \theta)\,dS=-\iint_{B_3}KH'\theta^2\,dS$$

which is negative semi-definite.

By the divergence theorem this is

$$\iiint_V K\,(\text{grad}\ \theta)^2\,dV+\iiint_V\frac{\partial}{\partial T}\,(\rho C_p\theta^2)\,dV$$

Initially $\iiint_V \rho C_v\theta^2\,dV=0$ since $\theta_1\,(x, y, z, 0)=\theta_2\,(x, y, z, 0)$

The derivative of $\iiint \rho C_p\theta^2\,dV$ cannot therefore be negative with respect to time. Hence θ and grad θ vanish everywhere.

This uniqueness theorem is independent of the non-isotropy of K and ρC_p with respect to space and temperature. Obviously if K is time-dependent the proof fails, but this is of no interest. Thus we conclude that if two systems satisfy equations like (1) and boundary conditions (2) which can be reduced to a common non-dimensional form, then they are physically similar irrespective of the non-isotropy.

If $$\frac{x}{\xi}=\frac{y}{\eta}=\frac{z}{\zeta}=L_1;\ \frac{T}{\tau}=T_1;$$

then (1) reduces to

$$\text{div}\ (K\ \text{grad}\ \theta)=\frac{L_1^2\rho C_p}{T_1}\frac{\partial\theta}{\partial\tau}.$$

APPENDIX II

UNIQUENESS THEOREM FOR ELASTIC MATERIAL UNDER THERMAL STRESS FIELD (SMALL STRAIN THEORY)

Equilibrium

$$\tau_{ij,j}+V_i=0 \quad . \quad . \quad . \quad . \quad (5)$$

Strain

$$2\varepsilon_{ij}=U_{i,j}+U_{j,i} \quad . \quad . \quad . \quad (6)$$

Stress strain

$$\varepsilon_{ij}=\frac{1+\nu}{E}\tau_{ij}-\delta_{ij}\left(\frac{\nu}{E}\tau_{kk}-\alpha\theta\right) \quad . \quad . \quad (7)$$

Subject to boundary conditions

$$\left.\begin{aligned}U_i&=U_{i0}\ \text{over part}\ B_1\ \text{of the boundary}\\ T_i&=\tau_{ij}n_j=T_{i0}\ \text{over part}\ B_2\ \text{of the boundary}\end{aligned}\right\} \quad (8)$$

Then if two solutions $(U_i)_1$, $(U_i)_2$ of this system exist with associated stresses $(\tau_{ij})_1$, $(\tau_{ij})_2$ the difference system

$$\left.\begin{aligned}U_i&=(U_i)_1-(U_i)_2\\ \tau_{ij}&=(\tau_{ij})_1-(\tau_{ij})_2\end{aligned}\right\} \quad . \quad . \quad (9)$$

with strains $\varepsilon_{ij}=(\varepsilon_{ij})_1-(\varepsilon_{ij})_2$

satisfies

$$\tau_{ij,j}=0$$

$$\varepsilon_{ij}=\frac{1+\nu}{E}\tau_{ij}-\frac{\nu\delta_{ij}\tau_{kk}}{E} \quad . \quad . \quad . \quad (10)$$

Uniqueness then follows in the usual way by considering

$$\iint_{B_1+B_2}U_i\tau_{ij}n_j\,dS=\iiint U_i\,(\tau_{ij,j})\,dV+\iiint(U_{i,j})\,(\tau_{ij})\,dV$$

$$=2\iiint\tau_{ij}\varepsilon_{ij}dV>0$$

since the strain energy is positive definite.

Over B_1 $U_i=0$, over B_2 $\tau_{ij}n_j=0$;

hence $\iint U_i\tau_{ij}n_j dS=0$ and the two stress systems are identical.

This proof shows in addition that if $(U_i)_1\neq(U_i)_2$, the only difference possible is a displacement vector leading to zero stress, *i.e.* a rigid body displacement.

Thus a common non-dimensional boundary value problem structure ensures similarity of strain and stress, and of displacement if the systems are suitably orientated.

Further the temperature dependence or non-constancy of E, ν does not affect the proof.

REFERENCES

1. Barzelay, Martin E. and Holloway, George F. (1957). Effect of an Interface on Transient Temperature Distribution in Composite Aircraft Joints. N.A.C.A. T.N. 3824, April 1957.
2. Barzelay, M. E., Tong, N. N. and Hollo, G. (1954). Thermal Conductance of Contacts in Aircraft Joints. N.A.C.A. T.N. 3167, March 1954.
3. Bernard, J. J. (1958). La Resistance Thermique des Joints. A.G.A.R.D. Structures and Materials Panel, Copenhagen, October 1958.
4. Biot, M. A. (1957). New Methods of Heat Flow Analysis with Applications to Flight Structures. *Journal of the Aeronautical Sciences* 24, 12, pp. 857-73, December 1957.
5. Bosworth, R. C. L. (1952). *Heat Transfer Phenomena*. Associated General Publications, Sydney, 1952.
6. Broglio, L. and Santini, P., *High Temperature Effects in Aircraft Structures*. AGARDograph 28, Chapter 10.
7. Duncan, W. J. (1953). *Physical Similarity and Dimensional Analysis*. Edward Arnold & Co., 1953.
8. Durelli, A. J., Phillips, E. A. and Tsao, C. H. (1958). *Introduction to the Theoretical and Experimental Analysis of Stress and Strain*. McGraw-Hill, New York, pp. 278-302, 1958.
9. Fishenden, M. and Saunders, O. A. (1950). *An Introduction to Heat Transfer*. Oxford University Press, 1950.
10. Green, A. E., Radok, J. R. M. and Rivlin, R. S. (1958). Thermo-elastic Similarity Laws. *Quarterly of Applied Mathematics*, XV, 4, pp. 381-393, 1958.
11. Heldenfels, R. R. *Models and Analogs*. AGARDograph 28, Chapter 16.
12. Hemp, W. S. (1956). Fundamental Principles and Theorems in Thermoelasticity. *Aeronautical Quarterly*, Vol. 7, p. 184, August 1956.
13. Hetenyi, M. (*ed.*) *Handbook of Experimental Stress Analysis*, Appendix II. Goodier, J. N., *Dimensional Analysis*, pp. 1035-1045. Also Chapter 16, *Analogies*, by Mindlin, Raymond D. and Salvadori, Mario G.
14. Hoff, N. J. (1951). Structural Problems of Future Aircraft. *Proceedings of the Third Anglo-American Aeronautical Conference*, Royal Aeronautical Society, London, 1951. Appendix I by Torda, P. and Hoff, N. J., pp. 103-110.
15. Hoff, N. J. (1956). Comparison of Radiant and Conductive Heat Transfer in a Supersonic Wing. *Journal of the Aeronautical Sciences*, 23, 7, pp. 694-5, July 1956.
16. Lucks, C. F. and Deem, H. W. (1958). Thermal Properties of Thirteen Metals. *American Society of Testing Materials*, Philadelphia, 1958.
17. McAdams, W. H. (1954). *Heat Transmission*, 3rd Edition. McGraw-Hill, 1954.
18. Madejski, Jan (1957). *Rozprawy Insynierskie*, LXXVI, pp. 487-91, 1957.
19. Meikle, G., Binning, M. S. and Wright, M. E. (1948). The Properties of some Aluminium Alloys at Elevated Temperatures. R.A.E. Tech. Note Met. 96, December 1948.
20. O'Sullivan, William J., Jr. (1957). Theory of Aircraft Structural Models subject to Aerodynamic Heating and External Loads. N.A.C.A. T.N. 4115, September 1957.

21. PARKES, E. W. (1953). Transient Thermal Stresses in Wings. *Aircraft Engineering*, XXV, 298, pp. 373-8, December 1953.
22. POHLE, FREDERICK V. *Heat Transmission in the Structure*. AGARDograph 28, Chapter 3.
23. POHLE, F. V. and OLIVER, H. (1954). Temperature Distribution and Thermal Stresses in a Model of a Supersonic Wing. *Journal of the Aeronautical Sciences*, 21, 1, pp. 8-16, January 1954.
24. SOKOLINKOFF, I. S. (1956). *Mathematical Theory of Elasticity*, 2nd Edition. McGraw-Hill, 1956.
25. TAYLOR, JAMES (1958). General Introduction to Thermal Structures. Paper presented to A.G.A.R.D. meeting on 21st October 1958.
26. TAYLOR, J. (1957). Research Equipment for the Investigation of Aircraft Structures at Elevated Temperatures. *Aircraft Engineering*, pp. 228-232, August 1957.
27. WALKER, P. B. (1955). The Structural Effects of Kinetic Heating in Supersonic Flight. *Journal of the Royal Aeronautical Society*, Vol. 59, September 1955.
28. ZEMANSKY, MARK W. (1951). *Heat and Thermodynamics*. McGraw-Hill, 1951.

Summary of the Discussion

MAUREEN E. MICHAEL, M.A., Grad.R.Ae.S. and JOAN BRUCE, B.Sc., A.F.R.Ae.S.

(Technical Department, Royal Aeronautical Society)

SOME FACTORS AFFECTING THE CHOICE OF MATERIALS

The first speaker in the discussion following Mr. Heath's paper was from Bristol Aircraft Ltd.; he noted that the paper could be divided into three parts, material properties, time-dependent effects and materials of the future. Commenting on the first part, he agreed that it would be a good idea to throw away existing curves of specific strength, but he would like someone to suggest a convenient method of presentation for the data on material properties necessary to the designer. In the second part of his paper Mr. Heath seemed to suggest that structures should be designed on the "fail-safe" principle because of the difficulty in achieving a full test life with some specimens. Surely the need for "fail-safe" structures arose primarily from other considerations? In giving guidance on material selection Mr. Heath had concentrated on the properties *at* temperature, but it was possible that in future aircraft the plan form might be such that at high speeds when heating was present the gust loads would be small, and the design criteria might well be landing and take-off loads when the material would be cool. He agreed with the lecturer that the present lack of knowledge on creep was rather frightening, and put in a plea for more compression creep testing, as in some cases compression buckling could be important. It could be shown that before creep buckling collapse there was a significant amount of lateral deformation and this extended over a considerable period of time before collapse, so that it would be possible to use inspection methods.

In his reply Mr. Heath said that it would be difficult to present data on material properties in a readily usable form; curves showing stiffness and tension and compression proof stresses would have to be given for each material for various lengths of time at any particular temperature. With some of the new materials it was remarkably difficult to ascertain their properties due to lack of published data, but they would probably have to be used for structures subject to temperatures above 500°C. Later on in the discussion he stressed the point that choice of material and choice of type of structure must go together, as one could not get a fair picture by looking solely at material parameters. The materials mentioned in his paper were those for which he had information readily available and they were to be regarded only as an illustrative selection. He feared that where some of the new materials were concerned it might ultimately be the workshops that governed the choice.

He agreed that the primary consideration in "fail-safe" design was the same as at room temperature; his reason was merely an extra one for such design.

Mr. Heath endorsed the plea for more compression creep testing and, in reply to another speaker, from A. V. Roe and Co. Ltd., suggested that the right proportion might be 60 per cent compression testing and 40 per cent tension testing.

Asked to give some indication as to which were the most important material properties for the designer to consider, he said he could not really help; he felt that the answer to such a question could only come from a large scale research programme. Although there were many establishments in this country carrying out research there was little or no co-ordination of their activities. Only by setting up a co-ordinating body could they hope to get such programmes as the one he envisaged carried out. He made a strong plea for such a body to be set up.

In replying to a question from the Chairman, Mr. Heath agreed that in testing large built-up structures subject to very severe kinetic heating, it would be impossible to separate fatigue and creep testing.

A speaker from the R.A.E. commented that, unlike the engine people who thought they knew all about creep, structural engineers did not want to know a great deal about the fundamentals of it. They wanted to know what creep problems would apply to structural elements used in supersonic transports.

A spokesman from Bristols considered the case of a supersonic transport having a pressurised aluminium alloy cabin. Taking into account a scatter factor he deduced a safe working stress due to pressure. In supersonic aircraft with thermal stresses, the working stress would have to be even lower. From a structural point of view the problem was simplified. The problem became not how to deal with these stresses when they arose, but how to stop them arising. He suggested that this could be done by cooling or by insulation to smooth out the thermal gradients.

A questioner from the Air Registration Board asked how the rapidly changing qualities of thermal structures

would affect the repair schemes for future supersonic transports. Mr. Heath replied that at the present time the only answer he could give was to put on a patch and hope for the best.

In reply to a questioner from Bristol Aircraft on the need for consideration of similitude when dealing with the specific strength curves, Mr. Heath agreed, and repeated again the point he had made in his paper, that the consideration of one facet was not enough. A completely misleading answer could be obtained if only one factor were taken into consideration.

In correspondence after the meeting it was suggested that basic fatigue data should be obtained on materials after soaking at maximum temperature for the appropriate time, the fatigue testing to be performed at temperatures appropriate to climb and descent manoeuvres. The same correspondent asked why continued use of alclad aluminium alloy sheet was allowed, stating that its fatigue strength could be about 40 per cent less than that of the bare forged material at any large endurance. It would surely be better to use anodic treatment and paint rather than a protective coating that seriously reduced the fatigue strength of the material.

In his reply Mr. Heath said he was interested to hear the suggested compromise between the "short time" tests at elevated temperature and the "long time" fully programmed tests, but he did not know if it would work—only actual test results could show. Concerning the other point, he doubted that cladding could make so much difference to fatigue strength and thought that a comparison of results using specimens containing typical joints would show that endurances were more alike than had been indicated. He wondered what paint the questioner would recommend for use at 300°C.

Design of Transparencies

The discussion following Dr. Przemieniecki's paper was opened by a speaker from the R.A.E. who said that although the lecturer had been dealing with the case where there was no heat flow on the inside of the transparencies, surely in any ordinary pressure cabin the heat flow on the inside would have an appreciable value? He pointed out also that transparencies had two rather unfortunate properties: (*i*) a very high resistance to heat flow which induced large temperature gradients, and (*ii*) low powers of radiation. He asked whether, in future aeroplanes designed to fly at very high speeds, dimensions of transparencies could be kept low enough to be cooled from the inside or, would it be possible to cool them from the outside?

Dr. Przemieniecki said that for his paper he had considered the simplest case only, *i.e.* the one where the heat flow on the inner surface was zero. This was perhaps a little unrealistic as there would obviously be some heat losses from this surface, but the principles remained the same in each case. The two unfortunate properties that the questioner had referred to were, of course, quite important, and in some practical calculations that had been made the temperature gradients had been found to be quite large. Some of the problems could be overcome by using a double panel construction and supplying cooling air between them. It was doubtful if it would be practical to supply cooling air to the external surface.

Another speaker from the R.A.E. asked if the lecturer would agree that the choice of materials for transparencies was very limited because of all the conditions that had to be met. In the comparison between the fused silica and toughened soda-lime glass it had been shown that fused silica had definite merits where the temperature change was high, but he felt that toughened soda-lime glass might still be considered favourably for use in civil air liners where any change of temperature would not be rapid.

In replying to this speaker Dr. Przemieniecki said that he had been dealing with temperatures and temperature effects associated with Mach numbers greater than two, and therefore the use of plastic materials had been eliminated. He agreed that there might be rather more scope than he had indicated for use of toughened soda-lime glass, but pointed out the danger that at very high temperatures it would lose its toughening.

Dr. Przemieniecki replied to a question on the use of transparencies and retractable blinkers in supersonic transport, by saying that this was not a practical solution and that he would prefer no passenger windows at all. Retractable shutters could perhaps be used on some special purpose windows, *e.g.* emergency hatches.

After commenting that he thought that the question of windows would be settled by the travelling public who obviously liked them, a speaker from the R.A.E. went on to say that he had been surprised to hear the lecturer assume zero heat transfer into the cabin. He stated that on fighters, a large proportion of the heat entering the cockpit entered through the transparencies. A usual cure was to increase the mass of air flow through the cockpit, but this usually involved increased air velocities over the transparencies and, hence, higher heat transfer coefficients, which was really no solution. He thought that the lecturer's proposal of cooling the space between two panels would be difficult to achieve.

Dr. Przemieniecki replied that although the assumption of zero heat transfer on the inside surface was an unrepresentative case it could be used effectively for design purposes. This assumption led to conservative designs since cooling of the inside surface resulted generally in a reduction of the maximum thermal stress. He thought that no appreciable difficulty would be encountered in cooling the interspace, but due to a very high thermal resistance of transparency panels this method was not very effective in reducing temperature of the outer panel; consequently outer panels would have to be designed to withstand maximum temperatures.

Some Practical Aspects of Kinetic Heating

Calculations

An aerodynamicist said that he was diffident on enlarging upon the complexities of the estimation of aerodynamic heating rates. He congratulated Mr. Bore on his manipulation of the formulae and the very convenient form of presentation but requested him not to ask the aerodynamicists to produce charts showing the values of the parameters over a range of Mach numbers.

A question was asked regarding the relation of enthalpy to Mach number. However, the complex nature of the problem meant that the answer could not be given briefly at this meeting. In later correspondence the questioner stated that he did not disagree with the form of equation (5), but felt that little error would arise in the estimation of recovery enthalpy ("forcing enthalpy") due to taking the coefficient of M^2 equal to 0·2. He agreed that the local temperature could be high in regions of much reduced flow speed, leading to changed values of the coefficient, but M_1 would be small in such cases, so that there would be little overall effect. He suggested that it was more convenient to use equation (1), thus avoiding any ambiguity over the value or definition of γ.

Mr. Bore replied that it was true that in many cases

little error would accrue from taking M^2 equal to 0·2, but it was quite easy to include the variations while preparing the charts, so there was little point in avoiding them.

Larger discrepancies occurred between the strict local enthalpies and those obtained by taking the approximate coefficient when the local temperature was large and M_1 was also large. If $M_0=5$ and $M_1=2{\cdot}5$, for example, the value of local enthalpy would be given about 2½ per cent too large.

The main reason for introducing the later forms of the energy equation was to facilitate calculations for regions where the local velocity was substantially different from free-stream velocity. In such regions he generally found it more convenient to estimate local Mach numbers than true local velocities which depended on the local temperatures, which were rather difficult to estimate when M_1 or U_1 were unknown.

Advantages and Limitations of the Use of Models

Concerning Mr. Sobey's paper the same aerodynamicist said he thought that the idea of the Hoff study wing was an abomination. He had never liked the idea of infinite accelerations and he could only accept it as a purely academic problem.

A speaker from Bristol Aircraft thought that Mr. Sobey had given rather a depressing picture of the use of models. It seemed that for a particular aircraft the use of models for determining the thermal effects did not have much future. Models had, however, been used with success in most fields of aerodynamics and structural research and they were valuable in that they provided a physical picture and a check on the mathematical theory.

He thought that the Hoff wing could be used to obtain an experimental check on the theory, and that theoretical models could then be elaborated and developed and checked with physical models approaching nearer to real aircraft structures.

For aeroelastic heating problems, simple models would be put in an air stream so that the heat transfer coefficients could be easily deduced, and various characteristics could be measured and assessed and taken into account in theoretical studies. He felt there was a danger of having a wealth of theory with very little experimental evidence. Mr. Sobey replied that he agreed that more models should be tested to check with theory, but the difficulties were largely experimental. Unless the tests were directed at a specific simple structure it was very difficult to acquire any useful information. This was particularly so in the case of rapidly transient phenomena, which should be avoided because of the limited test equipment available.

A speaker from the N.G.T.E. quoted the popular press as saying that future supersonic transports would travel at a Mach number of 2 or 3. As an engine man he said he would prefer a Mach number of 3 on the grounds of higher engine efficiency. He put forward the opinion that the future transport aircraft would be more important than the fighter aircraft.

The Chairman here pointed out that the discussion should consider all aircraft in the very broad sense. Missiles must also be considered.

A speaker from the R.A.E. supported the analogy with aerodynamics where any advances had come from small scale model tests rather than replica tests. At times, he said, the latter were necessary, but sometimes led to considerable difficulties. These difficulties were usually sorted out by the small scale model test when the problem was broken down into its component terms.

He agreed that in order to deduce the most significant parameters, crude theories had to be constructed to isolate those parameters.

Mr. Sobey replied that he did not really disagree but he felt there were times when replicas must be used. There was generally not the opportunity to do extensive tests from which to build up theory. A simple and single test was of great value. The small scale work piece was an instrument of scientific research, but did not obtain the useful structural information needed for preliminary design.

Closing Remarks

In his closing remarks the Chairman thanked the four principal speakers and said they had given very useful information which would be of benefit to all those interested in kinetic heating. He made two points in conclusion. The first, a general point, concerned the vital importance of really understanding the test technique so that this could keep ahead of the actual aeroplane.

The second point was that from the day's discussion it might appear that they were on new and dangerous territory. This was not altogether true. There were a large number of complex aeronautical devices flying around with complete success and suffering from quite severe kinetic heating problems. Quite a lot was known about kinetic heating already, but he stressed that more knowledge was needed in order to design with extreme efficiency.

Icing Flight Development*

by

B. T. CHEVERTON

(Chief Flight Development Engineer, D. Napier and Son Ltd., Luton Airport)

Introduction

The aircraft designer must clearly ensure that his aircraft will fly in all climatic conditions normally to be expected. Over and above this, aircraft must be able to cope with a change in weather also.

Since the last war, research into the problem of ice accretion on aircraft has done much to widen understanding of this serious flying hazard. In the flight testing and development of ice protection systems for aircraft, however, one of the principal difficulties encountered is that of finding natural icing conditions sufficiently uniform through which to fly the test aircraft. Because of this it has been found more profitable not to seek natural conditions, but instead to fly in clear air at temperatures below 0°C, while spraying the test surface from a water spray rake fitted to the test aircraft.

It is nevertheless essential to prove that the simulated conditions are closely related to the natural conditions that would give the severity of ice accretion specified for test purposes, and it is desirable therefore to know the precise severity of the contributory natural factors to the icing risk, namely, ambient temperature, water concentration and droplet size.

The Icing Risk

Aircraft icing may occur in natural atmospheric conditions if flight is made in droplet cloud, the particle size of which is greater than, say, three microns, and when the forward facing surfaces are at a temperature of 0°C or below. When ice crystals are encountered in cloud a different situation may exist since, if the surface is not wetted by the thawing out of crystals, adhesion of ice will not take place.

It is possible to produce an icing condition by descending a cold aircraft into warmer but moist air, or to avoid an icing condition because of a surface kinetic heating effect associated with forward speed. An aircraft flying at 10,000 ft., for example, on an I.C.A.N. day will be experiencing an ambient temperature of −5°C, but at a true air speed of around 250 m.p.h., the wet air kinetic rise will be about 5°C and the icing risk will be associated with an ambient air temperature of only zero. The icing severity for a particular aircraft depends therefore on forward speed such that at a Mach number giving a wet kinetic rise of 40°C, the icing risk in droplet cloud may be nil.

*Based on a lecture given to the Luton Branch of the Society on 5th December 1956.

The Icing Severity Standard

In flight, the icing severity experienced will vary from day to day and cloud to cloud, but it is necessary, for design purposes, to define a standard. This is given in A.P. 970 for military aircraft, and in B.C.A.R. papers for civil aircraft.

Three degrees of icing conditions are promulgated. The most intense is Instantaneous, which may occur for distances of up to half a mile and with concentrations up to 5 gm./m³. "Intermittent" conditions with concentrations up to 2·5 gm./m³, may occur at intervals of three miles below 30,000 ft., and at intervals of twenty miles above 30,000 ft. over distances of up to three miles. The severity for Continuous Maximum conditions is shown in Fig. 1. The severity is tied to ambient temperature, water concentration and droplet size. It will be seen that the concentration at 30 microns is half that for 20 microns, and that icing conditions may be expected at ambient temperatures from zero to −30°C.

It is by no means readily apparent which combination of these severity conditions would prove most hazardous. A short period at high concentration might seriously impair engine performance, whereas a long period at relatively low concentration might destroy aerodynamic lift or increase weight and drag to unacceptable limits.

It is partly to determine the relative seriousness of the several possible icing conditions that experimental flight testing is undertaken. Exploratory flight tests have been made at all conditions shown in Fig. 1 and also at Intermittent Maximum conditions.

Formation of Icing Cloud

The maximum amount of water vapour that can be present in an air mass without condensation occurring, depends mainly on the temperature of the air and becomes less as the temperature decreases. If air is cooled, condensation therefore occurs when that maximum is reached, the air then being saturated.

In the atmosphere, cooling is most often due to the adiabatic expansion that occurs when air is moved upwards to a lower pressure level, so that the amount of water vapour present may be described in terms of the pressure level to which air must be carried up for it to become saturated and for condensation to water droplets to take place. This will be the condensation level or the altitude at which cloud forms.

A cloud may form as the result of water vapour in the exhaust of an engine and this is an interesting study

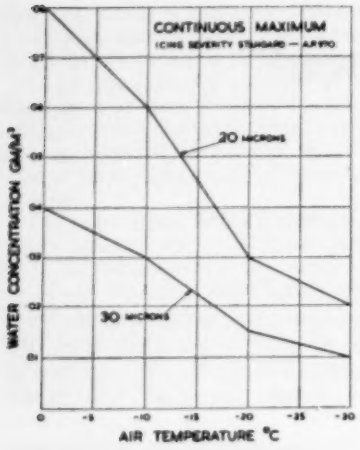

FIGURE 1. Icing severity standard.

but, from the icing consideration, an aircraft does not of itself condition the severity of the icing cloud through which it may subsequently fly.

In clear air the condensation of water takes place into water droplets and not ice crystals, and if the temperature is below freezing point the droplets are said to be supercooled. Ice crystals do not form in clear air when saturation is reached, they are formed as the result of subsequent freezing of water droplets.

Water Catch

The icing risk has been considered briefly and it is seen that by flying faster the temperature range over which icing occurs may be reduced. It is not normally practicable to do this, although as a general maxim "the sooner out of cloud the better." In flying faster however, the rate of catch is increased and it will be as well now to consider severity in terms of rate of catch and ambient temperature.

Clearly, catch rate will increase as water concentration and forward speed increase and it will be appreciated also, that large droplets have greater inertia and are more likely to be caught than small droplets. Catch increases also as frontal area is increased but that is inherent in design and may not be blamed on the weather.

FIGURE 2. Water spray boom, showing 43 nozzle spray head and camera housing.

Rate of catch is equal to the product of the water concentration, the velocity of the aircraft, the frontal area of the section and, the catch efficiency. An estimation of catch efficiency is difficult and tedious to obtain, and this becomes a major difficulty in the estimation of heating requirements. It is nevertheless necessary for the designer to know the efficiency and hence, the rate of catch, and also the peripheral limits of catch in order to produce a protective system. Because of difficulty in assessing rate of catch or heat transfer, flight tests of a specimen are undertaken to confirm the suitablity of an anti-icing or de-icing design.

The Test Aircraft

At the Luton Flight Development Establishment some early tests were completed with an electrical mat mounted on the leading edge of a Tempest aircraft. The test section was flown for 100 hours in a variety of weather conditions at ambient temperatures down to −48°C. Surrounding paintwork was damaged by climatic conditions, but the weathering properties of the mat were good and further installations were made.

A Lincoln aircraft was fitted with a water spray on a forward boom, more commonly known as "a proboscis." Water was sprayed from a 43 nozzle spray head into the ducted spinner intake of a Napier Naiad propeller-turbine engine (*see* Fig. 2). These tests were undertaken partly to prove the effectiveness in icing conditions of Spraymats fitted to spinner and intake splitters. A camera fitted to the boom allowed a photographic record of tests to be obtained—a scheme to fit a large mirror was rejected.

Excellent results were obtained, the spinner remaining ice-free in moderate icing conditions with a heat input of less than 4 watt/in.² as is shown in Fig. 3. During initial tests an excessively high heat input resulted in the open-circuiting of one phase of the three-phase circuit, but complete protection continued to be provided. Fig. 4 demonstrates what may happen if protection is not provided; a typical cauliflower head appearance after 6 minutes in icing conditions is shown. It is also of interest that in conjunction with these tests an investigation was completed with a momentum separating type of intake designed to protect the engine in icing conditions.

A Spearfish aircraft was used for spray nozzle development work. A tennis racket device was mounted

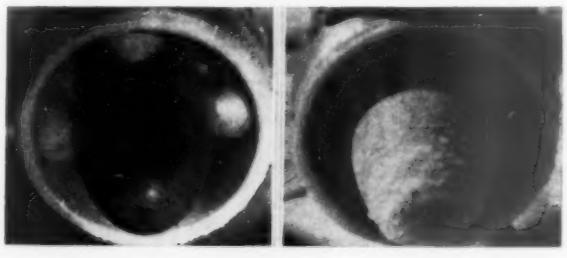

FIGURE 3 (*left*). Napier Spraymat ice-free in moderate icing conditions with heat input approx. 4 watt/in.²
FIGURE 4 (*right*). Spinner unprotected for 6 min.

in the spray of a single nozzle, and the area of spray was clearly established at several forward speeds and water flow rates. These tests, besides showing the clearly defined area of spray, produced the distinct types of ice normally encountered.

Slush ice is dirty in appearance, appears to be wet, is easily dislodged and forms at relatively warm effective temperatures of, say, zero to $-3°C$. Glaze ice forms at temperatures around -7 to $-8°C$; it is relatively smooth, tends to be transparent but is dirty in appearance. Rime ice has a white milky appearance, and is opaque and forms at lower temperatures where, due to the rapid rate of freezing, the ice formation contains a good deal of entrained air. Quite obviously the appearance of ice varies with ambient temperature and does not readily fall into "ice-tight" compartments. For example, to describe ice formation that appears to be neither glaze nor rime we have coined the word "glime."

This slight digression from a discussion of test aircraft demonstrates the difficulty that will inevitably be experienced in classifying types of ice formation during flight tests, particularly when it is considered that the appearance of ice is considerably affected by lighting effect, as for example when the sun is shining on to the surface or, from behind the surface. I have seen ice apparently dispersed merely by a change in aircraft heading.

The next aircraft used for icing research was a Vickers Viking; this aircraft was flown on icing tests for over 300 hours during the years 1951 to 1955. It had originally been intended to utilise the aircraft for a full scale de-icing investigation of mainplanes and empennage, and a Gypsy Queen auxiliary power unit capable of supplying sufficient electrical energy was installed. It was later agreed with the Bristol Aircraft Company to flight test a Britannia wing tip section in preference to other schemes.

To cope with the size of section involved, an overshoe to the aircraft fin was designed to house a variety of test sections. Cloud conditions were simulated by a water spray system with a spray rake mounted six feet in front of the test section.

It is unfortunately not possible to describe at length the most interesting tests and results obtained with the Viking aircraft. It was, however, a splendid test vehicle. Flight testing is not always achieved in such comfort.

Figures 5 to 8 show more recent installations on Lincoln aircraft, involving Beverley, Comet and N.A.C.A. 4414 type aerofoils. A number of heater mats have been added experimentally to the latter type section to provide easy clearance of run-back ice.

Water Spray System

It has already been inferred that the water spray system is probably the weakest link in the test system. There is the obvious difficulty of housing a sufficient quantity of water for a test programme, and pipe lines have become frozen, even in well heated hangars. The introduction of anti-freeze was considered but it was

FIGURE 5. Beverley aerofoil.

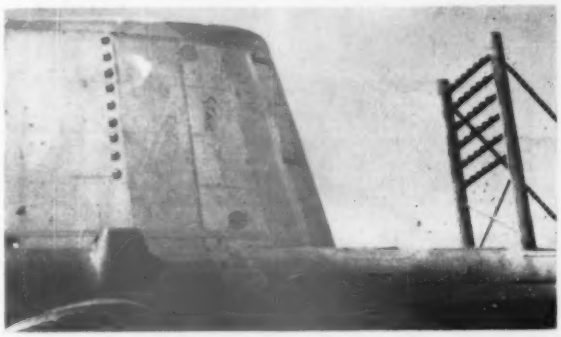

FIGURE 6. Comet 4 aerofoil.

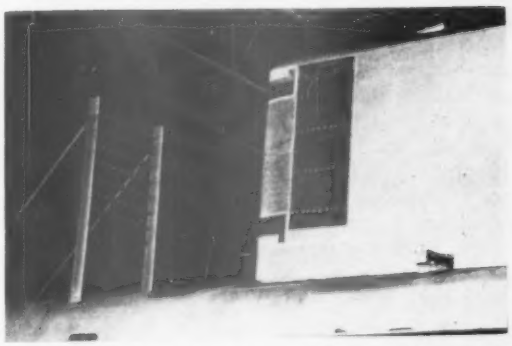

FIGURE 7. N.A.C.A. 4414 type aerofoil mounted on Lincoln fuselage, with experimental heater mats.

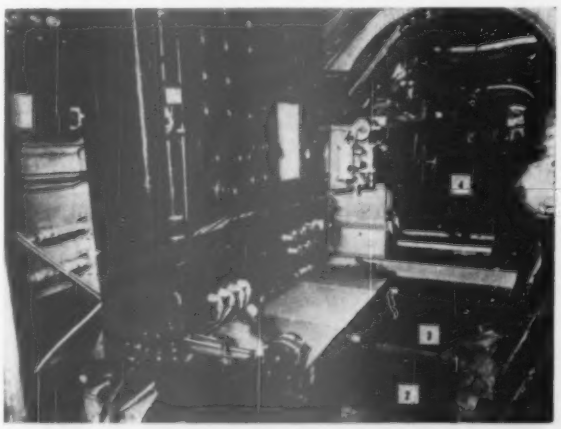

FIGURE 8. Lincoln RF 402 showing instrument panel and section hot gas controls (numbers refer to Observer stations, a maximum of four Observers being employed).

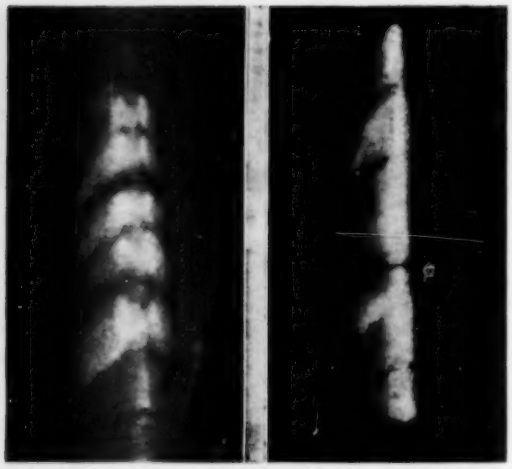

FIGURE 9 (*left*). Poor water spray distribution during initial tests on Viking VL 229 test section.

FIGURE 10 (*right*). Improved distribution after fitment of fairings to spray nozzles.

thought that the Air Registration Board might not approve.

There is then, the problem of passing a sufficient quantity of water to give high concentration but with atomisation adequate to give small droplet sizes. We have now reached the stage where we are able to achieve this, but it has only been possible as the result of lengthy testing in a cold wind tunnel and flight tests, as for example on the Spearfish aircraft. It is just not good enough to throw buckets of water at a test section or even to argue that conditions more severe than normal will adequately prove a section, particularly for de-icing tests.

The next requirement is that the water spray shall be directed over a sufficiently large area, and from a distance sufficient to ensure that complete supercooling of droplets is achieved. Exploratory tests were necessary and Figs. 9 and 10 show the poor distribution obtained at one time and the subsequent improvement resulting from fitment of nozzle fairings.

In association with the water system there must be a nozzle air system, an additional air flow being necessary to achieve the required degree of atomisation. A large quantity of air is required, and it has been necessary to employ a cabin type supercharger for the job. To illustrate the importance, for another project, a Palouste turbo-jet engine is used for this purpose only.

There is next the nozzle calibration necessary to ensure that correct droplet sizes are provided. This has entailed droplet sampling in flight and the programme has been of such magnitude that there was at one time a danger of mistaking a tail for the dog.

Droplet Sampling

If natural conditions are to be simulated, however, droplet size must be correct and it is most gratifying to be able to guarantee droplet size to within two microns.

Figures 11 and 12 show firstly, a sample obtained in natural cloud and secondly, a sample with the artificial spray system. Both are to the same scale. There is no suggestion that one is intended to simulate the other but the comparison demonstrates how far off from a true simulation we might be without precise calibration.

The sampling apparatus, which may readily be installed in other aircraft, consists of three independent components: an ice box in which oil slides prepared for exposure are stored, a sampling device for exposing the slides to a droplet stream for a controlled period, and an adapted Newman Sinclair camera fitted with a macro lens. Fig. 13 shows the observer station.

The type of oil used is important, it being necessary to obtain an even film with good photographic properties. Because the oil film takes and hold samples most efficiently at temperatures around 0°C, and because it is essential to keep the slides clean, they are stored in a dust-proof ice box. An appreciable rise in temperature would cause the oil to run and destroy the even depth of film, whereas a decrease in temperature below 0°C may cause droplets to freeze on impact and form ice crystals.

There would be a risk of condensation from observers' breath if care were not taken. We have

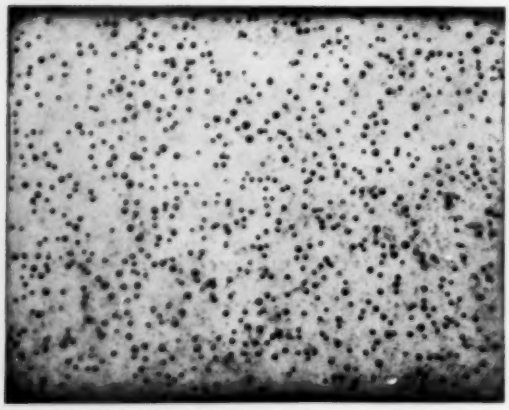

FIGURE 11. Droplet sample from natural cloud. Volume median 11 microns.

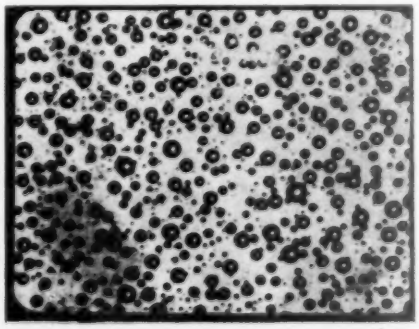

FIGURE 12. Droplet sample in simulated cloud.

FIGURE 13. Droplet sampling station in Viking VL 229.

estimated the risk of contamination through perspiration as slight, but there is a real danger of critical evaporation of droplets from the oiled slides if too long a period elapses between the taking and photographing of a sample.

The over-exposure of a slide will cause too many droplets to be caught with the result that adjacent droplets coalesce, causing an exaggeration in the subsequent calculations. A correction factor determined experimentally may then have to be applied.

To control the exposure time a simple pneumatic sampling device was used at first in the form of an air-operated piston by which single slides are moved past an aperture in a tube that is raised by the observer to project into the droplet stream. The mechanism is designed to ensure that while the aperture is exposed the slide passes it once only.

After sampling, areas of approximately one square millimetre are magnified and photographed on 35 mm. film; three or four shots are obtained to give representative views, although, with a uniform spectrum, variation in mean droplet size calculated from each photograph should be negligible. The globular appearance by which droplet images are identified as droplets or otherwise

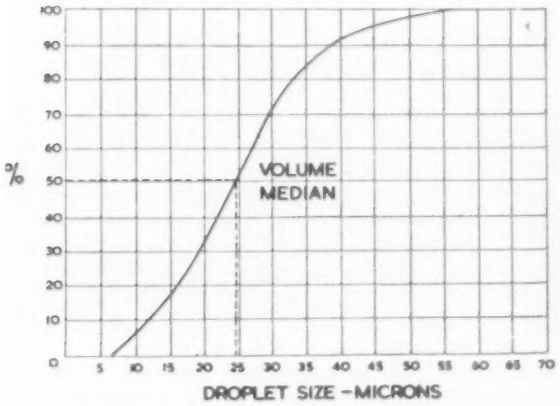

FIGURE 14. Curve used to calculate volume median droplet size.

FIGURE 15. Catch limits associated with droplet size of (*a*) 20 microns and (*b*) about 55 microns

is well illustrated in Fig. 12, together with the clear definition required for measurement.

The film is next projected on to a suitable screen and by super-imposing a calibrated scale, the droplets are then counted into size bands of 5, 10, 15, 20 and so on, microns diameter. It is next required to determine the mean droplet size but before describing the method some explanation of its significance may be useful.

The essential feature of droplet size that affects the amount and distribution of ice accretion is the droplet weight, which is proportional to the volume. However, since the droplet size is not uniform throughout any cloud it is necessary to establish an expression of droplet volume in terms relevant to the icing severity produced by the particular droplet size composition of the cloud. The relevant expression is not an average volume but a median volume which is stated in units of droplet diameter at which, for the example concerned, the total volume of droplets contained in the spectrum of diameter less than the median is equal to the total volume of droplets of larger diameter.

This value, known as the volume median, is usually given when natural icing conditions are specified in meteorological data, and is determined from a sample by constructing a curve to data from the count. A curve, as shown in Fig. 14, is plotted to co-ordinates of nominal droplet size in microns and aggregate percentage of the total weight of droplets counted. The droplet volume median is then determined by reading off the nominal droplet size at the position on the curve corresponding to 50 per cent by weight of the total.

The critical nature of droplet size is shown clearly in Fig. 15.

The Protective System

The icing risk and the problem of providing artificial simulation having been considered, some reference must now be made to the protective system to be employed, although a comprehensive list of the various systems that might be employed will not be attempted.

One form of protection is to use a mechanical ice-breaking device on the leading edge of an aerofoil surface. An inflatable rubber tube might be used so that when expanded at intervals it would serve to break off ice adhering to it. The disadvantages are plain in that it may not always clear satisfactorily and that in

high speed aircraft the presence of an inflatable bag is not compatible with aerodynamic efficiency.

Another method of protection is to spread on the surface to be protected a film of some liquid, such as alcohol, which serves to lower the freezing point when mixed with water. Even mixing is essential but difficult to control and, apart from being messy, a large amount of fluid must be carried with consequent reduction in payload.

Special pastes and even warm engine oil have been used for anti-icing and, although useful for limited application, as is for example anti-freezing grease on control actuators, these methods do not recommend themselves for use on aircraft lifting surfaces.

There are two methods readily employable and both were tested on the Viking test aircraft—they are hot gas anti-icing and electrical de-icing methods.

Anti-icing presumes that heating becomes effective before encountering an icing hazard. The entire surface on which water may catch or run back should be maintained at a temperature above 0°C. De-icing presumes that ice may be allowed to form, being subsequently cleared in a selected sequence from separately heated mats.

Anti-icing and de-icing systems may be compared but the overall suitability of one system as against the other is tied up with installation requirements, interchangeability, liability to damage and so on, not excluding cost.

For flight test experimental work, however, it must be accepted that during an immediate flight programme we are mainly concerned with the mechanical reliability, endurance and functional ability of a component under test.

Flight Testing an Anti-Icing System

The hot gas anti-icing system as flight tested will now be considered. Hot air must be ducted to the test section which must be set at representative incidence to the effective air flow. The heat input in terms of air mass flow and temperature differential must be measured, further instrumentation will be required to allow for reproduction on full scale tests and may take the form of surface thermocouples and reference for internal structure temperature and air flow distribution. The hot gas may be supplied from engine exhaust or compressor tapping, or from a separate ram source through a combustion heater or other heat source.

In an experimental installation the entire anti-icing system may not be standard. For example on the Viking aircraft it was necessary to employ an electrically-heated element to replace a combustion heater. Correct simulation of the actual section was essential, particular care being taken neither to exclude nor introduce cold spots.

In order to determine the lift coefficient at particular section incidence, pressure plots have sometimes been obtained in flight and, to determine section incidence, yawmeters have been used.

Anti-icing systems may be classified into two kinds,

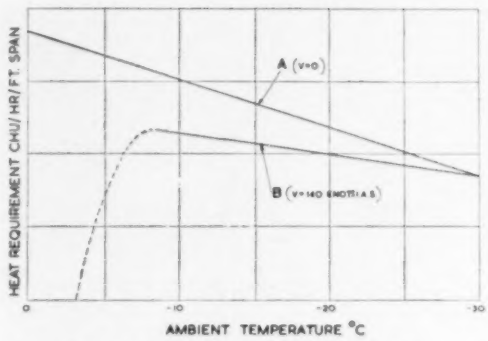

FIGURE 16. Anti-icing heat requirements.

either "wet" or "dry." A wet system is designed to keep a protected surface ice-free while allowing water not evaporated to run back and form on unheated portions aft where it will not necessarily be an embarrassment. A dry system presumes complete evaporation of all water caught and therefore requires a larger heat input.

In determining the heat requirement, therefore, run-back is the main guide, although at very low ambient temperatures associated with low rates of catch ice may form directly on the heated portion.

The testing technique is to set initially to a high heat input and then to reduce progressively, maintaining inlet temperature or air mass flow constant as pertinent to the system being tested, working always within the temperature limits for the type of aerofoil construction under test. At the heat input just insufficient to evaporate, or otherwise clear, all water running back to the unheated portion, a streak of ice will be detected.

It has been observed that run-back forms initially behind a region of low heat input, as for example, multiple skinning on a wing. Run-back will also occur in a region of high water catch due to poor spray nozzle configuration or local roughness of the skin as, for example, when external thermo couples are fitted.

A task for the Flight Observer is to detect this first instance of run-back and this calls for continuous viewing and frequent change in aircraft loading to provide variation in solar lighting. In fact when working to close limits, we have observed that run-back ice clears more rapidly from a surface on which the sun is shining.

For a particular icing severity condition tied to forward speed and section incidence, the maximum heat requirement may be determined. Theoretically, as shown in Fig. 16 at curve *A*, the heating intensity required at Continuous Maximum severity and zero speed is a maximum at 0°C. The heat input required is a compound of heat to raise the water temperature from ambient to surface temperature, heat to maintain a surface temperature and heat to evaporate the water caught.

The maximum temperature at which icing may occur depends on forward speed and curve *B* shows the heat input actually found to be necessary. The dotted part of curve *B* is difficult to obtain, there being a

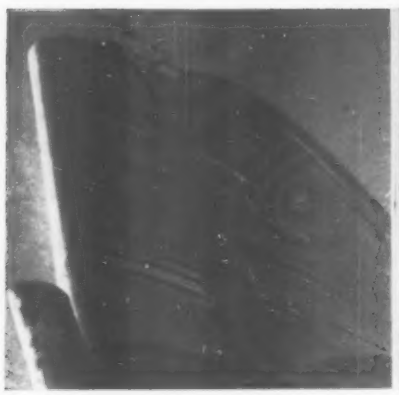

FIGURE 17. Ambient −5°C. Concentration 1·18 gm./m³. Encounter time 13 min. "Cruise" configuration.

FIGURE 18. Ambient −7½°C. Concentration 1·14 gm./m³. Encounter time 17 min. "Cruise" configuration.

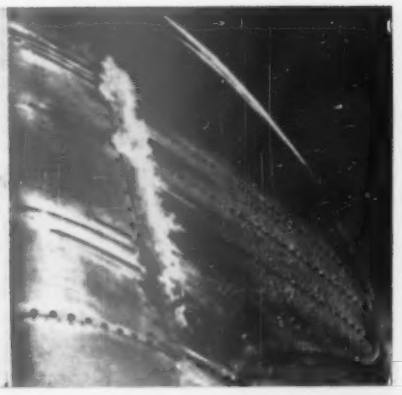

FIGURE 19. Ambient −10°C. Concentration 1·10 gm./m³. Encounter time 15 min. "Climb" configuration.

very small ambient temperature difference between that giving zero heating requirement and that giving maximum heating requirement.

An interesting feature is the difference between *A* and *B*; briefly the reason is to be found in: —

(*a*) That not all of the water caught needs to be evaporated since some blows off the section and does not subsequently catch.

(*b*) That the boundary layer becomes heated, thus allowing some run-back water to flow on to the unheated portion from which further evaporation takes place.

In practice, it has also been found that water may run back in rivulets so that the entire heated surface area behind the catch area is not wetted even at the point of breakdown. This effect, and the practically impossible task of determining, firstly, transition points in wet air from laminar to turbulent flow, and secondly, the resulting heat transfer coefficient, makes compilation of curve *A* difficult.

At −30°C, however, there is no bonus since breakdown occurs as the result of ice freezing on the heated portion and there is a small margin of heat input only between that necessary to keep the leading edge ice-free and that required to keep the heated position ice-free. The first instance of run-back determines the ice-free heat input. This may, however, be an extravagant intensity, and it has been shown that a reduction in heat input value at −10°C may be tolerated without embarrassment.

As heating is further reduced the ice build-up increases and moves towards the leading edge, ultimately forming on the heated portion. It has been found that once this condition has been reached only a small further reduction in heating intensity is required to cap the leading edge. The difference in heating intensity between the ice-free and ice-capped state is therefore greater at −10°C than at −30°C.

Figure 16 is of further interest since it shows that at constant indicated forward speed and section incidence, the higher concentration at −8°C ambient produces a more severe condition than the lower

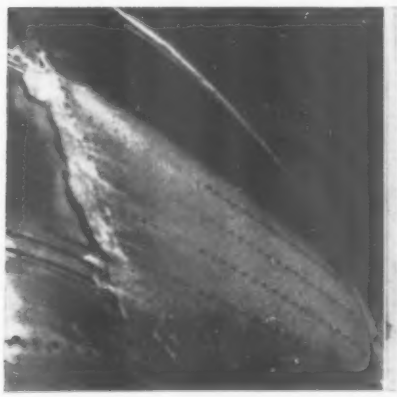

FIGURE 20. Ambient −15°C. Concentration 0·98 gm./m³. Encounter time 20 min. "Climb" configuration.

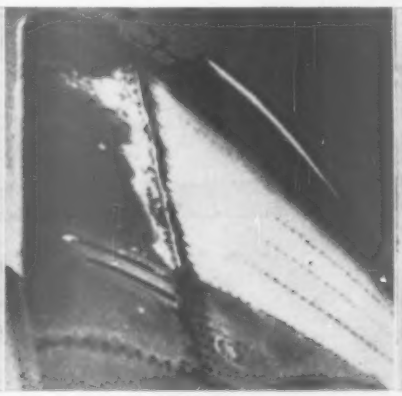

FIGURE 21. Ambient −30°C. Concentration 0·5 gm./m³. Encounter time 18 min. "Climb" configuration.

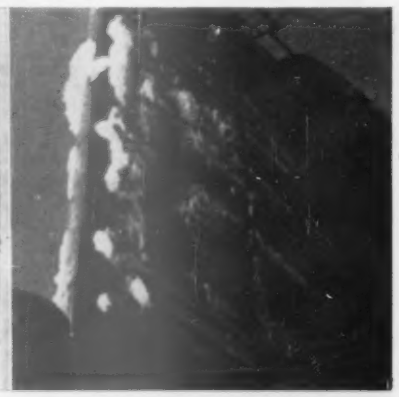

FIGURE 22. Ambient −10°C. Concentration 1·10 gm./m³. (Simulated reduced heat condition with 10 min. at final heat input.)

concentration (and temperature) at $-30°C$. The design condition then for the particular section under review would be $-8°C$, and the heat to be supplied is the theoretical value multiplied by the ratio B to A.

A number of photographs taken at various icing conditions are shown in Figs. 17 to 22. Tests were at Intermittent Maximum severity although heat input was that found adequate to cope with Continuous Maximum conditions; this accounts for the run-back ice experienced. Attention should be given to the following features:—

(*a*) The location of run-back ice with respect to the heated portion.
(*b*) The chordwise extent of run-back ice.
(*c*) The formation of rime ice behind run-back, due possibly to turbulence caused by the run-back deposition.

Flight Testing a Cyclic De-icing System

A cyclic de-icing system has two essential features:—

(*a*) Continuously-heated parting strips are provided along the leading edge and between primary heated areas.
(*b*) A number of separately heated mats operate to a time sequence best calculated to ensure adequate shedding without danger of bridging the parting strips.

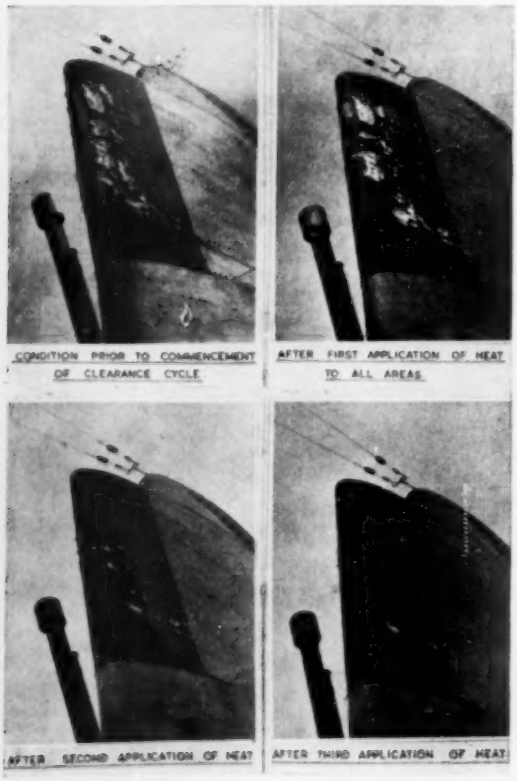
CONDITION PRIOR TO COMMENCEMENT OF CLEARANCE CYCLE
AFTER FIRST APPLICATION OF HEAT TO ALL AREAS
AFTER SECOND APPLICATION OF HEAT
AFTER THIRD APPLICATION OF HEAT

FIGURE 23. De-icing clearance cycle.

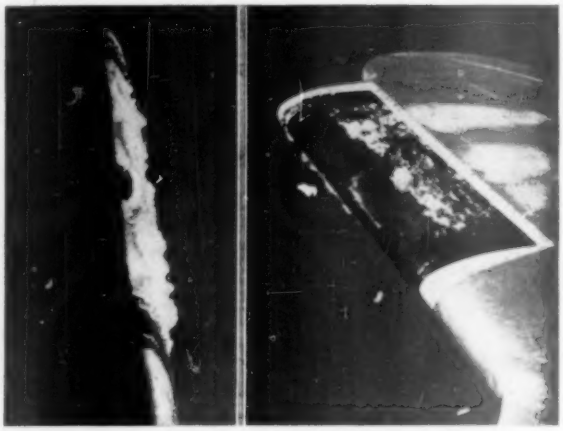

FIGURE 24 (*left*). Minimum acceptable leading edge gap width.
FIGURE 25 (*right*). Clean shedding from primary areas.

Clean shedding is helpful but not a criterion, since ultimate shedding with a cyclic system may be achieved by re-selecting mats on after flying out of cloud as shown in Fig. 23.

A de-icing system must inevitably be a compromise, since it must cope with the most severe condition likely to be encountered without bridging of the leading edge, and it must operate in low severity conditions without producing run-back. Fig 24 shows what was taken as a minimum acceptable leading edge gap width at $-16°C$ ambient temperature. The condition was excessively severe, water concentration being 1·12 gm./m³. Leading edge heating intensity was 14·5 watt/in.² with 10 watt/in.² to primary areas. The photograph shows the condition at the begining of the fourth primary cycle, that is after nearly 18 minutes at this severity condition. Fig. 25 shows the subsequent clean shedding obtained from primary areas *B*1 and *B*2.

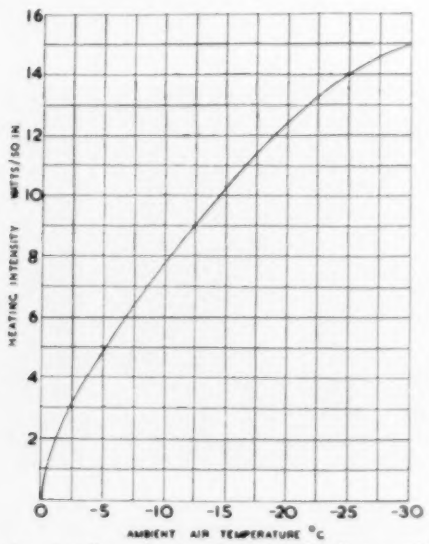

FIGURE 26. Leading edge breaker strip heating requirements.

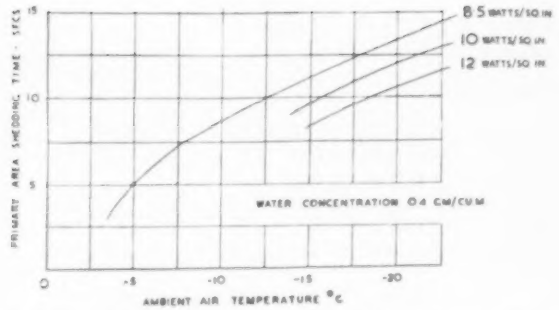
8·5 WATTS/SQ IN
10 WATTS/SQ IN
12 WATTS/SQ IN
PRIMARY AREA SHEDDING TIME - SECS
WATER CONCENTRATION 0·4 GM/CU M
AMBIENT AIR TEMPERATURE °C

FIGURE 27. Relationship between heating intensity and primary area shedding time.

During flight development of a de-icing system the following requirements must be established:—

(*i*) The heating intensity and breaker strip width particularly at the leading edge. Fig. 26 shows a typical requirement curve.

(*ii*) Whether variation in this requirement justifies a multiple-way heating intensity switch, to cope for example with ambient temperature range of say 0 to $-10°C$, -10 to $-17\frac{1}{2}°C$ and $-17\frac{1}{2}$ to $-30°C$, requiring heating intensities of 8, 12 and 15 watt/in.^{2} respectively.

(*iii*) The optimum length of complete operation of cyclic sequence, this being allied to the time that each mat will be on, and equally important, the time that each mat will be off. Fig. 27 shows a typical plot obtained of shedding time against ambient temperature at constant watts loading. The "heat on" time determines the "heat off" time and, hence indirectly the sizes of mats required and total wattage for cyclic area.

(*iv*) The optimum heating intensity for primary areas. Here the observer comes into his own, it is not a matter one can prove subsequently with curves and figures.

(*v*) The usefulness of graduated heat input from front to rear of the section must be determined.

(*vi*) Whether secondary areas are necessary.

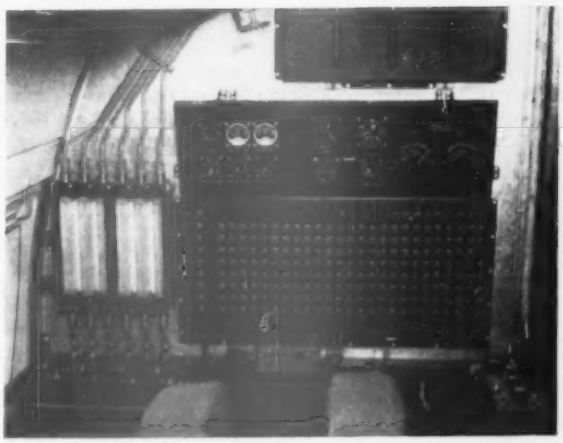

FIGURE 28. Control panel for electrical thermal de-icing experimental tests on Viking VL 229.

There are, of course, other considerations. A considerable amount of rig-testing will have been necessary and it must be accepted that some testing may more usefully be done in closely controlled and observed laboratory conditions before flight testing begins, particularly when it is necessary to determine trends toward optimum configuration.

With an electrical system, heating intensities are closely controlled and readily predicted. A selected watts loading remains constant at all forward speeds, altitude, ambient temperature and distances from the heat source. There is not the same need therefore for extra instrumentation to ensure simulation of heat output in full-scaled tests. This makes life easier for the observers, although it will be sobering to look at the special test cyclic control panel (Fig. 28). There was in this installation plenty for at least one observer to do.

The observer crew requirements were largely as for the anti-icing investigation. The auxiliary power unit was operated by a Flight Engineer who had the least comfortable ride, being closeted in a sound-proof cabin with a 150 s.h.p. piston engine. His job was to maintain

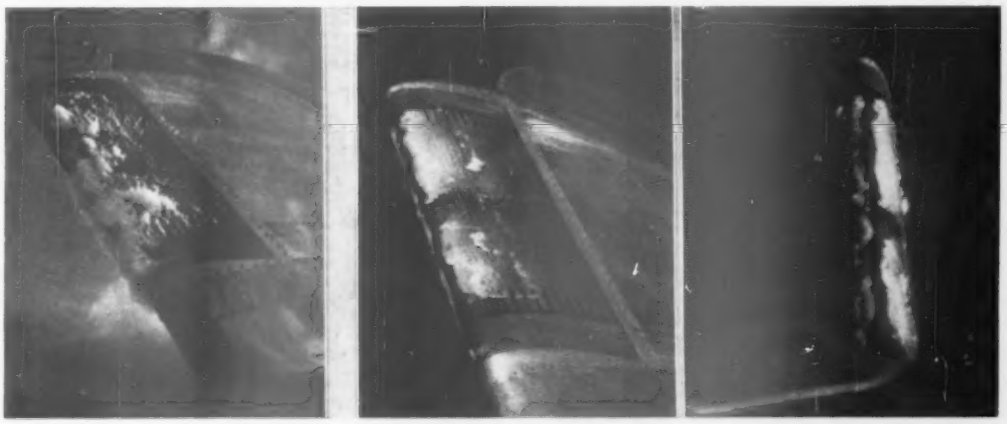

FIGURES 29, 30 and 31. Inadequate heat input. Effectiveness of continuous heated areas on Spraymat. Water concentration 0·24 gm./m^3. Ambient $-10°C$.

A.P.U. r.p.m. constant thereby maintaining constant spray nozzle pressure and alternator output.

No. 1 observer was able to view the section through a slit in the cabin roof (Fig. 24). Additional viewing was provided from a blister in the entrance door (Fig. 25). Later in the programme a blister was fitted to the starboard side giving yet another view of the test section. No. 2 observer controlled the water flow rates and nozzle air pressures, selecting the concentration and droplet size required at each test level. No. 3 observer controlled watts loading to the heated section and was also chief permutator of the cyclic panel. No. 4 observer had the dual role of assistant photographer and droplet sampler.

It will be instructive to observe the penalty to be paid at Continuous Maximum severity conditions of supplying insufficient heat as is shown in Fig. 29. Comparative views of satisfactory operations are shown in Figs. 30 and 31.

Recent Experience

In conclusion some technical data relevant to a more recent clearance undertaken with the Lincoln aircraft, that for the Comet 4 is of interest. Twenty-four flights were made, involving a flying time of about 46 hours.

The flight conditions of climb and descent were demonstrated and the climb was shown to be the more severe; two combinations of climbing speed and incidence were used.

It was also required to cover an air temperature and altitude operating range of from I.C.A.N. +25°C to I.C.A.N. −5°C. Demonstration was concentrated on the I.C.A.N. +25°C condition.

The heat outputs and working temperatures to be expected on the Comet were set up on the Lincoln as shown in Table I. The water flow rates required to meet the maximum Comet rates of catch were employed.

Climb on the Comet 4 is at 7,350 engine r.p.m. and a working air temperature of 200°C is maintained for anti-icing purposes by diluting compressor air by cold air bleed as necessary. The air flow available for anti-icing purposes becomes less as altitude is increased and varies from 0·088 lb./sec. per foot run at −5°C on an I.C.A.N. −5°C day, to 0·038 lb./sec. per foot run at −30°C on an I.C.A.N. +15°C day; the latter case implying a high altitude.

TABLE I

Regime		*Ambient* °C	*Inlet temp.* °C	*Heat input chu./hr./ft. run*
Climb	ICAN+25°C	−10	200	9980
Descent	ICAN+25°C	−10	167	7470
Climb	ICAN+25°C	−20	200	8850
Climb	ICAN+15°C	−30	200	9100
Descent	ICAN+15°C	−30	149	6840

Heat input is defined as $= m\,Cp\,(tgi - to)$.
where m = mass flow of hot gas in lb./sec.
where tgi = inlet temperature °C.
where to = ambient air °C.

Descent is at 6,000 r.p.m. and satisfactory performance was demonstrated. At this lower r.p.m. a working temperature of 200°C is no longer obtainable, and both temperature and air flow are dependent on altitude, being 167°C and 0·077 lb./sec. per foot run on an I.C.A.N. −5°C day at −5°C, and 149°C and 0·036 lb./sec. per foot run at −30°C on an I.C.A.N. +15°C day.

It was demonstrated that with the design heat inputs, anti-icing performance was satisfactory at B.C.A.R. Continuous Maximum severity conditions.

Based on the Lincoln tests, the A.R.B. agreed that airframe icing approval would be granted for the Comet 4 in the event that the same dry air surface temperatures were achieved in flight as were associated with the satisfactory heat input conditions during Lincoln tests. This was achieved on the Comet as evident from the clearance obtained.

Footnote

The Lincoln has since been converted to carry wing and tailplane sections of the Sud Aviation Caravelle, and tests to Continuous Maximum and Intermittent Maximum severity have been satisfactorily completed.

The aeroplane is now being converted to carry a wing tip section of the Avro 748 aircraft; this will be followed by testing of the A.W. 650 tailplane.

TECHNICAL NOTES

Iterative Solutions of the Equations for Plane Oblique Shock Waves

by

A. R. COLLAR, M.A., D.Sc., F.I.A.S., F.R.Ae.S.

(Department of Aeronautical Engineering, University of Bristol)

1. THE PRINCIPAL EQUATION

If a plane oblique shock wave, inclined to the free stream at the angle ε, is produced in two-dimensional supersonic flow of Mach number M by (for example) a wedge which deflects the flow through an angle δ, the equation connecting these quantities may be written

$$\tan\delta=\cot\varepsilon\,\frac{2\,(M^2\sin^2\varepsilon-1)}{(\gamma+1)\,M^2-2\,(M^2\sin^2\varepsilon-1)}\quad . \qquad (1)$$

In this form, δ is given explicitly when M, ε are fixed. Similarly, we may obtain M explicitly when ε, δ are fixed; equation (1) may be written (*see*, for example, Liepmann and Puckett[1], Equation 4.27)

$$\frac{1}{M^2}=\sin^2\varepsilon-\left(\frac{\gamma+1}{2}\right)\frac{\sin\varepsilon\sin\delta}{\cos(\varepsilon-\delta)}\quad . \quad . \qquad (2)$$

Unfortunately, it is rare to meet a problem in which M, ε or ε, δ are given. It is nearly always the case that M, δ are given and that it is required to find ε and to derive pressure ratios, and so on. Equations (1) and (2), for given M, δ, yield a cubic equation for the determination of ε: one of the roots is physically inadmissible, and of the other two, only the one corresponding to the weaker shock wave appears in practice. Because of the difficulty of solving a cubic and obtaining the relevant root, it is often the case that equation (1) is used to draw a chart or set of charts from which ε may be read off when M, δ are given. However, such charts are often either too large to be convenient, or too small for accurate reading. The writer suspects that there may be many who, like himself, have neither the inclination nor the eyesight for reading such charts, even if one remembers where the chart is to be found. Accordingly, he feels that it is worth noting an arithmetical method of solution of equation (1) which automatically yields the correct root of the cubic equation determining ε. The method proposed is one of iteration; it will yield results to any desired degree of accuracy.

2. THE REQUIRED SOLUTION

In equation (1) write

$$x=\cot\varepsilon\quad . \quad . \qquad (3)$$

and re-arrange the equation to read

$$x=\left\{(M^2-1)-\frac{\left(\frac{\gamma+1}{2}\right)M^4\tan\delta}{x+\left(\frac{\gamma+1}{2}M^2+1\right)\tan\delta}\right\}^{\frac{1}{2}} \qquad (4)$$

We then adopt the iterative process

$$x_{n+1}=+\left\{A-\frac{B}{x_n+C}\right\}^{\frac{1}{2}},\quad . \quad . \quad . \qquad (5)$$

Received 10*th August* 1959.

where

$$\left.\begin{aligned}A&=M^2-1,\\ B&=\left(\frac{\gamma+1}{2}\right)M^4\tan\delta,\\ C&=\left(\frac{\gamma+1}{2}M^2+1\right)\tan\delta.\end{aligned}\right\}\quad . \quad . \qquad (6)$$

Note that A, B, C are positive for all M, δ. We begin the iteration with x_0 large. If, in fact, the initial choice is infinitely large, the next value is evidently $A^{1/2}$, and this is thus a suitable choice for x_0. It is easy to see that this is greater than the root sought, since

$$A^{1/2}=(M^2-1)^{1/2}=\cot\mu,$$

where μ is the Mach angle. Since ε is necessarily greater than μ, it follows that $A^{1/2}$ is greater than cot ε. However, it is, of course, not necessary to choose $x_0=A^{1/2}$, if a closer approximation is known or can be inferred. It is, in fact, not necessary to begin with x_0 large: the iteration (5) converges to the greatest positive root of the cubic implied by (4) (if a positive root exists; that is, if an attached shock is possible) provided only that the initial value x_0 is greater than the second (positive) root. If an attached shock cannot exist, then after a number of steps x_{n+1} becomes imaginary.

3. THE CUBIC EQUATION

If we rationalise equation (4) we obtain

$$f(x)\equiv x^3+Cx^2-Ax+(B-AC)=0,\quad . \qquad (7)$$

where A, B, C are given by equation (6), so that

$$B-AC=\left(\frac{\gamma-1}{2}M^2+1\right)\tan\delta.\quad . \quad . \qquad (8)$$

It is to be noted that the coefficient of x^2 is positive, that of x negative, while the constant term is positive, for all values of M, δ. This implies certain properties: in particular, that the cubic has one, and only one, real negative root. To prove this, we observe that $f(x)$ changes sign in the range $-\infty<x<0$; there will therefore be either one or three real negative roots. But if there are three, then $f(x)$ must have its maximum and minimum values for x negative. This, however, is not so, for the constant term in $f'(x)$ is negative. There are thus not three negative roots: there must be one and one only. If the remaining two roots are real, they must be positive.

This, of course, accords with the well-known fact (demonstrated, for example, by the hodograph of the flow) that for given M, δ there are two shock inclinations ε which are physically possible; of these, it is always the weaker shock (smaller ε, larger x) which appears to be stable and which is observed in practice.

4. EXAMPLES OF THE ITERATIVE PROCESS

As a first, simple example, let $M^2=10$, $\tan\delta=0{\cdot}1$. Then, with $\gamma=1{\cdot}4$, we have

$$A=9,\ B=12,\ C=1{\cdot}3.$$

These numbers give, for the roots of the cubic (7), the values $-3{\cdot}73267$, $0{\cdot}03350$, $2{\cdot}39917$. The iteration procedure is, by (5)

$$x_{n+1}=\left\{9-\frac{12}{x_n+1{\cdot}3}\right\}^{1/2} \quad . \quad . \quad (9)$$

If we begin with $x_0=3$, the successive values of x_i, as computed with a slide rule, are

x_0	x_1	x_2	x_3	x_4
3	2·49	2·42	2·40	2·40

Similarly, if we begin with $x_0=0{\cdot}5$, we obtain

x_0	x_1	x_2	x_3	x_4	x_5	x_6
0·5	1·53	2·18	2·36	2·39	2·40	2·40

This is an example of an initial choice lying between the positive roots. However, if we begin with $x_0=0$, the process will not converge; one step gives x_1 imaginary. This example shows that, in the absence of any knowledge of the required value, it is safest to begin with $x_0=(M^2-1)^{1/2}$, since this is known to be greater than the root sought.

If a desk calculating machine and table of square roots is available, a calculation can be carried through very rapidly without recording any of the steps in the iteration. For example, let

$$M=2{\cdot}37,\ \delta=15^\circ\ (\tan\delta=0{\cdot}26795).$$

Then the iteration formula is

$$x_{n+1}=\left\{4{\cdot}6169-\frac{10{\cdot}1445}{x_n+2{\cdot}0740}\right\}^{1/2} \quad . \quad . \quad (10)$$

We begin by looking up $4{\cdot}6169^{1/2}$ in the Tables, setting it on the machine and adding 2·0740; use the sum to build up 10·1445, set up the multiplier found, subtract from zero, and add 4·6169. The square root of the answer is again found from the Tables and the procedure repeated. In this way we find the required root to be 1·2516.

Finally, as an example of a flow in which an attached shock wave cannot exist, let

$$M^2=10,\ \tan\delta=1{\cdot}0.$$

Then

$$x_{n+1}=\left\{9-\frac{120}{x_n+13}\right\}^{1/2} \quad . \quad . \quad (11)$$

This yields the sequence

x_0	x_1	x_2	x_3	x_4	x_5	x_6
3	1·225	0·751	0·523	0·355	0·121	imaginary

5. CONVERGENCE

It is usually easier to use iterative processes of the kind proposed than to demonstrate rigorously their convergence or to find the limits to which they converge. The following discussions are not claimed to be rigorous, but they may help in giving some insight into the convergence or otherwise of the process.

5.1. *Analytical Treatment*

Let the system be such that an attached shock can exist. We know from the previous discussion (Section 3) that $f(x)=0$ has three real roots, one negative. Let X_1 be the greatest (positive) root, X_2 the second positive root.

Now the iterative process is

$$x_{n+1}=\left\{A-\frac{B}{x_n+C}\right\}^{1/2} \quad . \quad . \quad . \quad (12)$$

and the desired solution is X_1, where

$$X_1=\left\{A-\frac{B}{X_1+C}\right\}^{1/2} \quad . \quad . \quad (13)$$

If now a step in the iteration begins with x_n, where

$$x_n>X_1,$$

it follows, since A, B, C are positive, that

$$A-\frac{B}{x_n+C}>A-\frac{B}{X_1+C},$$

or, in view of (12) and (13),

$$x_{n+1}>X_1. \quad . \quad . \quad . \quad (14)$$

Also, in view of (12),

$$x_n^2-x_{n+1}^2=x_n^2-\left\{A-\frac{B}{x_n+C}\right\}$$

$$=\frac{f(x_n)}{x_n+C}.$$

Now since $x_n>X_1$ and X_1 is the greatest root of $f(x)$, it follows that $f(x_n)$ is positive, whence

$$x_n>x_{n+1}. \quad . \quad . \quad . \quad . \quad (15)$$

From (14) and (15) we see that

$$x_n>x_{n+1}>X_1,$$

and each iteration therefore yields a closer approximation to X_1 than its predecessor.

If we begin with $x_n<X_1$, we obtain similarly the final result

$$X_1>x_{n+1}>x_n,$$

provided $f(x_n)$ is negative; that is, provided x_n lies between X_2 and X_1. If $x_n<X_2$, then $f(x_n)$ is again positive, and the iterative process clearly diverges.

Finally, if no positive roots exist, equation (14) is no longer applicable, but equation (15) is still true, since $f(x_n)$ is now positive for all positive x. Hence the iteration procedure eventually leads to a negative value for x_{n+1}^2.

5.2 *Graphical Treatment*

We can regard the iteration process (5) as an attempt to find the intersection of the two lines

$$y=x \quad . \quad . \quad . \quad . \quad . \quad . \quad . \quad (16)$$

$$y=g(x)\equiv\left\{A-\frac{B}{x+C}\right\}^{1/2} \quad . \quad . \quad (17)$$

The curve (16) passes through the first and third quadrants. As regards (17), it is (in view of the radical) symmetric about the x-axis. In the third quadrant, it has a branch asymptotic to $y=-A^{1/2}$; $g(x)$ is increasingly negative as x increases and the curve tends to the asymptote $x=-C$. Clearly (16) and (17) will have one intersection in this quadrant.

For $-C < x < (B-AC)/A$, $g(x)$ is imaginary. It becomes real again for $x \geq (B-AC)/A$, and in the first quadrant rises from zero with initial slope infinite, curves over and tends ultimately to the asymptote $y=+A^{1/2}$. Differentiation of equation (17) shows that the slope decreases monotonically from infinity when $g=0$ to zero for x infinite.

Figure 1 shows the curves (16) and (17) for the first example of Section 4, that is, $M^2=10$, $\tan\delta=0{\cdot}1$. The iteration procedure is equivalent to following the paths $PQRST\ldots$ or $P_1Q_1R_1S_1T_1U_1\ldots$ to the root X_1. For if we begin with x infinitely positive and substitute in (17), $y=g(\infty)=A^{1/2}$. Substitution of this value of y in (16) gives the point P with x also equal to $A^{1/2}$. This value of x in (17) gives Q, which in (16) gives R, and so forth. The two paths $PQR\ldots P_1Q_1R_1\ldots$ shown correspond to the two iteration tables of Section 4.

It is also clear that if the curve of $g(x)$ does not intersect $y=x$ in the first quadrant, an iteration will give a zigzag path alternating between the curves until a vertical step misses the curve $g(x)$: that is, an imaginary value of g is obtained.

Finally, it is also clear that if $g(x)$ and $y=x$ approach tangency (whether they just intersect or just miss) a large number of small steps in the iteration will occur.

6. OTHER ITERATIVE PROCESSES

The iteration process (5) is, of course, not unique; it is however, the most satisfactory the author has found. However, a few remarks on other formulae may be of interest.

Equation (1) may be transformed by the substitution

$$z=M^2\sin^2\varepsilon-1$$

to the form

$$z_{n+1}=\left(\frac{\gamma+1}{2}M^2-z_n\right)\left(\frac{M^2}{1+z_n}-1\right)^{-1/2}\tan\delta.$$

If this process is begun from $z_0=0$ (which, like $x_0=A^{1/2}$ earlier, corresponds to $\varepsilon_0=\mu$) it converges to the required result. However, each step requires two substitutions of z_n, so that the process takes longer, even though the number of steps required may be less.

An iteration of interest is derived from (5), but with the negative sign, namely,

$$x_{n+1}=-\left\{A-\frac{B}{x_n+C}\right\}^{1/2}. \qquad (18)$$

If we begin with x infinitely negative, we find the next value to be $-A^{1/2}$. Fig. 1 then demonstrates the quasi-spiral path $P_2Q_2R_2S_2T_2\ldots$ which converges in this case on the negative root:

x_0	x_1	x_2	x_3	x_4	x_5
-3	$-4{\cdot}01$	$-3{\cdot}66$	$-3{\cdot}75$	$-3{\cdot}73$	$-3{\cdot}73$

When the negative root has been found, it can be extracted from the cubic, and the positive roots, if any, then found. However, this iteration does not always converge; it does so only if the negative root lies at a point for which

$$-\frac{dg}{dx}<1.$$

If the (negative) slope exceeds unity, the process will clearly diverge. For example, if we attempt to solve (11) with the negative sign, beginning with $x_0=-3$, x_1 is imaginary. However, we can proceed in reverse; (11) gives x_n in terms of x_{n+1} as

$$x_n=\frac{120}{9-x_{n+1}^2}-13,$$

and if we take $n=0$, this gives the reverse sequence

x_1	x_0	x_{-1}	x_{-2}	x_{-3}
$-\infty$	-13	$-13{\cdot}75$	$-13{\cdot}67$	$-13{\cdot}67$

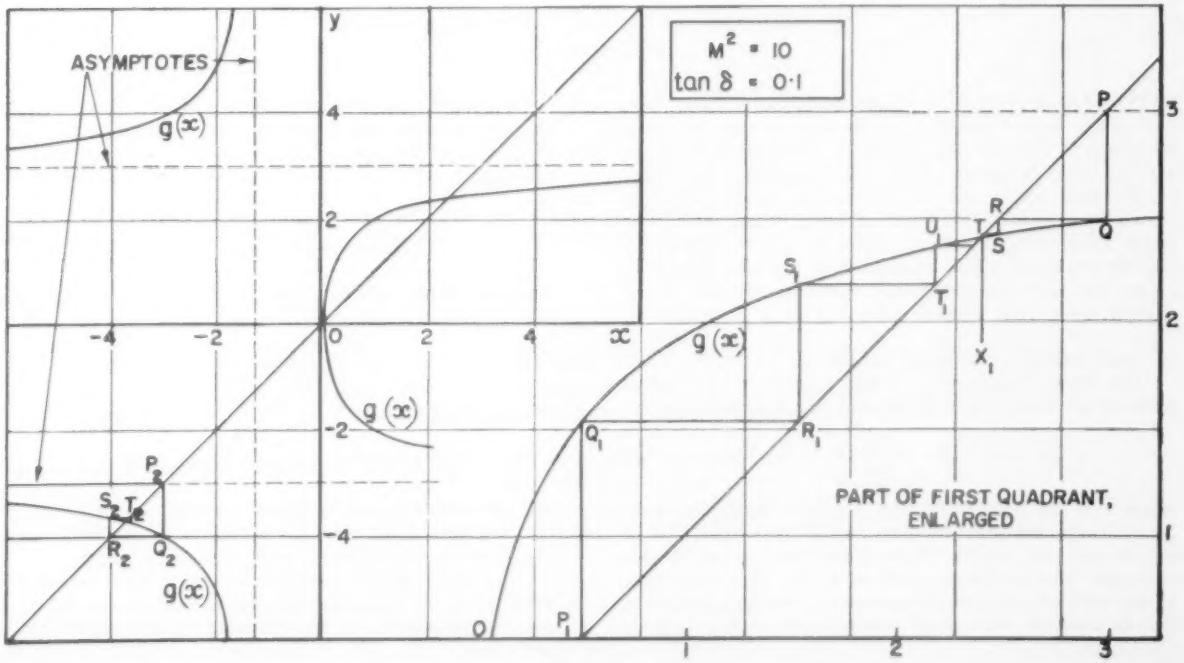

FIGURE 1.

We can also use this reverse iteration to obtain convergence toward the second positive root. If we revert to equation (9), for example, and write it as

$$x_n = \frac{12}{9 - x_{n+1}^2} - 1{\cdot}3,$$

we find, if we begin with $x_1 = 2$,

x_1	x_0	x_{-1}	x_{-2}	x_{-3}	x_{-4}
2	1·1	0·24	0·042	0·0336	0·03350

while the same result is achieved in two steps from an initial choice of zero.

However, these iterations are principally of academic interest, as an underlining of the conclusions of Section 5 on convergence. The important requirement for an iterative process is, in this case, that it can be used with confidence in all circumstances and that it should lead to the root sought, if such a root exists. The iteration (5) satisfies these requirements.

7. COMPLETION OF THE SOLUTION

The iteration process determines $x = \cot \varepsilon$; when this has been found, the Mach number normal to the shock, namely, $M \sin \varepsilon$, may be calculated and the pressure and density ratios, and so on, then determined. However, with a little manipulation, formulae involving x directly may be established; we have

$$\frac{p_2}{p_1} = 1 + \frac{\gamma M^2 \tan \delta}{x + \tan \delta} \quad . \quad . \quad . \quad . \quad . \quad (19)$$

$$\frac{\rho_2}{\rho_1} = 1 + \frac{M^2 \tan \delta}{x + \left(\frac{\gamma - 1}{2} M^2 + 1\right) \tan \delta} \quad . \quad . \quad (20)$$

and the temperature ratio can be found from these. For example, using the illustration of Section 4, we have, with $\gamma = 1{\cdot}4$,

$$M^2 = 10, \ \tan \delta = 0{\cdot}1, \ x = 2{\cdot}39917.$$

Then

$$\frac{p_2}{p_1} = 1{\cdot}5602; \ \frac{\rho_2}{\rho_1} = 1{\cdot}3705; \ \frac{T_2}{T_1} = \frac{1{\cdot}5602}{1{\cdot}3705} = 1{\cdot}1384.$$

Lastly, if M_s is the Mach number after the shock, it is given explicitly by the energy equation in the form

$$M_s^2 + \frac{2}{\gamma - 1} = \frac{T_1}{T_2}\left(M^2 + \frac{2}{\gamma - 1}\right), \quad . \quad (21)$$

or with $\gamma = 1{\cdot}4$

$$M_s^2 = \frac{T_1}{T_2}(5 + M^2) - 5.$$

REFERENCES

1. LIEPMANN, H. W. and PUCKETT, A. E. (1947). *Introduction to Aerodynamics of a Compressible Fluid*. Wiley and Sons, New York, 1947.

The Effect of Initial Lateral Tension or Slackness on the Deflection of Long, Thin Plates under Normal Pressure

by

H. L. COX, M.A., F.R.Ae.S. and D. DAWSON, G.I.Mech.E.

(*The National Physical Laboratory*)

THE BASIC THEORY of the deflection of long, thin plates under normal pressure is extended to cover the effects of initial lateral tension or slackness in the plate and the effect of deformation of the supports at the edges of the plate under the lateral tension developed. The procedure is illustrated by application to a case of a plate under initial tension with its edges held apart elastically, and the computed values of the strains are compared with values measured experimentally. The application to an initially slack plate is also illustrated by a diagram.

1. BASIC THEORY: THE DEFLECTED FORM

The deflection (w) of a long plate under normal pressure (p) is governed by the von Kármán equation,

$$EI\frac{d^4w}{dx^4} - T\frac{d^2w}{dx^2} = p \quad . \quad . \quad (1)$$

where T is the tension per unit length of the plate across its width (in the direction Ox), and EI is the modulus of section per unit length of the plate for bending in this direction. For moderate values of w (say up to one-tenth of the width b) T may be regarded as independent of x, but its constant value may depend upon initial slack or tension in the undeflected plate and upon the stiffness of the side supports which hold the edges of the plate apart.

The von Kármán equation (1) may be rewritten in the form

$$\frac{1}{(\alpha b)^2}\frac{d^4w'}{dx'^4} - \frac{d^2w'}{dx'^2} = \frac{pb}{T} \quad . \quad . \quad (1a)$$

where $w' = w/b$, $x' = x/b$ and $\alpha^2 = T/EI$, and the solution may be written in the form

$$w' = (pb/T)\,\psi\,(x/b, \ \alpha b) \quad . \quad . \quad (2)$$

The general form of ψ is

$$\psi = -\tfrac{1}{2}(x/b)^2 + A\,(x/b) + B + C\cosh \alpha x + D \sinh \alpha x \quad (3)$$

and the values of the arbitrary constants A, B, C and D are determined by the four conditions of deflection and rotational support, two at each edge of the plate.

The form of the function ψ is therefore completely determined by these edge conditions and by the value of αb, and the effect of elastic restraint against movement of the edges of the plate in the plane of the plate is entirely comprised in the value of αb.

Received 10*th August* 1959.

2. BASIC THEORY: DETERMINATION OF THE MEMBRANE STRESS

If the edges of the plate were held at a fixed distance apart, the centre line of the plate in the deflected form would be extended by a fraction proportional to $(w/b)^2$. Therefore this extension takes the form $(pb/T)^2\,\phi\,(\alpha b)$, where the function ϕ of (αb) depends otherwise only on the condition of support of the plate edges against deflection normal to the plate and against rotation. The condition of support against movement of the edges of the plate in the plane of the plate is a separate issue yet to be considered.

The actual extension of the centre line of the plate is $\{(T-T_0)/E't\}$ where T_0 is the initial tension in the plate, $E'=E/(1-\sigma^2)$ for the plate material, and t is the thickness of the plate; but the effective extension is further increased by the elastic deflection of the supporting members at the sides of the plate under the loading $T-T_0$. Thus the total effective extension of the centre line is $\{(T-T_0)/E't\}+2\{(T-T_0)/kb\}$, where k is the stiffness (load per unit width per unit deflection) of the supports at each edge of the plate to movement in the plane of the plate*. The value of T is therefore to be determined from the equation

$$\left(\frac{T-T_0}{T}\right)\left(1+\frac{2E't}{kb}\right)\frac{T}{E't}=\left(\frac{pb}{T}\right)^2\phi\,(\alpha b)\ . \qquad (4)$$

The mean stress f_s in the plate

$$\frac{T}{t}=\alpha^2\frac{EI}{t}=\frac{1}{12}E'\,(t/b)^2\,(\alpha b)^2$$

so that $\{f_s/E\,(t/b)^2\}$ is a function of αb only. On the other hand the bending stresses which are functions of αb are also proportional to w and therefore to pb/T; and so, of course, is the deflection also.

3. EXTENSION OF APPLICATION OF ROYAL AERONAUTICAL SOCIETY STRUCTURES DATA SHEETS IN THE 02.09 SERIES

The data presented in R.Ae.S. Structures Data Sheets of the 02.09 series represent solutions of equation (4) for the case $T_0=0$ and $(1/k)=0$. If we define a nominal pressure

$$p_n=p\left\{\left(1-\frac{f_s'}{f_s}\right)\left(1+\frac{2E't}{kb}\right)\right\}^{-1/2},$$

where f_s' is the initial lateral stress, equation (4) reduces to

$$\frac{T}{E't}=\left(\frac{p_nb}{T}\right)^2\phi\,(\alpha b)\ . \qquad (4a)$$

and the Data Sheets are once more directly applicable.

*If the two stiffnesses are k_1 and k_2, $(1/k_1)+(1/k_2)$ should be substituted for $(2/k)$.

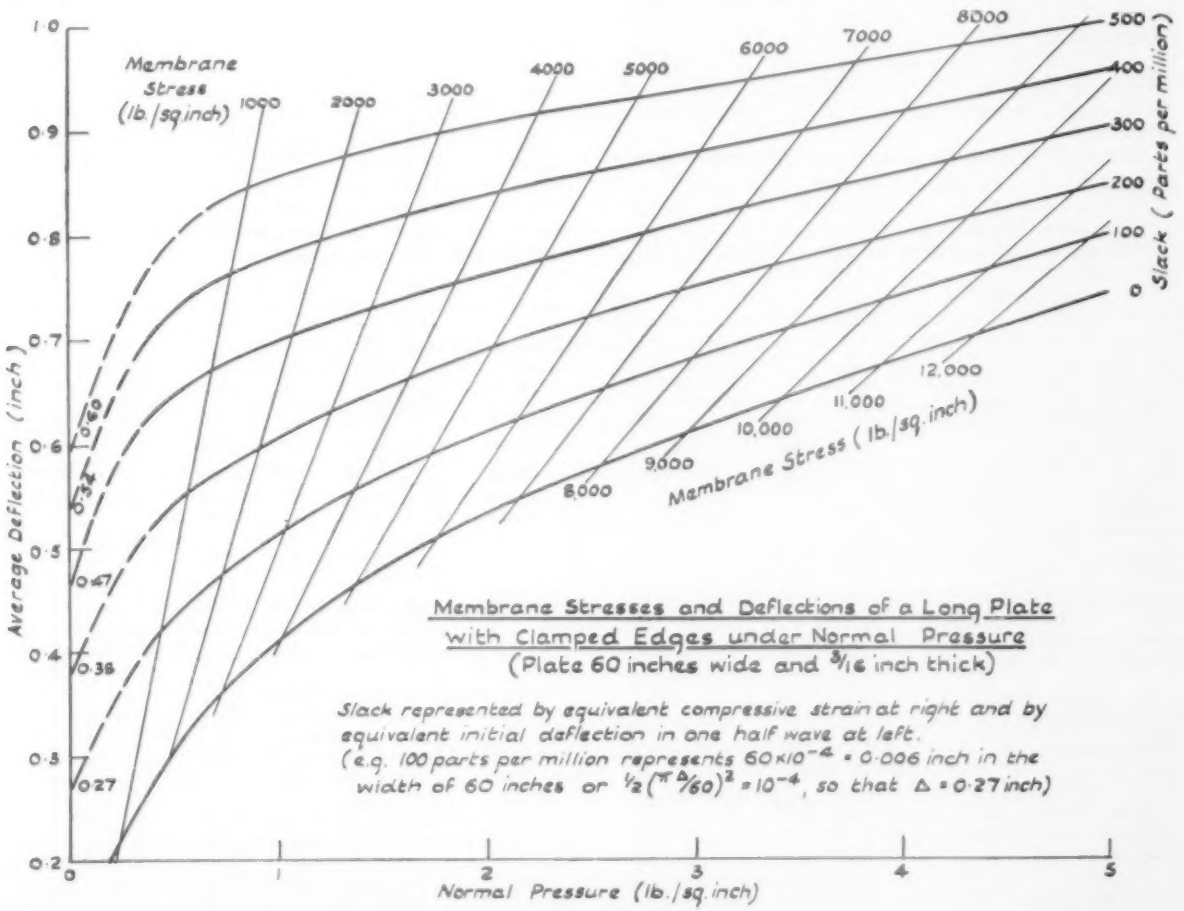

FIGURE 1

The procedure is to assume a value of p_n and to read the value of f_3 from 02.09.01 or 02. Then, the values of f_3' and k being specified, the value of p is found by multiplying p_n by the factor

$$\left\{\left(1-\frac{f_3'}{f_3}\right)\left(1+\frac{2E't}{kb}\right)\right\}^{1/2}$$

The values of δ and f_1-f_3 read from the Data Sheets must also be multiplied by the same factor, because they are proportional to pb/T that is to $(p/p_n)(p_nb/T)$, whereas the values read from the data sheets are proportional to (p_nb/T).

The procedure is demonstrated in Table II and comparison with experimental measurements is described in Section 5 and Table I.

4. APPLICATION TO PLATES INITIALLY SLACK

The general method is applicable if the plate were initially under transverse compression, that is when f_3' is negative. However, if $-f_3' > (\pi^2/3)(t/b)^2$ the plate would buckle and therefore a lower value of f_3' would represent initial slack in the plate. If the slack consisted in waviness of half wavelength λ and half amplitude A, the corresponding strain would be $(\pi A/2\lambda)^2$ and the value of $-(f_3'/E)(b/t)^2$ would be roughly $-\{3{\cdot}6+(n\pi A/2t)^2\}$, where n is the number of half waves across the width b. Using this formula to assess the value of f_3' from measurements of (A/t) and n, the general method may be used to compute the behaviour of an initially slack plate.

It is true that this application must be limited to positive values of f_3 (final); but this restriction is of no consequence, because until $f_3 > 0$ the initial waviness would persist.

The application of the method to a slack plate is illustrated in Fig. 1.

5. EXPERIMENTAL CHECK

The plate tested was 24 in. long, 4 in. wide and $\frac{1}{16}$th in. thick. The ends of the plate were clamped to supports 20 in. apart; these clamps held the edges of the plate firmly against rotation, but afforded only elastic restraint against movement of the edges in the plane of the plate. One support was adjusted relative to the other so as to apply an initial lateral tension of 1000 lb./in.² to the plate. This lateral tension was measured by means of resistance wire strain gauges glued to both top and bottom surfaces of the plate at the centre of its length, and these gauges were subsequently used to measure the stresses developed when normal pressure was applied. The normal pressure was applied by dead weights distributed over a sheet of sponge rubber one inch thick laid on top of the plate.

Measurements were also made of the lateral movement of the side supports by means of dial gauges in contact with each support just below the plate fixing. The results of the test are listed in Table I.

TABLE I

Pressure (*lb./in.²*)	*Change of Lateral Stress* (*lb./in.²*)		*Total Lateral Movement at Edges* (*in.*)
	Top Surface	*Bottom Surface*	
3	−2,500	13,600	0·0049

Note: Compressive stress is indicated by a negative sign. Since the measured change of average stress, 5,600 lb./in.², corresponds to a loading of 350 lb./in. on the side supports, the value of $k = 350/0{\cdot}00245 = 0{\cdot}14\times10^6$ lb./in.². Taking $E' = 33\times10^6$ lb./in.²,

$$1+\frac{2E't}{kb} = 2{\cdot}5.$$

The computed values of the stresses and deflection are listed in Table II. It will be seen that the computed value of f_1-f_3' is in good agreement with the measured value, although the computed value of f_4-f_3' is rather too low.

TABLE II

(*All stresses in lb./in.²: deflections in inches*)

p nom.	1·0	1·5	2·0	2·1	3·0	4·0
f_3 act. (read from 02.09.02)	4000	5200	6900	7300	9300	11400
$1-\frac{f_3'}{f_3}$	3000/4000	4200/5200	5900/6900	6300/7300	8300/9300	10400/11400
$\frac{p\text{ act.}}{p\text{ nom.}} = \sqrt{\left[2{\cdot}5\left(1-\frac{f_3'}{f_3}\right)\right]}$	1·36	1·43	1·47	1·47	1·49	1·51
p act.	1·36	2·15	2·94	3·08	4·47	6·04
$\frac{\delta}{t}$ nom. (read from 02.09.02)	2·21	2·59	2·85	2·97	3·29	5·05
$\frac{\delta}{t}$ act.	3·01	3·68	4·18	4·35	4·90	7·60
(f_1-f_3) nom. (read from 02.09.02)	4250	4730	5100	5300	6000	6600
(f_1-f_3) act.	5780	6740	7480	7750	8930	9950
δ	0·19	0·23	0·26	0·27	0·31	0·47
f_1	9780	11940	14380	15050	18230	21350
f_4	−1780	−1540	−580	−450	370	1450
f_1-f_3'	8780	10940	13380	14050	17230	20350
f_4-f_3'	−2780	−2540	−1580	−1450	−630	450
f_3-f_3'	3000	4200	5900	6300	8300	10400

Graduates' and Students' Section

Annual Dance: Friday 20th November

The dance this year will be held in the Library of the Society at No. 4 Hamilton Place, W.1. Dancing will be, as usual, to the music of Hugh McCamley. Double tickets cost only 14s. and include free drink and refreshments. No single tickets will be available this year.

Get your tickets from your nearest Committee member or representative, or write to Mr. J. D. Duncan, 8 Carlisle Avenue, St. Albans, Herts. Cheques and Postal Orders should be made payable to "Graduates' and Students' Section, Royal Aeronautical Society."

Visit to Hanover

We would be interested to know if there would be support for a visit to the Hanover Fair (24th April-3rd May 1960) on the same lines as the Paris Air Show visit. Part of the Fair is devoted to Air Transport and should prove of great interest. The cost is bound to be greater than the Paris visit and will depend on the numbers interested, so write as soon as you can to the Hon. Visits Secretary: Mr. A. R. M. Pickering, "Riverside," Vicarage Walk, Bray, Berks.

FUTURE LECTURES AND VISITS

The Flight Testing of Rotorcraft

Just to remind you of Sqdn. Ldr. Gellatly's lecture on Wednesday 11th November; full details were given in the October JOURNAL.

Atomic Energy Research Establishment, Harwell

There may still be a few places left for this very popular visit on Saturday 21st November, when these words appear in print. Write quickly to the Visits Secretary, at the address above.

Aerodynamics of Racing Cars

Mr. F. A. Costin will be speaking to us on Wednesday 2nd December on a very specialised subject of which he is an acknowledged expert. Shapes of record breaking Lotus, Vanwall, Maserati and Lister cars have been evolved from his careful work, and those who have met him will know that his fund of experience will ensure an interesting and entertaining evening. Frank Costin will be responsible for future shapes of projects from the Speedwell Company.

College of Aeronautics, Cranwell

A visit has been arranged for Saturday 5th December.

Letter to the Editor

Sir,

I wish to comment on Mr. Wilby's letter published in the Graduates' and Students' Section of the July 1959 JOURNAL regarding the professional status of members of the Society.

I wish to concur fully with Mr. Wilby's sentiments. In my experience as an Aeronautical Engineer in both the U.K. and Canada, I have noticed this apparent lack of knowledge concerning the Royal Aeronautical Society and its qualifications and also the *professional* status of its members.

In Britain (16 years ago) I found that preferential treatment in job status and salary was given to holders of B.Sc. degrees, who had no previous experience in the Aeronautical or any other Industry and were not members of the Society in any grade, over holders of a Grad. R.Ae.S. qualification.

In Canada, when prospective employers question you regarding Professional Qualifications, an answer involving the Royal Aeronautical Society brings, in a surprising number of cases, the query "What does that mean?" or "Who are they?" The same confusion does not exist regarding the status of Mechanical, Electrical and Civil Engineers and membership in their respective Associations.

I personally feel that today, professional recognition is becoming increasingly important for the Engineer as his work is becoming increasingly important to world progress, and it is essential that the public recognise and support this fact.

I submit that the R.Ae.S. has fallen somewhat behind other institutions in recognising (or acting on this recognition of) this fact of their *raison d'être*.

I have always been proud to be a member of the R.Ae.S. and continue to attach great importance to my association with this body. I certainly feel however, that more importance should in future be attached to the points raised in Mr. Wilby's letter.

Yours faithfully,
(*signed*) J. MACNAUGHTON,
Grad.R.Ae.S., P.Eng., M.C.A.I.

(A check on current advertising shows that only Blackburn and General Aircraft Ltd. specifically mention A.F.R.Ae.S. as a desirable qualification. The R.A.F. brochure on commissions in the Technical Branch does not mention it. The Royal Navy has at present no vacancies for careers as a Technical Officer for anyone except Cadet entrants (and Electrical Engineers) and we must therefore reserve judgment—*Section Editor*).

Lunar Probes

In his recent lecture to the Section about moon probes Mr. J. E. Allen outlined the flight paths and orbits which could be achieved and went on to examine the accuracy requirements for launching. He also discussed the design of the moon-probe vehicles and the launchings which have already been made by the U.S. and Russia.

Mr. Allen showed that very small variations in the final velocity of a probe had a big influence on the journey time taken to reach the moon. He also gave figures for the accuracy needed if a probe were guided only during its launching phase. For a vehicle intended to hit the moon the acceptable velocity error was only 75 ft./sec—in a total speed of about 36,500 ft./sec—if the injection angle was exactly correct. If the correct injection speed were achieved, the acceptable error in angle was only 0·01°.

For more complicated missions even greater accuracies were essential. If the probe was to pass round the moon and return to make a braking ellipse around the Earth, the initial accuracy required was 1 ft./sec. in velocity if the direction were correct; if the velocity were correct the direction error should be no more than 0·001°. Such accuracies were impossible with current guidance systems and mid-course or terminal corrections to the probe's trajectory would be needed.

The relative success of Russian and U.S. moon-probe launchings was mentioned in the discussion. Although the Russians may well have made abortive launchings, Mr. Allen thought it significant that recent Lunik shots had been timed to coincide with Kruschev's visit to the U.S. and the second anniversary of the Sputnik I launch. This indicated that the Russians could make successful launchings on planned dates, which had not always been the case with U.S. efforts.

Mr. Allen's complete lecture will be published in a future issue of the JOURNAL.—J. R. C.

THE LIBRARY

Reviews

SOUNDING ROCKETS. *Homer E. Newell, Jr. McGraw-Hill. 334 pp. Illustrated. 97s.*

In Dr. Newell's words "The essential feature of a sounding rocket is its ability to carry scientific instruments into the upper atmosphere." In his book he has gathered together descriptions of a very wide range of rockets with this ability and has outlined both the nature and the purpose of the instruments which are carried. The fact that Dr. Newell has nineteen collaborators, as authors of various chapters, stems from the fact that the book is based on papers presented in November, 1956 to a Symposium on High Altitude Sounding Rockets organised by the American Rocket Society. In the course of compilation the material has been kept up to date so that it, in effect, gives the "state of the art" at the start of the International Geophysical Year in July 1957.

To the separate descriptions of some fifteen basic sounding rockets and their variants, Dr. Newell has added two introductory chapters and two concluding chapters. The first introductory chapter outlines the essential features of sounding rockets and goes on to give the basic mathematics of rocket propulsion, the thermodynamics of rocket jets and the theory of the convergent-divergent nozzle. Why these particular topics are given so much weight is puzzling for they do not seem any more peculiar to sounding rockets than other important aspects of rocket flight, such as aerodynamics, which are not discussed. The second introductory chapter outlines the application of rockets to geophysical and solar research. In six pages the physical properties of the atmosphere (density, pressure, temperature, composition, clouds, winds and turbulence, the ionosphere, magnetic field, aurora, airglow, cosmic rays, meteors) are summarised. In the following seven pages the principal methods and the results obtained in measuring the above properties by rocket techniques are given. The high degree of condensation required to cover such a wide field in thirteen pages results in an account which should be of interest to those on the fringe of this field but is unlikely to appeal to either the novice or the expert.

The bulk of the book consists of fourteen chapters, each of which is devoted to a particular rocket or rocket family. In addition to American rockets (Aerobee, Viking, and so on) the sounding rockets developed by the British (Skylark), the French (Veronique and Monica) and the Japanese (Kappa and Sigma) are described in detail. For each rocket the historical background is given; the propulsion, launching and constructional features described and the performance characteristics stated. In some instances rocket costs are quoted. The techniques involved in launching from balloons or aircraft as a means of achieving greater altitude are described.

In his penultimate chapter Dr. Newell describes briefly the rocket firing ranges available in the U.S.A., Canada, Australia, French N. Africa and Japan. In his final chapter he discusses that complement to the sounding rocket—the artificial satellite. In this he derives the basic orbits and the relationships which have to be established in order to achieve orbital motion. The Vanguard launching vehicle is very briefly described.

I would have welcomed an extra chapter which attempted to bring together and compare the main characteristics of the rockets so that the reader was left not with a confused impression of many rockets, but an integrated picture of the trends in sounding rocket development.

The main value of the book undoubtedly lies in its being a detailed, in places too detailed, history of sounding rockets up to mid-1957.—J. J. GAIT.

GUIDED MISSILE ENGINEERING. *Allen E. Puckett and Simon Ramo (Editors). McGraw-Hill, London, 1959. 497 pp. Illustrated. 77s. 6d.*

Despite its title, this book is not really concerned with engineering: it might more suitably have been called "The fundamental theory of guided missiles." In seventeen independent chapters, by separate authors, the theory underlying nearly all aspects of guided missile design and operation is developed *ab initio* up to a point where a reader previously unfamiliar with the theory can see how it applies to actual missiles. The editors chose most of the authors from their own organisations, the Hughes Aircraft Company and the Ramo-Wooldridge Corporation, but there need be no regrets over this touch of clannishness, for the book is an excellent one.

The first section is a deft outline of aerodynamics by A. E. Puckett, and this is followed by chapters on aerodynamic stability and control, rockets, and ram-jets. Then come surveys of information theory and missile guidance, navigation, random phenomena, servos and feedback control, and gyroscopy. Next there are three chapters on electronics—entitled Radio Propagation, Microwaves, and Radar. Thus far, the book is consistently good: the general plan seems to be that each author should start at the most elementary level and develop the essentials of the theory, sometimes to quite an advanced stage, without digressing into matters of detail. The authors succeed in this aim and are often refreshingly direct in cutting through the tangle of jargon which shrouds their subject, most notably perhaps in F. P. Adler's presentation of information theory and its application to missile guidance, topics notoriously difficult to explain. The overlapping, omissions and sudden changes of style which often mar multiple-author books are avoided. The last four chapters, on analogue computers, digital computers, trajectory analysis and flight simulators, and the integration of design, are however less satisfactory, chiefly because of overlapping and a drift into generalities.

The editors, like the compilers of a verse anthology, can scarcely hope to escape criticism over their choice of subjects, on which opinions are bound to vary. To the reviewer it is astonishing, especially in view of the book's title, that there is no chapter on missile structural design: the intercontinental ballistic missile, which is, at least to the general public, the guided missile *par excellence*, depends more upon efficient structural design than upon any other factor. The balance of the book is questionable in a few other respects, too. For example, it is rather surprising to find a 40-page chapter, backed up by an Appendix, on such a specialised subject as instrumental gyroscopy, when the other chapters are much wider in scope.

With these few reservations, the book can be strongly recommended as an introduction to guided missile theory; and it conforms to the high standard of production which one expects of McGraw-Hill books.—D. G. KING-HELE.

BRITISH CIVIL AIRCRAFT 1919-59. Vol. 1. *A. J. Jackson. Putnam, London, 1959. 571 pp. Illustrated. 63s.*

In his preface, the author of this latest book in Putnam's historical series points out that the progress of civil aviation in Britain falls into two well-defined 20-year cycles, the first distinguished by relatively unfettered operation of privately-owned light aeroplanes, the second dominated by fiercely competitive transport fleets and strict legislation. Somewhere about halfway through the first cycle, the author was inspired to begin collecting photographs and data of aeroplanes bearing British civil registration marks. G-EBZZ had just been followed by G-AAAA and both had been in the news, the former with a solo flight to West Africa and the latter with a new altitude record. Even at that date the possibility of compiling anything like a complete record must have seemed remote, but by fortunate coincidence, he, living in Essex, made contact with another of like mind living in the North of England. Their collections, being regional in origin, were found to be complementary and so began the fruitful partnership between A. J. Jackson and the late E. J. Riding, to whom this book is dedicated.

Their complete records, compiled for personal satisfaction, form an unparalleled archive of one aspect of civil aviation over a period of forty years, but are obviously far too voluminous and detailed for publication at length. Mr. Jackson has had a difficult task in epitomising this record in a book of reasonable compass even though his publishers have allowed him two pint pots into which to distil his imperial gallon. No room could be spared for excursions into anecdote or design philosophy, and some readers may regret this, but Mr. Jackson is to be congratulated on providing a very readable text containing all the essential facts, dimensions, fates and dates on his subject. This volume ranges from A.B.C. to Dudley Watt, the remainder being reserved for Volume 2.

The production and quality of the photographs is fully up to Putnam's highest standards, and what a store of hidden treasure they reveal! For the first time this reviewer sees in print the Airspeed Ferry with all three engines inverted, the Avro Cabin Cadet, the Bristol 83E with geared Titan, the Parnall-built Airdisco-engined C.11 gyroplane, the Avro 538 sporting variant of the Spider scout, the Beardmore W.B.X., the Dart Flittermouse, the only civil Bristol Scout C and the D.H. Hound with its original direct-drive Lion. The other 500 photographs, although less rare, are all excellently chosen and in many cases hitherto unpublished. There are over 100 three-view general arrangement drawings, which exhibit Mr. L. E. Bradford's customary skill and accuracy, although unavoidably constrained to a small scale in certain cases.

The main body of the book deals with 210 types and variants of production civil aircraft, giving each main type or family group a concise and informative account of development and operation averaging some 1500 words. This section is followed by four Appendices, of which the first briefly describes and illustrates a further 141 civil aeroplanes, mainly prototypes; the second deals similarly with 45 civil-registered military aeroplanes; the third describes the mere dozen civil-registered types of which no illustrations have so far come to light; while the last gives in tabular form the registration particulars and individual histories of aircraft described in the main text, so far as they are on record.

No book of this size and scope can entirely avoid errors, but very few are apparent and those are of minor importance. For instance, the Genet-Avian G-AABR (a most interesting close-cowled variant) is captioned as "wooden" although stringers visible through the fuselage fabric are typical of metal construction; surely, too, the Cirus III Avian AACV and Tommy Rose's Hermes Avian AAHJ had metal fuselages and antedated AATL which is quoted as being the first metal Avian? There is some confusion over the type number of the Avian IVM—on page 91 it is given as Avro 616 but elsewhere as Avro 594. The Beardmore W.B.X is identified in the text as G-EAQI whereas the photo clearly shows it as EAQJ; on page 133 Mr. J. E. Carberry is wrongly styled "Sir John," which may annoy him, and there are a few mis-spelled names (*e.g.* Wooley Dod), which should have been avoided. These will not mislead any reader but ought to be eliminated from the next edition, in which, too, the opportunity should be taken to bring last-minute data up to date, *e.g.* Britannia AOVT should be added to the B.O.A.C. fleet list in Appendix D. An author's difficulties in gleaning the last grain of information are not confined to current events, for, after this volume had gone to press, news came from Australia indicating almost certainly that Harry Butler's preserved Bristol monoplane VH-UQI was bought by him from the Disposal Board at Waddon as C-5001 at an earlier date than G-EAER was registered; consequently the surmise given in good faith on pages 186 and 534 must now be discounted.

An interesting sidelight on the small productive capacity of the British aircraft industry in the late twenties is implied on page 164, where it is mentioned that Bluebird IV production was subcontracted to Saunders-Roe because Blackburn's had just received a military order (presumably for Ripons). What Mr. Jackson does not say is that Saro themselves were so overwhelmed by the Bluebird commitment that they in turn sub-contracted the wings to Boulton and Paul at Norwich. Mr. Jackson writes as a lifelong flying club enthusiast and is an active and talented amateur holder of a P.P.L., who has flown a representative sample of the vintage light aeroplanes he describes. He seems, moreover, to have captured much of the zest which was so characteristic of Eddie Riding's own reporting.

This is a book in the high tradition set by J. M. Bruce's "British Aeroplanes 1914-18," and a thoroughly worthy companion to Thetford's two precursors in the same format. One has only one fear, that Volume 2 may not be out in time for Christmas—but that is no reason for not ordering both volumes now.—SENRAB.

NINE LIVES. *Group Captain A. C. Deere, D.S.O., O.B.E., D.F.C. Hodder and Stoughton, London, 1959. 262 pp. Illustrated. 15s.*

Alan Deere, the most famous of the New Zealand fighter pilots, though a forceful character, as his autobiography makes clear, is a very modest man. His personal courage in conditions of desperate war against the enemies Luftwaffe and Fatigue was a great inspiration to all who worked, flew and fought with him. His story of a very unpleasant yet thrilling experience as a pilot in the Battle of Britain is probably the best yet published. As a word picture it has everything to commend it. The book is written in the first person and the author takes the reader with him, as a guide shows a visitor a military museum. He shows from personal experience how the battle ebbed and flowed, as he saw it rather than as it affected him. Of course, he was tremendously affected, as several incidents make clear, but his personal enthusiasm for the job of making war on a vicious enemy submerges his personal sense to a remarkable degree. This book is well worth reading.—A.S.C.L.

Additions to the Library

Air Aces of the 1914-1918 War. Bruce Robertson (*Editor*). Harleyford Publications, Letchworth. 1959. 211 pp. 45s. *To be reviewed.*

Asbestos: its Industrial Applications. D. V. Rosato. Reinhold (C. and H.). 1959. 214 pp. Illustrated. 46s. A small book on uses of asbestos in industry. Chapters include insulation, textiles and plastics. A bibliography is appended.

British Civil Aircraft 1919-59, Volume I. A. J. Jackson. Putnam, London. 1959. 571 pp. Illustrated. 63s. *Reviewed on p.* 677.

Construction of Research Films, The. D. H. Densham. Pergamon. 1959. 104 pp. 30s. No. 33 in the Agardograph series, this has been compiled by the Adviser on Films at the Ministry of Supply. Thirteen chapters deal with all aspects and a useful glossary is appended.

Famous Airships of the World. J. A. Sinclair. Muller, London. 1959. 144 pp. Illustrated. 9s. 6d. There are 18 other titles in this series—airports, air routes, battleships and so on through the alphabet to waterways. The late Captain Sinclair was one of the few people still left with an interest in airships. Such a small book cannot be exhaustive and most of it deals with the bigger craft of the later years.

Handbook of Supersonic Aerodynamics. Volume 3, Section 7. Three Dimensional Aerofoils. U.S. Bureau of Ordnance and Johns Hopkins University. U.S.G.P.O. 1957. Sectional pagination. $1.50.

Numerical Control of Machine Tools, The. R. C. Brewer. Engineer's Digest. 1959. 69 pp. Illustrated. 6s. A second edition of *Engineer's Digest* Survey No. 5, originally published in that journal in September 1958 and January 1959. A long list of acknowledgments indicates co-operation from many firms.

Outer Space Propulsion by Nuclear Energy. U.S. Congress. U.S.G.P.O. (H.M.S.O.). 1958. 232 pp. 5s. 5d. Minutes of hearings before subcommittees of the Joint Committee on Atomic Energy. This Committee contributed to the Nautilus project and now has Project Rover underway. "It was the consensus among witnesses who appeared before the Committee that of all propulsion systems currently under consideration, nuclear propulsion appears to offer the greatest advantage for carrying large payloads great distances, such as interplanetary travel."

Proceedings of the Society for Experimental Stress Analysis. Volume XVI, No. 2. C. V. Mahlmann and W. M. Murray (*Editors*). S.E.S.A. 1959. 165 pp. Illustrated. No price. 17 papers on a range of aspects of stress analysis, including photoelasticity, triaxial stress testing, acoustical testing, impact loading and the use of digital computers.

Raumfahrt—technische Überwindung des Krieges. Eugen Sänger. Rowohlt, Hamburg. 1958. 142 pp. D.M. 1.90. *To be reviewed.*

Rockets and Satellites Work Like This. John W. R. Taylor. Phoenix House London. Roy Publishers, New York. 72 pp. Illustrated. 9s. 6d. One of the "Science Works Like This" series, intended for boys but suitable for anyone who wants a simple, logical presentation of the history and development of rockets and satellites. It is well co-ordinated and illustrated, and could be used as a reference book for a short, clear description of nine basic categories of guided weapon and eleven types of guidance system.

S.A.E. Transactions 1959. Society of Automotive Engineers. New York, S.A.E. 1959. 672 pp. Figs. $8 to libraries. $11 to non-members. Contains some of the more notable papers read in 1958 including Van Every on design for very high speed flight, Stepniewski on wings and vertical thrust in VTOL, Ekvall on strength and limitations of materials for airframes (Titanium) and Stasinger on inertial navigation systems.

Seven Skies, The: a Study of B.O.A.C. and its Forerunners Since 1919. John Pudney. Putnam, London. 1959. 320 pp. Illustrated. 30s. *To be reviewed.*

Sixth Anglo-American Aeronautical Conference. Folkestone, 1957. Royal Aeronautical Society, London. 1959. 524 pp. 6 guineas. The complete record of the Technical Sessions, including the 16 papers, all formal discussions and the list of delegates. The subjects covered include: N.A.C.A. Research on V.T.O.L. and S.T.O.L., Nuclear Propulsion for Aircraft, Control of Supersonic Propulsion Systems, Electrical Control of Power Plants, Kinetic Heating, Titanium, Non-metallic Materials at High Temperatures, Blast Loading of Aircraft Structures, Safety in Relation to Structural Damage, Aircraft Instruments, Aeroelasticity, Boundary Layer Control, Experimental Hyperballistics, Civil Turbine Engines and The Human Pilot.

Two Residents of Bexley, Part I—Sir Hiram Maxim. Patricia H. Hazael. Bexley. 1959. 55 pp. Illustrated. No price. A teacher's thesis which, with its local interest and modern approach is more readable and interesting than the conventional works.

Reports

AERODYNAMICS

BOUNDARY LAYER *see* SCIENCE—GENERAL

COMPRESSIBLE FLOW

An experimental investigation of the interference between bodies of revolution at transonic speeds with special reference to the sonic and supersonic area rules. G. Drougge. Appendix: Application of the transonic principle of equivalence to a pair of bodies of revolution. S. B. Berndt and L. O. A. Hilding. F.F.A. Report 83. 1959.

Certain aspects of the sonic and supersonic area rules have been investigated experimentally, mainly by interference tests on a pair of slender bodies of revolution at transonic and low supersonic speeds. The investigations make it possible to test the transonic similarity rules for bodies of revolution, and a convincing confirmation is obtained.—(1.2.2×1.2.3).

FLUID DYNAMICS *see also* STABILITY AND CONTROL

The effect of density on jet flow at subsonic speeds. A. H. Craven. C.o.A. Report 120. *July* 1959.

On the assumption that the velocity and density distributions across a jet of one gas issuing into a stream of a second gas are of exponential form, the momentum integral approach has been used to find the variation of centre-line velocity downstream of the potential core. The results for the particular case of a jet issuing into a gas at rest are equivalent to those found theoretically by Blottner and experimentally by Keagy and Weller. The results for the jet issuing into a moving stream agree with the author's limited experiments.—(1.4).

A fluid-dynamic mechanism of meteorite pitting. D. T. Williams. Smith: Cont. to Astro. Vol. 3, *No.* 6. 1959.

Flow lines on meteorites were photographed to determine the nature of air flow inside the "thumb pits" in the surface.—(1.4.3×8.1).

LOADS *see* WINGS AND AEROFOILS

STABILITY AND CONTROL *see also* TESTING AND INSTRUMENTS

Effect of body incidence on two afterbodies with a rearward facing jet. A. H. Craven. C.o.A. Note 92. *Dec.* 1958.

The results of an experimental investigation into the effect of a jet issuing from two afterbodies (one a right cylinder and the second conical) at incidence to a uniform subsonic flow are given. The tests were performed at a Reynolds number of $0{\cdot}3\times10^6$ based on a body diameter and maximum tunnel velocity.—(1.8.0.2×1.4).

*The influence of non-stationary stability derivatives on the snaking motion at high subsonic speed. J. Yff. N.L.L. Report TR.F.*208. *Nov.* 1957.
Some lateral stability calculations with two degrees of freedom for flight at high subsonic speed have been performed to study the influence of the non-stationary stability derivatives on the damping of the snaking motion.—(1.8.1.1).

WINGS AND AEROFOILS

Efforts d'un fluide incompressible sur un profil oscillant autour d'une incidence non nulle. G. Couchet. O.N.E.R.A. Pub. 96. 1959. (*In French*).—(1.10.1.1×1.6.3×2).

Experimental investigation of transonic flow past two-dimensional biconvex circular-arc airfoils at small angles of attack. R. Kawamura and K. Karashima. Aero. Res. Inst. Tokyo Report 342. *April* 1959.
The results of an experimental investigation of transonic flows past biconvex circular-arc aerofoils with thickness-chord ratios of 10·6, 8·08 and 5·44 per cent are presented. Aerodynamic characteristics of the aerofoils are analysed from the surface pressure distributions obtained by interferometry.—(1.10.2.1).

TESTING AND INSTRUMENTS *see also* FLIGHT TESTING

Measurement of aerodynamic damping and stiffness derivatives in free oscillation with automatically recycled feedback excitation. K. J. Orlik-Rückemann. N.R.C. Report LR-246. *June* 1959.—(1.12.6×2×1.8.0.2).

Interpretation and applicability of results of wind-tunnel flutter and control surface buzz investigations. A. G. Rainey. AGARD Report 219. *Oct.* 1958.
Several aspects of the rôle of the wind tunnel in the overall picture of flutter investigations, model simulation, tunnel suitability and application to flight are considered. The types of flutter amenable to wind tunnel study, the degree of model simulation required, the value of the small scale aeroelastic component model and, the application of wind tunnel results in the determination of critical flutter ranges or margins of safety are described.—(1.12.1×2).

A summary of design techniques for axisymmetric hypersonic wind tunnels. Y-N Yu. AGARDograph 35. *Nov.* 1958.
A family of perfect fluid co-ordinates for axisymmetric effusers with the exit Mach number range of 5 to 20 has been computed by the method of characteristics. A conical source flow front and a centre line Mach number distribution are used as initial conditions. Design techniques and other related problems of interest in the development of hypersonic facilities are summarised.—(1.12.1.3×1.12.6.1).

AEROELASTICITY

See AERODYNAMICS—WINGS AND AEROFOILS
TESTING AND INSTRUMENTS

AIRCRAFT

See DESIGN AND CONSTRUCTION

DESIGN AND CONSTRUCTION

Tire-to-surface friction-coefficient measurements with a C-123B airplane on various runway surfaces. R. H. Sawyer and J.J. Kolnick. N.A.S.A. Report 20. *June* 1959.
An investigation was conducted to obtain information on the tyre-to-surface friction coefficients available in aircraft braking during the landing run. The tests were made with a C-123B aeroplane on both wet and dry concrete and bituminous pavements and on snow covered and ice surfaces at speeds from 12 to 115 knots. Measurements were made of the maximum (incipient skidding) friction coefficient, the full-skidding (locked wheel) friction coefficient, and the wheel slip ratio during braking.—(4.2.2.3×5.3×3.6).

United States Air Force development of aircraft arresting gear. V. V. Vary. AGARD Report 227. *Oct.* 1958.
For many years Navy aeroplanes have required arresting gear and catapults for carrier operation. This has meant a considerable weight penalty to the aeroplane structure, which has had to be designed to withstand horizontal arresting accelerations up to 6*g* and also large vertical accelerations due to the relatively high vertical speed of contact with the deck. A relatively low stalling speed—to keep within required launching and arresting energies—has been another penalty. Land based Air Force aeroplanes have, until recently, gone in for longer runways and, consequently, can operate at greater loads and speeds. This makes the design of arresting gear for Air Force aeroplanes much more difficult than for the short-stroke, high-*g* Navy aeroplane. Various devices by which engagement can be effected and the aeroplane successfully arrested are discussed.—(4.2.3).

AIRCRAFT OPERATION

See also DESIGN AND CONSTRUCTION
FLIGHT TESTING
AIRPORTS

Origin and prevention of crash fires in turbojet aircraft. I. I. Pinkel et al. N.A.C.A. Report 1363. (*Supersedes N.A.C.A. T.N.* 3973). 1958.
The tendency for the jet engine rotor to continue to rotate after crash presents the probability that crash-spilled combustibles suspended in the air or puddled on the ground at the engine inlet may be sucked into the engine. Studies showed that combustibles drawn into the engine in this way ignite explosively within the engine. Flames that could set the major fire appear at the engine tailpipe and often at the inlet when this explosive ignition occurs. This ignition may occur on the hot metal of the engine interior even after the combustor flame is extinguished and the engine rotor is coasting to rest.—(5.3×27.4).

An evaluation of the factors which influence the selection of landing approach speeds. F. J. Drinkwater et al. *AGARD Report* 230. *Oct.* 1958.
The aim was to increase understanding of factors influencing pilots' choice of approach speeds by an evaluation of landing techniques of a wide variety of aeroplanes, using the constant speed, constant angle, type of approach.—(5×13).

AIRPORTS

Measurements and power spectra of runway roughness of an airport. (*Airport* 1). *AGARD R.M.* 1. *March* 1959.
Measurements of the surface roughness obtained by a profile survey method are presented in the form of tables giving the survey data and in the form of power spectra.—(6.1).

Measurements and power spectra of runway roughness of an airport. (*Airport* 2). *AGARD R.M.* 2. *March* 1959.
Measurements of the surface roughness obtained by a profile survey method are presented in the form of tables giving the survey data and in the form of power spectra.—(6.1).

EXTRA-ATMOSPHERIC TECHNOLOGY

See also AERODYNAMICS—FLUID DYNAMICS
MATHEMATICS
MISSILES

Minimum propulsion for soft moon landing of instruments. D. S. Carton. C.o.A. Note 94. *July* 1959.—(8×27·3).

FLIGHT TESTING

See also AIRCRAFT OPERATION

Review of aircraft altitude errors due to static-pressure source and description of nose-boom installations for aerodynamic compensation of error. W. Gracey and V. S. Ritchie. N.A.S.A. Memo 5-10-59*L. T.I.L.* 6491. *June* 1959.
Aircraft altitude errors due to static pressure source are briefly reviewed. Wind tunnel test information concerning nose-boom pressure installations for aerodynamically compensating static-pressure errors due to position and angle of attack at subsonic and low supersonic speeds are also presented.—(13×1.12.2).

Several methods for aerodynamic reduction of static-pressure sensing errors for aircraft at subsonic, near-sonic, and low supersonic speeds. V. S. Ritchie. N.A.S.A. Report 18. *June* 1959.
Tests were conducted in transonic wind tunnels to investigate and verify experimentally methods for aerodynamically reducing errors due to sensor position, bow-wave passage, and angle of attack.—(13×1.12.2).

The performance testing of military aircraft-carrier aircraft. R. P. Dickinson. AGARD Report 232. *Oct.* 1958.
The operation of carrier-borne aircraft and the ways in which it differs from the operation of other military aircraft from the

viewpoint of performance assessment are described. The factors affecting the determination of recommended approach speed and of wind speed limitations for catapult take-off are discussed and an indication is given of the extensive instrumentation needed during trials.—(13.3×5).

FUELS AND LUBRICANTS

Aviation fuel problems at high altitudes and high aircraft speeds. E. M. Goodger. C.o.A. Report 119. *Jan.* 1959.
Much useful data has appeared concerning the problems incurred by continued increases in operational altitudes and aircraft speeds. A representative amount of these data is presented in a form suitable both for general information and for project design reference.—(14).

INSTRUMENTS AND EQUIPMENT

R.P.M. indicator and overspeed trip. R. J. Harron. N.R.C. Report MI-819. May 1959.
The function of this dual-purpose instrument is (*i*) a coarse r.p.m. indicator and (*ii*) an adjustable overspeed trip relay having two overlapping ranges of 11,000 to 16,000 r.p.m. and 15,000 to 20,000 r.p.m.—(18.1).

MATERIALS

See STRUCTURES—THEORY AND ANALYSIS

MATHEMATICS

See also MISSILES

Periodic orbits of a planetoid passing close to two gravitating masses. R. R. Newton. Smith: Cont. to Astro, Vol. 3, *No.* 7, 1959.
A study of periodic orbits in the restricted three-body problem in which the small mass passes close to each of the large masses is presented. The orbits are classified according to the types of motion involved and methods are given for estimating initial conditions for various classes of orbit. Sample orbits determined by a digital computer are presented.—(22.3×8).

Actes du colloque de calcul numérique. Perigueux 1957. *Pubs Sc et Tech N.T.* 80. (*In French.*) 1959.—(22.1).

MECHANICAL ENGINEERING

On helical-spring suspension. L. G. Lidin. Inst. of Machine Elements. Chalmers University of Tech. Report 6. 1959.
The problem of determining the natural frequencies for a device suspended by helical springs is treated. The method is applicable also to other spring types, provided their elastic properties are known. There are two different types of springs that are used for this purpose, namely springs with hinged ends (hooks) and compression springs with ends clamped. An account of the elastic properties of both types is given. Then for each type the general frequency determinant for a spring-suspended system is derived from the movement equation. The significance of the natural frequencies for forced vibrations is demonstrated. General schedules are given for obtaining the determinants for any case of helical-spring suspension. Experiments have been made of both types of springs.—(23).

MISSILES

1958 *NASA/USAF space probes* (*Able*-1). *Final Report Vol.* 1. *Summary. Space Technology Labs. N.A.S.A. Memo* 5-25-59W. *TIL* 6490. *June* 1959.
The three NASA/USAF lunar probes of 17 Aug., 13 Oct. and 8 Nov. 1958 are described. Details of the programme, the vehicles, the payloads, the firings, the tracking, and the results are presented. Principal result was the first experimental verification of a confined radiation zone of the type postulated by Van Allen and others.—(25.3×27.3×8).

Lieu des racines d'une équation algébrique dépendant d'un paramètre: application a la stabilité et au guidage des fusees. F. Salles. Pubs Sc et Tech. 351. 1959. (*In French*).—(25.1×22.1).

POWER PLANTS

See also AIRCRAFT OPERATION
EXTRA-ATMOSPHERIC TECHNOLOGY
MISSILES

The effect of combustor outlet temperature profiles on ramjet thrust. M. R. Williams and S. W. Greenwood. C.o.A. Note 59. *July* 1957.
The desirability of obtaining an even distribution of temperature at the outlet of a ram-jet combustor is indicated theoretically. Results of experiments on a particular combustion system over a limited range of conditions using a series of mixers are presented.—(27.4).

Theoretical performance of liquid hydrogen with liquid oxygen as a rocket propellant. S. Gordon and B. J. McBride. N.A.S.A. Memo 5-21-59E. *TIL* 6492. *June* 1959.
Theoretical rocket performance for both equilibrium and frozen composition during expansion was calculated at four chamber pressures (60, 150, 300 and 600 lb./in.^{2} abs.) and a wide range of pressure ratios (1 to 4000) and oxidant-fuel ratios (1·190 to 39·683). Data are given to estimate performance parameters at chamber pressures other than those for which data are tabulated.—(27.3×34.1.1).

SCIENCE—GENERAL

La resistance thermique des joints. J. J. Bernard. AGARD Report 212. *Oct.* 1958. (*In French.*)—(32.2.2×34.3.3).

Recherches expérimentales sur les ondes de choc produites par les décharges condensées dans les gaz rares. M. Cloupeau. Pubs Sc et Tech. 352. 1959. (*In French.*)—32.2.1×1.2.3.2).

STRUCTURES

THEORY AND ANALYSIS

An improved first-approximation theory for thin shells. J. L. Sanders. N.A.S.A. Report 24. *June* 1959.
A theory is derived in which all strains vanish for any rigid-body motion in contrast to the results of Love's theory. Expressions for the stress resultants and couples which satisfy the homogeneous equilibrium equations are given in terms of three stress functions. The special forms of the equations of the new theory in the case of a circular cylinder are given.—(33.2.4.11).

Sandwich structure for high temperature vehicles. H. R. Ashley. AGARD Report 216. *Oct.* 1958.
A review of high temperature sandwich structure from the viewpoints of theoretical structural efficiency and of practical design and manufacturing is presented. The physical properties of five materials (R.R.58 light alloy, F.V.520 stainless steel, 6 Al 4 Va titanium alloy, Nimonic 90 and 0·5 titanium molybdenum) are summarised and, in conjunction with core data, used to present a series of graphs showing the efficiency of both honeycomb and corrugated sandwich at high temperatures for specific structural index values. Thermal stress factors for these materials at various temperatures are also presented. The practical design and production aspects of sandwich construction is discussed.—(33.2.4.14.9×21.2.3).

Transient thermal stresses in the elastic slab. C. H. J. Johnson. ARL Note ME 232. *March* 1959.
As part of an investigation of thermal stresses in turbine blades a solution has been obtained to the problem of determining the transient thermal stress distribution in an infinite elastic slab due to the sudden simultaneous application of a temperature T_1 to one face and a temperature T_2 to the other face, the initial conditions being zero and with zero surface tractions. The solution is given in series form, the successive terms of which, in effect, give the stress at a particular depth in a semi-infinite solid with a constant temperature boundary condition. This result is analogous to the solution of problems in transmission line theory in terms of multiple reflected waves. The solution in this form converges quite rapidly except for large values of the time.—(33.2.4.5.9).

TESTING

A calibrator for strain gauge bridges. I. G. Scott. ARL Note SM 251. *March* 1959.
A very simple calibrator for strain gauge bridges is described. —(33.3.1).

THERMODYNAMICS

See also POWER PLANTS
SCIENCE—GENERAL

The freezing and melting times of slabs and cylinders. D. C. Baxter. N.R.C. Report MK-1. *Feb.* 1959.
General results for the time required to freeze or melt slabs or circular cylinders of a pure substance initially at the fusion temperature and exposed to a constant ambient temperature have been obtained on the PACE analogue computer.—(34.3.4).

Heat conduction in solids at hypersonic speeds. L. Broglio. AGARD Report 209. *Oct.* 1958.
Part I is an extension of a general approach to the heat conduction problems presented in a previous paper to a body whose thermal properties are dependent on temperature. Part II is an application of Part I to the heat conduction problems in hypersonic flight. Part III is a numerical application of Part I and Part II to a hollow steel hemisphere at hypersonic speed.—(34.3.3).

APPOINTMENTS

This section of THE JOURNAL *is available for advertisements of appointments in the Industry, the Ministries, Research Establishments, Universities and Colleges.*

Press Day—20th of the month preceding publication.
Rates—8/- a line. Each paragraph is charged separately and name and address must be counted. Semi-displayed setting £4 0s. 0d. per column inch.
Box Numbers—1/- extra. Replies should be addressed to: Box 000, care of THE JOURNAL of the Royal Aeronautical Society, One Arundel Street, Strand, London W.C.2.

Remittances—Cheques and postal orders should be made payable to the Journal of the Royal Aeronautical Society, One Arundel Street, Strand, London, W.C.2.
The Society reserves the right to decline any copy or advertisement at its discretion and accepts no responsibility for delay in publication or for clerical or printer's errors, although every care is taken to avoid mistakes.

Blackburn

offer
interesting and progressive careers to Designers and Technicians in the Aircraft and Gas Turbine industries. If you are an A.F.R.Ae.S. or possess an equivalent qualification,

please write to : The Technical Staff Manager

BLACKBURN & GENERAL AIRCRAFT LIMITED
BROUGH, EAST YORKSHIRE

C106/a

AN INTRODUCTION TO AERONAUTICAL ENGINEERING

Vol. 1: Mechanics of Flight.
By A. C. Kermode, O.B.E., M.A. 6th Edition.
The well-known standard work on the subject. It forms an essential and extremely valuable book for those engaged in all branches of aeronautical work. 25/- net.

THE HELICOPTER AND HOW IT FLIES

By John S. Fay. Meets the need for a simple book giving basic information about helicopter theory without resorting to mathematical formulae. Containing over 100 illustrations, this is a most useful book for the pilot, apprentice, and the technician transferring to helicopters. 12/6 net.

FROM ALL BOOKSELLERS

PITMAN AERONAUTICAL BOOKS
Parker St., Kingsway, London, WC2

UNIVERSITY OF BRISTOL

Applications are invited for a **LECTURESHIP** (Grade II) in **AERONAUTICAL ENGINEERING.** Applicants should have a good Honours Degree and some relevant research or teaching experience, preferably in the field of High Speed Flow.

The salary will be in the range £900—£1,300 (bar)—£1,650.

The appointment will be made as soon as possible and the successful candidate will be required to take up duty not later than 1st January, 1960.

Applications, including the names of two persons to whom reference may be made, should be sent to the Registrar, The University, Bristol, 8, from whom further particulars may be obtained.

FATIGUE DATA SHEETS

A supplementary issue to the Fatigue Data Sheets will be issued shortly. The new sheets will cover Basic Statistical Concepts and Methods; the Effect of Interference in Pin Joints; Fatigue Testing Machines Data and Geometric Stress Concentration Factors

further particulars are available from

THE ROYAL AERONAUTICAL SOCIETY
4 Hamilton Place, London W.1
Grosvenor 3515-9

TRADE MARKS SECTION

AIRCRAFT MATERIALS LTD.

AML

STRUCTURAL MATERIALS
and COMPONENTS

ASSOCIATED ELECTRICAL INDUSTRIES LTD.

AEI

ELECTRICAL EQUIPMENT
for Aircraft
Associated Electrical Industries Ltd.
Aircraft Equipment Group

BOULTON PAUL AIRCRAFT LTD.

BPA

THE BRITISH REFRASIL CO. LTD.

REFRASIL

LIGHTWEIGHT, HIGH TEMPERATURE INSULATION

DOWTY GROUP LTD.

DOWTY

UNDERCARRIAGES
HYDRAULIC & ELECTRICAL EQUIPMENT
FUEL SYSTEMS FOR GAS TURBINES
RUBBER SEALS

FIRTH-VICKERS STAINLESS STEELS LTD.

FV

"Stayrite"
STAINLESS STEEL

HUNTING AIRCRAFT LTD.

KELVIN & HUGHES (AVIATION) LTD.

KH

(HENRY HUGHES & SON LTD.
KELVIN, BOTTOMLEY & BAIRD LTD.)

K.L.G. SPARKING PLUGS LTD.

K·L·G

SPARKING PLUGS AND
IGNITION EQUIPMENT

LIGHT-METAL FORGINGS LTD.

LMF

LOCKHEED PRECISION PRODUCTS LTD

ALL-BRITISH
Lockheed
hydraulics

SAUNDERS-ROE LTD

SAUNDERS-ROE
LIMITED
OSBORNE EAST COWES · ISLE OF WIGHT
Phone Cowes 2211 and at Trafalgar 5448
CFH/SR0/15

JOSEPH LUCAS (GAS TURBINE EQUIPMENT) LTD

LUCAS

SMITHS AIRCRAFT INSTRUMENTS LTD.

SMITHS
SMITHS AIRCRAFT INSTRUMENTS LTD.

REDIFON LTD.

Redifon
FLIGHT SIMULATOR
DIVISION
CRAWLEY - SUSSEX - ENGLAND

THE UNITED STEEL COMPANIES LTD.

"RED FOX"
HEAT RESISTING
STEELS
S. FOX & CO. LTD. SHEFFIELD

F299

ROTAX LTD

ROTAX
AIRCRAFT ELECTRICAL ENGINEERS

WESTLAND AIRCRAFT LTD.

WESTLAND
The Hallmark of British Helicopters
Westland Aircraft Limited, Yeovil, England

DIRECTORY OF ADVERTISERS

AIR PICTORIAL
Rolls House, Breams Buildings, London, E.C.4. *Holborn* 5708

AIR TRAINERS LINK LTD.
Bicester Road, Aylesbury, Bucks. *Aylesbury* 4611

AIRCRAFT MATERIALS LTD.
Midland Road, London N.W.1. *Euston* 6151

ALBRIGHT & WILSON (MFG.) LTD.
1 Knightsbridge Green, London S.W.1. *Kensington* 3422

BERFIELD INDUSTRIES LTD.
Aviation Division, Stratford House, London W.1. *Grosvenor* 7090

BLACKBURN AND GENERAL AIRCRAFT LTD.
Head Office: Brough, E. Yorks. *Brough* 121
London Office: 43 Berkeley Square, W.1. *Grosvenor* 5771-8

BLACKHEATH STAMPING CO. LTD.
Blackheath, Birmingham. *Blackheath* 1448-9

BOOTH, JAMES, & CO. LTD.
Argyle Street Works, Birmingham 7. *East* 1521

BOULTON PAUL AIRCRAFT LTD.
Wolverhampton. *Fordhouses* 3191

B.P. AVIATION SERVICE SHELL-MEX AND B.P. LTD.
Shell-Mex House, Strand, London W.C.2. *Temple Bar* 1234

BRISTOL AEROPLANE CO. LTD.
Filton House, Bristol, Gloucestershire. *Filton* 3831

BRISTOL SIDDELEY ENGINES LTD.
London Office: Mercury House, 195 Knightsbridge, S.W.1. *Kensington* 7090
Bristol: P.O. Box 3, Filton, Bristol, England. *Filton* 3871
Coventry: P.O. Box 17, Coventry, Warwickshire, England. *Coventry* 62666

BRITISH OVERSEAS AIRWAYS CORPORATION
Head Office: London Airport, Hounslow, Middx. *Skyport* 5511
Passenger Reservations and Enquiries: Airways Terminal, Buckingham Palace Road, S.W.1. *Victoria* 2323

BRITISH REFRASIL CO. LTD.
Stillington, Co. Durham. *Stillington* 351

BRITISH THOMSON-HOUSTON CO. LTD.
Lower Ford Street, Coventry *Coventry* 64181

CIBA (A.R.L.) LTD.
Duxford, Cambridge. *Sawston* 2121

CROSS MANUFACTURING CO. (1938) LTD.
Bath, Somerset. *Combe Down* 2355/8

DECCA NAVIGATOR CO. LTD., THE
Decca House, Albert Embankment, S.E.11. *Reliance* 8111

DE HAVILLAND AIRCRAFT CO. LTD.
Hatfield, Herts. *Hatfield* 2345

DELANEY GALLAY LTD.
Vulcan Works, Edgware Road, London N.W.2. *Gladstone* 2201

DOWTY EQUIPMENT LTD.
Cheltenham, Glos. *Cheltenham* 53471

ELECTRO-HYDRAULICS LTD.
Liverpool Road, Warrington. *Warrington* 35241

ENGLISH ELECTRIC CO. LTD.
Marconi House, Strand, London W.C.2. *Covent Garden* 1234

ESSO PETROLEUM CO. LTD.
36 Queen Anne's Gate, S.W.1.
Aviation Technical Service *Reliance* 1262

FAIREY AVIATION LTD.
Hayes, Middlesex. *Hayes* 3800
24 Bruton Street, London W.1. *Mayfair* 8791

FERRANTI LTD.
Hollinwood, Lancashire. *Failsworth* 2000
London Office: Kern House, 36 Kingsway, W.C.2. *Temple Bar* 6666

FIRTH, THOS. & JOHN BROWN LTD.
Atlas Works, Sheffield 4. *Sheffield* 40871
11 Hamilton Place, London W.1. *Grosvenor* 8781-6

FIRTH-VICKERS STAINLESS STEELS LTD.
Staybrite Works, Sheffield. *Sheffield* 42051

FLIGHT REFUELLING LTD.
Tarrant Rushton Airfield, Blandford, Dorset. *Blandford* 501

FOX, SAMUEL, & CO. LTD. (UNITED STEEL COMPANIES LTD.)
17 Westbourne Road, Sheffield 10. *Sheffield* 40871

GENERAL ELECTRIC CO. LTD.
Magnet House, Kingsway, London W.C.2. *Temple Bar* 8000

GRAVINER MANUFACTURING CO. LTD.
(Aircraft Division Sales Department), Poyle Mill Works, Colnbrook, Bucks. *Colnbrook* 2345

HANDLEY PAGE LTD.
Cricklewood, London N.W.2. *Gladstone* 8000

HAWKER SIDDELEY AVIATION LTD.
Richmond Road, Kingston-on-Thames. *Kingston* 7741
Duke's Court, Duke Street, St. James's, London S.W.1. *Whitehall* 2064

HAWKER SIDDELEY GROUP LTD.
18 St. James's Square, London S.W.1 *Whitehall* 2064

HIGH DUTY ALLOYS LTD
Slough, Bucks. *Slough* 23901

HOBSON, H. M. LTD.
Hobson Works, Fordhouses, Wolverhampton. *Fordhouses* 2266

HUNTING AIRCRAFT LTD.
Luton Airport, Luton, Bedfordshire. *Luton* 6060

IMPERIAL CHEMICAL INDUSTRIES LTD.
Plastics Division, Black Fan Road, Welwyn Garden City, Herts. *Welwyn Garden* 3400

IMPERIAL CHEMICAL INDUSTRIES LTD. (TITANIUM)
London S.W.1. *Victoria* 4444

INTEGRAL LIMITED
Birmingham Road, Wolverhampton. *Wolverhampton* 24984

JABLO PLASTICS INDUSTRIES LTD.
Jablo Works, Waddon, Croydon, Surrey. *Croydon* 2201

KELVIN & HUGHES (AVIATION) LTD.
New North Road, Barkingside, Essex. *Hainault* 2601

K.L.G. SPARKING PLUGS LTD.
Putney Vale, London S.W.15. *Putney* 8111

LAPORTE CHEMICALS LTD.
Kingsway, Luton. *Luton* 4390

LIGHT-METAL FORGINGS LTD.
Oldbury, Birmingham. *Broadwell* 1152

LOCKHEED PRECISION PRODUCTS LTD.
Tachbrook Road, Leamington Spa. *Leamington Spa* 2700

LUCAS, JOSEPH (GAS TURBINE EQUIPMENT) LTD.
Shaftmoor Lane, Birmingham 28 *Springfield* 3232
Burnley. *Burnley* 5051 & 5027

MAGNESIUM ELEKTRON LTD.
Lumms Lane, Clifton Junction, nr. Manchester. *Swinton* 2511-9
5 Charles II Street, London W.1. *Trafalgar* 1646

NAPIER, D., & SON LTD.
Acton, London W.3. *Shepherds Bush* 1220

NORMALAIR LTD.
West Hendford, Yeovil, Somerset. *Yeovil* 1100

PERGAMON INSTITUTE
4 & 5 Fitzroy Square, W.1. *Euston* 4455

PERGAMON PRESS LTD.
4 & 5 Fitzroy Square, London W.1. *Euston* 4455

PHILLIPS & WHITE
61 Queen's Gardens, London W.2. *Ambassador* 8651, 2764

PITMAN, SIR ISAAC & SONS LTD
Parker Street, Kingsway, London W.C.2. *Holborn* 9791

QANTAS EMPIRE AIRWAYS LTD.
Qantas Corner, Piccadilly and Old Bond Street, London W.1. *Mayfair* 9200

REDIFON LTD.
Crawley, Sussex. *Crawley* 1540

ROBERT RILEY LTD.
Milkstone, Spring Works, Rochdale. *Rochdale* 2237

ROLLS-ROYCE LTD.
Derby. *Derby* 42424
14-15 Conduit Street, London W.1. *Mayfair* 6201

ROTAX LTD.
Willesden Junction, London N.W.10. *Elgar* 7777

ROTOL LTD.
Cheltenham Road, Gloucester. *Gloucester* 24431

SAUNDERS-ROE LTD.
Osborne, East Cowes, Isle of Wight. *Cowes* 2211

SHELL-MEX & B.P. LTD.
Shell-Mex House, Strand, London W.C.2. *Temple Bar* 1234

SMITHS AIRCRAFT INSTRUMENTS LTD.
Cricklewood Works, London N.W.2. *Gladstone* 3333

SPERRY GYROSCOPE CO. LTD., THE
Great West Road, Brentford, Middlesex. *Ealing* 6771

SUPER OIL SEALS & GASKETS LTD.
Factory Centre, Birmingham 30. *Kings Norton* 2041

TEDDINGTON AIRCRAFT CONTROLS LTD.
Merthyr Tydfil, South Wales. *Merthyr Tydfil* 666
London Airport Office: Colnbrook By-Pass, West Drayton, Middlesex.

ULTRA ELECTRIC LTD.
Western Avenue, Acton, London W.3. *Acton* 3434

VICKERS-ARMSTRONGS (AIRCRAFT) LTD.
Vickers House, Broadway, Westminster, S.W.1. *Abbey* 7777
Weybridge Works, Weybridge, Surrey. *Weybridge* 5555
Supermarine Works, South Marston, Swindon, Wilts. *Swindon* 3451

WESTLAND AIRCRAFT LTD.
Yeovil, Somerset. *Yeovil* 1100

PLEASE NOTE:—The advertisement office of the JOURNAL is now at One Arundel St., Strand, W.C.2. Tel: Covent Garden 1612-3-4

AIR PICTORIAL

The non-technical monthly for the enthusiast

★

Exciting exclusive articles on past and present aircraft

★

Superb photographs — scores of them in each issue — keep you up to the minute on new developments

★

Large scale drawings provide information on world's aircraft

At your bookseller or newsagent 1/6d

★

Or send £1.2.6d for a year's subscription to Dept. A.S., AIR PICTORIAL, ROLLS HOUSE, BREAMS BUILDINGS, LONDON, EC4

if you would like a FREE COPY fill in the form

1/6d monthly

AIR PICTORIAL

the magazine to keep you in touch with aviation

Get this month's issue— and every month's

TO ROLLS HOUSE PUBLISHING CO LTD
ROLLS HOUSE
2 BREAMS BUILDINGS LONDON EC4

Please send me a specimen copy of ***AIR PICTORIAL*** for which I enclose 6d in stamps for postage and packing

BLOCK LETTERS PLEASE

NAME .....

.....

ADDRESS .....

.....

.....

A.S.

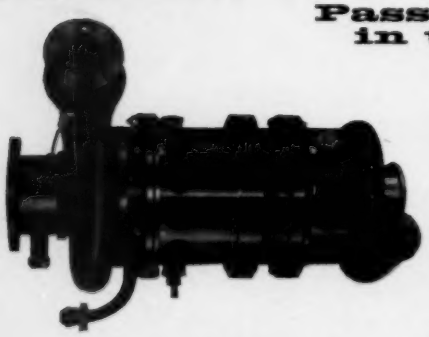

Passenger Comfort Assured in the air AND on the ground

NORMALAIR vapour cycle cooling systems will provide full refrigeration even when an aircraft is stationary with engines stopped, or taxying with engines turning at low r.p.m. They can also serve as a means of reducing the relative humidity of the cabin air supply, thereby ensuring an acceptable effective temperature in the cabin. The separate ground conditioning trucks used with air cycle systems can, therefore, be dispensed with.

As well as offering these important advantages, NORMALAIR vapour cycle systems make much smaller demands on power supplies than comparable air cycle systems. In general, they compare favourably with air cycle systems in the matter of weight, and where heat loads are high, are significantly lighter.

In addition to these aircraft systems, which are available for aircraft of all classes, and which can be based on either reciprocating or centrifugal compressors, NORMALAIR are producing systems for guided missiles and other applications.

NORMALAIR YEOVIL ENGLAND

The only designers and manufacturers in Great Britain of complete cabin air conditioning systems for all classes of military and civil aircraft

NORMALAIR (CANADA) LTD TORONTO

NORMALAIR (AUSTRALIA) PTY LTD MELBOURNE

PRINTED BY THE LEWES PRESS, WIGHTMAN & CO. LTD., LEWES, SUSSEX, ENGLAND, AND PUBLISHED BY THE ROYAL AERONAUTICAL SOCIETY, 4 HAMILTON PLACE, LONDON, W.1, ENGLAND.